

ATLAS Deliverable 2.2

Integrated physiological experiments and models

Project acronym:	ATLAS
Grant Agreement:	678760
Deliverable number:	2.2
Deliverable title:	Integrated physiological experiments and models
Work Package:	2
Date of completion:	30/06/2019
Authors:	Marina Carreiro-Silva (IMAR-UAz), Dick Van Oevelen (NIOZ) (see next page for full author list)



This project has received funding from the European Union's Horizon 2020 research and innovation programme under grant agreement No 678760 (ATLAS). This output reflects only the author's view and the European Union cannot be held responsible for any use that may be made of the information contained therein.

Author list: Marina Carreiro-Silva¹, Covadonga Orejas³, Maria Rakka¹, Stephanie Lieffman⁴, Evert de Roe², Johanne Vad^{4,5}, Sandra Maier², Meri Bilan¹, António Godinho¹, Inês Martins¹, Patricia Puerta³, Sebastian Hennige⁴, Theodore B. Henry⁵, Murray Roberts⁴, Karline Soetaert⁶, Dick van Oevelen⁶

¹IMAR-University of Azores, Portugal carreirosilvamarina@gmail.com

²Department of Ocean Systems, Royal Netherlands Institute for Sea Research (NIOZ-Yerseke), Utrecht University, Yerseke, The Netherlands

³Instituto Español de Oceanografía, Centro Oceanográfico de Baleares, Palma, Spain

⁴School of GeoSciences, The University of Edinburgh, UK

⁵School of Energy, Geoscience, Infrastructure and Society, Heriot-Watt University, Edinburgh, United Kingdom

⁶Department of Estuarine and Delta Systems, Royal Netherlands Institute for Sea Research (NIOZ-Yerseke), Utrecht University, Yerseke, The Netherlands

Contents

1	Executive summary	3
2	General introduction.....	6
3	Experimental studies conducted during ATLAS	7
3.1	Feeding ecology of cold-water corals	7
3.1.1	Capture rate efficiency for black corals and gorgonians in the Azores	12
3.1.2	Capture rate efficiency for scleractinian <i>Lophelia pertusa</i> , the bivalve <i>Acesta excavata</i> and the sponges <i>Geodia barretti</i> , <i>Stryphnus sp.</i> and <i>Phakellia ventilabrum</i> in Norway	23
3.1.3	Food preference and assimilation rates of habitat-forming cold-water corals in the Azores	42
3.1.4	Competition for food between two coexistent species in Azores coral gardens, <i>Dentomuricea aff. meteor</i> and <i>Viminella flagellum</i>	50
3.2	Assessing the impact of ocean acidification under variable food supply on the octocoral <i>Viminella flagellum</i>	55
3.3	Ecotoxicological studies on the sponge <i>Halichondria panicea</i>	69
4	Physiological model of cold-water corals and sponges under different scenarios of environmental change (flow velocity and food supply)	80
5	Conclusions and way forward	90
	References	90
	Document Information	101

1 Executive summary

A major objective of ATLAS is to produce a new class of predictive modelling tools that integrates food supply and biogeochemical cycling for mapping deep-sea species and ecosystems at management relevant spatial scales. To produce these models it is necessary to integrate field data on hydrodynamic conditions, organic matter concentration and settling flux to the seafloor with *ex situ* aquarium studies conducted to determine how deep-sea organisms respond to altered food supply regimes and changes in ocean conditions, such as ocean acidification. Here we report results of the *ex-situ* experiments using scleractinian corals, black corals, octocorals, bivalves and sponges conducted by different ATLAS partners and then use this data together with data available from the literature (DL 2.1) to produce physiological models for selected cold-water coral and sponge species.

Four types of experiments were carried out to:

(1) Assess the capacity of selected CWC species to capture live zooplankton prey under different hydrodynamic conditions (section 3.1). For this purpose, a set of experiments were performed in the Azores (section 3.1.1) and Norway (section 3.1.2). Experiments in the Azores tested capture rate efficiency of the black coral *Antipathella wollastoni* and the gorgonians *Viminella flagellum* and *Dentomuricea meteor* using the rotifer *Branchionus plicatilis* as prey under flow velocities of 1.5, 4 and 6 cm/sec for the black coral and 3, 6 and 9 cm/sec for the gorgonians, using laminar flow experimental flumes. Results obtained for *A. wollastoni* show the capacity for this species to consume high amounts of prey and this capacity seems to be enhanced in intermediate flow velocities (4cm/sec). This explain the natural abundance of *A. wollastoni* in crevices protected from strong currents. Experimental results obtained for the gorgonians, demonstrated higher capture rates per polyp for *V. flagellum*, with maximum capture rates at 6 cm/sec, compared with *D. meteor* with maximum capture rates at 9cm/sec. These results may be related to the larger size of polyps of *V. flagellum* and might reflect different feeding strategies by the two species due to their different morphological shape. All species studied showed lower capture rates per polyp when compared with the reef-forming *Lophelia pertusa* likely related with the smaller polyp size of black corals and gorgonians but preference for higher flow rates. These species-specific effects corroborate the hypothesis that flow regime can be a very important factor in describing species presence, density and success among different areas and may an important prediction factor of the distribution of species under present and future conditions.

Studies conducted in Norway tested capture rate efficiency for the reef-forming species *Lophelia pertusa*, the sponges *Geodia barretti*, *Stryphnus* sp. and *Phakellia ventilabrum*, and the bivalve *Acesta excavata* under 2 natural seston concentrations and water flow treatments using a flow through

chamber. Results of these studies found higher consumption rates for *L. pertusa* and *A. excavata* when compared with sponges. Interestingly, the sponge *P. ventilabrum*, a species characterized as having low abundance of associated microbial organisms (Low Microbial Abundance (LMA) sponges), had higher consumption rates when compared with *Geodia barreti* and *Stryphnus* sp, which characterized as High Microbial Abundance (HMA) sponges. This may be due to the fact that HMA sponges may complement their diet with their own symbionts and dissolved organic matter. Furthermore, *L. pertusa* and *A. excavata* showed a wider range of food sources consumed when compared with sponges which preferentially fed on algal and bacterial particles.

(2)) Determine the feeding preferences of selected habitat forming CWC species in the Azores (black corals and gorgonians) to different food source using live algae, zooplankton and DOC fed with isotopically labelled OM (^{13}C and ^{15}N) ; and estimate the incorporation of carbon and nitrogen and metabolic activity under ingestion of these different food sources (section 3.1.3). Results of these experiments showed that the black coral *A. wollastoni* and gorgonians *V. flagellum* and *D. meteor* can feed on a variety of food sources (DOC, algae and zooplankton), but preferentially fed on zooplankton. This was translated into higher incorporation of carbon and nitrogen in to coral tissues and higher oxygen consumption rates in coral feeding on zooplankton, suggesting that this food source is of high importance for the growth and metabolism of black corals and gorgonians, as it has been already documented for CWC scleractinian species. The gorgonian *D. meteor* showed higher tracer incorporation and oxygen consumption for all food sources consumed when compared with *V. flagellum*, suggesting different metabolic strategies between these two co-existing gorgonians. While fragments of *D. meteor* appeared to be more efficient in removing prey than *V. flagellum* (section 2.1.1.) under similar flow velocities, further studies are needed to determine if the lower values displayed by *V. flagellum* can be attributed to lower capture and ingestion of prey or if ingested prey was used for other metabolic processes such as excretion, calcification or growth of the main skeletal axis, which was not considered in this study.

(3) Understand competition interactions of two co-occurring octocoral species *D. meteor* and *V. flagellum* under different water flow conditions. Results showed that both species have higher incorporation rates under 4cm s^{-1} in comparison to 2cm s^{-1} likely because of higher prey encounter rate. *D. meteor* had higher incorporation of C and N tracers for all treatments when compared to *V. flagellum* likely related to the more branching and fan shape colony morphology of *D. meteor* that can maximize prey capture (see also 3.1.2). *Viminella flagellum* is a whip coral that stands higher in the water column and likely gets access first to food particles. These different feeding strategies may

contribute to their co-existence in the same coral garden. However if food becomes scarce, *D. meteor* may gain a competitive advantage in relation to *V. flagellum*.

(4) Understand the impacts of OA on coral garden forming octocorals in Azores by testing the interactive effects of OA and food availability. Specific objectives of this experiment were to determine if and how food concentration alters the impacts of OA on the physiology of the tested species; and to assess the impact of OA on food uptake and food assimilation. *Viminella flagellum* displayed a decrease in polyp activity under OA conditions for all food treatments although this was more pronounced under starvation. This can consequently lead to lower energy input, although during the course of the experiments main metabolic rates such as oxygen consumption and tracer C respiration remained stable or even increased under acidified conditions. The increased oxygen consumption and tracer C respiration observed under acidified conditions are indications of increased metabolic demands. Nevertheless, the uncoupling between the patterns in tracer C respiration and oxygen consumption in the case of *V. flagellum* fragments under acidified conditions is a strong indication of a change in metabolic processes among fragments under low and high conditions, i.e. under low food concentrations energy may be diverted towards survival physiological mechanisms instead of growth and reproduction. Negative impacts of acidification on the species physiology, such as the one described for *V. flagellum*, may not directly affect their survival but are expected to impact other processes such as long-term growth and reproduction with possible detrimental effects on the population level which can cascade to the whole community.

(5) Determine the physiological impacts of crude oil and dispersants on the marine shallow-water sponge *Halichondria panicea* as model species. Respiration rates from the single concentration experiment and the dose-response experiments were highly variable and did not seem to change with exposure to hydrocarbons. However, clearance rates decreased sharply in sponges exposed to crude oil fractions or chemically enhanced oil fractions, even at low oil loading. It is likely that stopping its filtration activity for extensive periods of time will strongly impact survival of *H. panicea*. The capacity of sponges to survive longer exposure periods should therefore be further investigated.

In the last section of the report (section 4), physiological models for passive (i.e. CWC) and active (i.e. sponges) suspension feeders were constructed based on literature and experimental data (see section 3) using physiological parameters such as respiration and assimilation efficiency. For illustrative purposes, these models linked the respective physiological models to theoretical trajectories of variable food supply using *L. pertusa* as representative passive filter feeder of the Rockall Bank and the sponge *Geodia* sp. as a representative of a suspension active filter feeder from Davis Strait. These

physiological models will be coupled in D2.5 to the environment using the hydrodynamic model (developed in D2.4) factors and calibrated by field data in D2.3.

Overall, experiments conducted in this DL have contributed to a better understanding of the feeding ecology and ecophysiology of understudied habitat-forming species such as black corals, octocorals, bivalves and sponges. It has also elucidated how octocorals, and the coral gardens they form, may be impacted by future predicted changes in seawater chemistry (OA) and food supply (OM concentration) and how sponges may be impacted by anthropogenic impacts such as oil spills. We have also demonstrated how this data can be integrated in physiological models of CWC and DWS as a proxy for the environmental status of the ecosystems.

2 General introduction

Cold-water coral (CWC) reefs and deep-water sponge (DWS) grounds are important for global biogeochemical cycles and the ocean's benthic pelagic coupling loop, being responsible for nearly 30% of the coupling between organic matter (OM) produced at the ocean surface and the seafloor (Cathalot et al., 2015). Several studies have shown OM export from the surface to the seafloor may decrease with a changing global climate (Sweetman et al., 2017; Wohlers et al., 2009), but the consequences to vulnerable marine ecosystems (VMEs) such as CWC reefs and DWS grounds remains elusive. These ecosystems provide complex three-dimensional structural habitat that support high levels of biodiversity by providing refuge, feeding opportunities, and spawning and nursery areas for a wide range of organisms, including commercially important fish species (Buhl-Mortensen et al. 2010, Pham et al. 2015). In addition, they represent hotspots of ecosystem functioning processing substantial amounts of OM (White et al., 2012, Cathalot et al., 2015; Rovelli et al., 2015) and release nutrients back into the surrounding water (Van Oevelen et al., 2009; Cathalot et al., 2015; Rovelli et al., 2015). Yet these ecosystems are lacking in global and regional (Regnier, et al., 2013), meaning existing mass balance estimates are inaccurate. Close associations between these ecosystems and regional hydrodynamics means that effects of an Atlantic Meridional Overturning Circulation (AMOC) slowdown, changing food supply, or resource exploitation on biomass, food webs and ecosystem functioning are not known.

Unlike some sponges and reef framework-forming corals, very little is known about whether other VME indicator taxa such as octocorals, which also support biologically rich communities, can survive variable food concentration and flux. For example, in the Azores, octocorals are the most prominent habitat builders with more than 90 species recorded for the region (Braga-Henriques et al. 2013, Tempera et al. 2013) but little is known on the life history of these organisms such as growth, age,

reproduction, feeding ecology and the role they play in ecosystem functioning. Effects of environmental variability on food uptake rates in sponges and corals has also not been verified, but the feeding ecology and ecophysiology of all these taxa need to be studied in order to better predict outcomes of altered AMOC and food supply.

In addition, compared to reef-framework corals, little is known on the impacts of climate change and anthropogenic impacts on octocorals and sponges and the ecosystem functions they provide (Xavier et al., 2019). However, this information is necessary to produce predictive modelling tools that integrates food supply and biogeochemical cycling under different environmental change conditions for mapping species and ecosystems at management relevant spatial scales. These modelling tools need to integrate field data on hydrodynamic conditions, OM concentration and settling flux to the seafloor (provided in D2.3 and 2.4) with *ex situ* aquarium studies conducted to determine how corals and sponges respond to altered food supply regimes and changes in ocean conditions, such as ocean acidification (OA). Here we report results of the *ex-situ* experiments using scleractinian corals, octocorals, bivalves and sponges conducted by different ATLAS partners and use this data to produce physiological models based on data produced from these experiments. We also present results on an additional experiment on the impact of chemical pollution (oil and dispersants) on sponges that will help us understand the potential impacts of oil pollution on these organisms.

3 Experimental studies conducted during ATLAS

3.1 Feeding ecology of cold-water corals

The study of the CWC feeding ecology under aquaria conditions has been investigated for approximately a decade. The precursory studies for CWC feeding were conducted by Orejas et (2001, 2003) on the capture rates of some Antarctic hydroids and anthozoans; these studies were also based on previous studies conducted *in situ* in Mediterranean waters with gorgonians (see Ribes et al. 1999).

The first aquaria studies dealing with the ability of CWCs to capture prey were conducted with “artificial prey” (i.e. *Artemia salina* nauplii and adults) with Mediterranean specimens of *Lophelia pertusa*, *Madrepora oculata*, *Desmophyllum dianthus* and *Dendrophyllia cornigera* (Tsounis et al. 2010), and almost simultaneously with North Atlantic specimens of *L. pertusa* (Purser et al. 2010). For these studies, small circulation flumes were used (Figure 1a). Details on the functioning and characteristics of these flumes can be found in the publications mentioned above as well as in the recently published review chapter on experimental work conducted with CWCs (Orejas et al. 2019).

Cylindrical flumes (Figure 1b) have been also used to investigate CWC capture rates. The work by Orejas et al. (2016) used this type of aquaria with natural living prey, analysing the ability of *L. pertusa* specimens from the NE Atlantic in capturing different prey types and sizes (OM, algae and copepods).

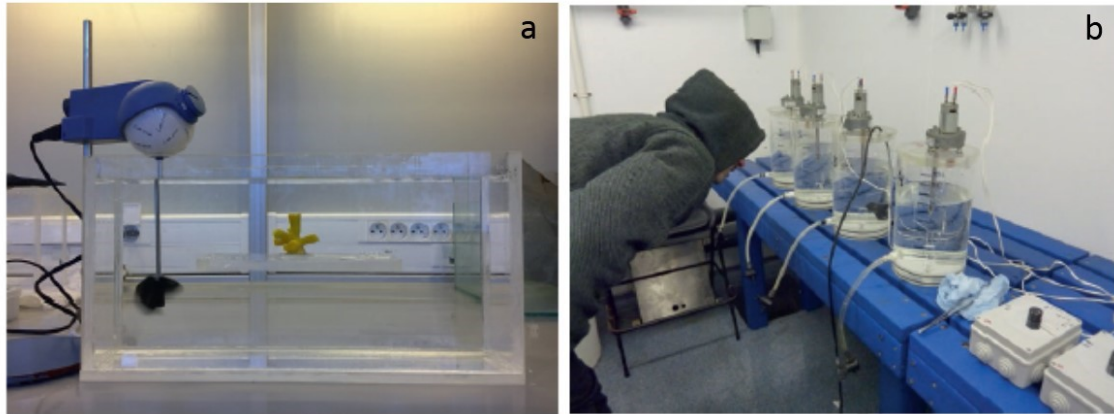


Figure 1: a) Closed recirculation flume (7 L volume) used at the CSM to conduct feeding experiments (Photo: © S. Reynaud), b) Cylindrical flumes (5 L) used for feeding experiments. The motor in the top of the chambers is connected to a blade, which keep the water moving at constant flow speed. The speed of the flow can be switched with the controllers (white boxes in the right part of the image). (Photo: © C. Orejas).

The work by Tsounis et al. (2010) compared the ability of *L. pertusa*, *M. oculata*, *D. dianthus* and *D. cornigera* to capture the same prey types under the same current speed (1 cm s^{-1}). The results reveal a better ability of *L. pertusa* to capture *Artemia* nauplii, and higher capture rates of *A. salina* adults for *D. dianthus* and *L. pertusa*, although the differences among the four species where not significant.

Following studies tested the ability of *L. pertusa* to capture prey under different current speeds (Purser et al. 2010; Orejas et al 2016). Although the experimental set-up (circular vs cylindrical) was quite different, the results obtained were similar for the experiments conducted with zooplankton as prey, and flow speeds of 2 to 2.5 cm s^{-1} were revealed as the most suitable for an effective capture of these prey items by *L. pertusa*, whereas the capture of microalgae seems to be more effective by 5 cm s^{-1} (Orejas et al. 2016). These studies demonstrated that seawater turbulence should be just below the limit for the polyp's ability to manage (and thus be able to feed): that is, there should be a noticeable strong flutter of the tentacles due to turbulence, but not too high to prevent the polyps from positioning its tentacles to catch food. Also, in some cases, when the current is too high the tentacles retracted, being also unable to capture food (see Orejas et al. 2019).

The findings that low current speeds are fundamental to assure the effective capture of prey by *L. pertusa*, may seem to be contradictory, considering that this CWC species frequently grows in locations where current speeds are considerably high, such as 20 cm s^{-1} in the Mingulay Reef Complex

(NE Atlantic) (Davies et al. 2009) and up to 80 cm s^{-1} in the Cap de Creus underwater canyon (NW Mediterranean), (Palanques et al. 2006). However, recorded data in continuum and over several days, showed remarkable differences in current speed regimes in a single day, ranging from less than 2 cm s^{-1} and up to 20 cm s^{-1} (Davies et al. 2009). This indicates that CWC feeding may be maximized at times when current speed is lowest (Davies et al 2009).

Although most studies on capture rate efficiency have been conducted with *L. pertusa*, studies with other CWC species have emerged in recent years that may better explain the CWCs capture rate efficiency under varying environmental conditions.

For example, Gori et al (2015) tested the ability of *D. cornigera* to capture two different prey sizes (i.e. mesozooplankton: *Artemia salina* nauplii and microzooplankton: *A. salina* adults) under three different current speeds (2, 5 and 10 cm s^{-1}) and three different temperatures (8, 12, and $16 \text{ }^{\circ}\text{C}$). Flow speeds did not significantly affect the capture of mesozooplankton by *D. cornigera*, whereas capture of macrozooplankton was significantly enhanced with increasing flow speed (Gori et al., 2015). Both meso- and macrozooplankton captures were not significantly affected by temperature. However, even if temperature did not directly affect the capture rates of *D. cornigera*, it may still influence the feeding capacity of this CWC since the capture rates at $8 \text{ }^{\circ}\text{C}$ were always in the lowest range of the observed values at each flow speed. In addition *D. cornigera* maintained at $8 \text{ }^{\circ}\text{C}$ required a longer time to fully expand their polyps once they were placed in the incubation chambers, than corals maintained at 12 and $16 \text{ }^{\circ}\text{C}$. Overall, this study demonstrated that *D. cornigera* is more efficient in capturing zooplankton under a larger range of flow velocities than *L. pertusa*, whose capture efficiency significantly decreased from low to high flow speeds (Orejas et al. 2016).

Although, prey capture studies have contributed to improve our knowledge of food preferences and rates of uptake of food particles, this approach cannot account for food that was lost as sloppy feeding (Moeller et al., 2005; Pitt et al., 2008) or cannot be assimilated, and thus food uptake rates cannot be directly translated to assimilation. In addition, organisms utilize the assimilated food in its total energy budget, which includes maintenance and growth respiration, tissue growth and storage, reproduction (Davies, 1984; Kooijman, 2000), calcification (Cohen and Holcomb, 2009; McCulloch et al., 2012) and the release of mucus as particulate and dissolved organic matter (Crossland, 1987; Maier et al., 2019; Naumann et al., 2011; Wild et al., 2008; Zetsche et al., 2016). The partitioning of the assimilated carbon (C) and nitrogen (N) amongst these processes is difficult to determine from traditional incubation studies as the measured physiological processes, such as respiration, are also fuelled by previously assimilated compounds.

The use of resources that are enriched in stable isotopes provides a unique tool to quantitatively follow the uptake and processing of organic and inorganic resources in freshwater and marine organisms (Fry, 2006; Middelburg et al., 2015). The general principle is relatively straightforward: an (in)organic resource, with a substantially higher than natural ratio of the heavy isotope (e.g. ^{13}C for carbon and ^{15}N for nitrogen) over the lighter isotope (e.g. ^{12}C for carbon and ^{14}N for nitrogen) is offered to the organism and the 'heavy isotope' pulse is used to trace the fate of the resource in the tissue and metabolic products of a consumer (Figure 2, e.g. Middelburg et al., 2000; Moodley et al., 2000). Stable isotopically enriched resources can be obtained in various ways. Inorganic resources (e.g. $\text{NaH}^{13}\text{CO}_3$, or $^{15}\text{NH}_4\text{Cl}$) can be commercially purchased, while organic resources (e.g. phytoplankton or bacteria) can be produced by culturing them in a ^{13}C or ^{15}N enriched medium (e.g. Moodley et al., 2000; Mueller et al., 2014). Enriched dissolved organic material (DOM) can be extracted from an enriched algal culture (De Goeij et al., 2008), while herbivorous zooplankton can be grown by feeding them with enriched algae (Mueller et al., 2014, Rakka et al, in prep).

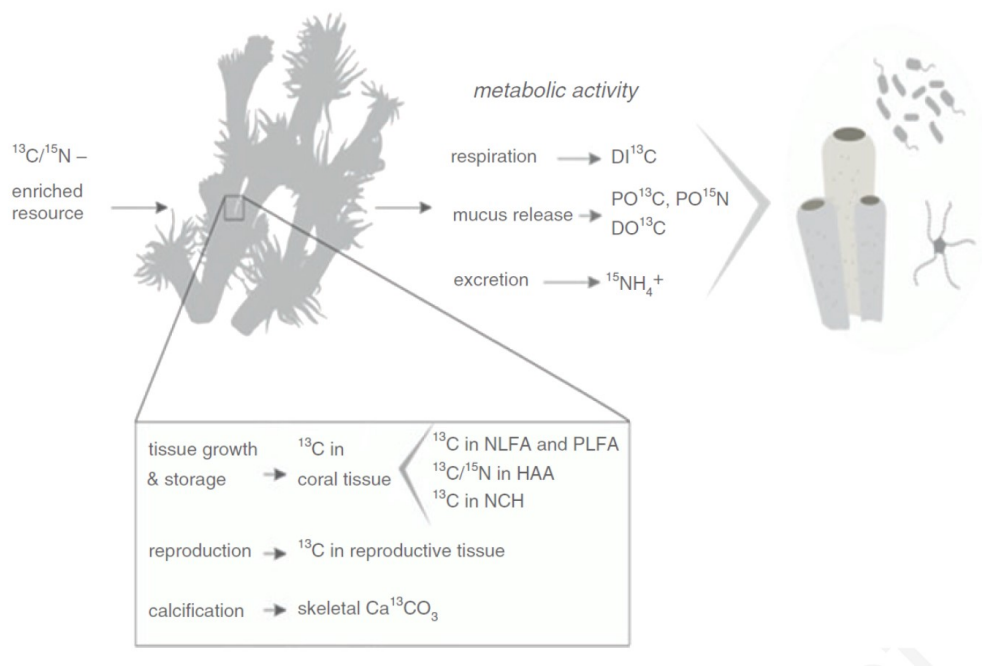


Figure 2. Uptake and processing of organic and inorganic resources of a cold-water coral feeding on a $^{13}\text{C}/^{15}\text{N}$ enriched resource, from assimilation to utilisation for metabolic activity, for tissue and skeletal growth and reproductive tissue formation. The resource ^{13}C and ^{15}N can be 'traced back' in metabolic products such as DIC dissolved inorganic carbon, POC/PON particulate organic carbon/nitrogen, NH_4^+ ammonium, and into coral (reproductive) tissue plus tissue molecules, NLFA neutral lipid-derived fatty acids, PLFA phospholipid-derived fatty acid, HAA hydrolysable amino acids, NCH neutral carbohydrates, and in skeletal calcium carbonate. (Scheme by © S.R. Maier reported in Orejas et al 2019).

Pulse-chase stable isotope tracer studies have shed light on the physiology of DWS and CWCs in various ways. Mueller et al. (2014) found opportunistic use of *L. pertusa* of different ^{13}C and ^{15}N -enriched substrates ranging from algal-derived amino acids (Dissolved Organic Matter) to

zooplankton. In addition, de novo lipid synthesis by *L. pertusa* was apparent from the ^{13}C enrichment of individual phospholipid-derived fatty acids (PLFAs) in the coral that were absent in the added food sources, a finding which may complicate the interpretation of coral nutrition based on lipid composition profiles alone (Mueller et al., 2014). Van Oevelen et al. (2016) found that selective feeding of *L. pertusa* were offered algae and bacteria in a cross-labeling approach, dependent on food concentration as algae were preferred over bacteria only at higher food concentration. Maier et al. (2019b) studied the metabolization of ^{13}C -labeled phytodetritus following the exposure of *L. pertusa* to a short food pulse. They found distinct temporal dynamics, with an initial preferential use phytodetritus-derived C for respiration and particulate mucus production. These fluxes declined exponentially to <20% within 2 weeks after feeding and then remained stable, which indicated that the remainder of the incorporated phytodetritus had entered a tissue pool with lower turnover. Analysis of ^{13}C in individual FAs revealed a mismatch between the FAs incorporated from phytodetritus and the FA requirements of the coral. Van Oevelen et al. (2018) found a niche overlap between the coral *L. pertusa* and the DWS *Hymedesmia coriacea* using isotopically-enriched algae and bacteria as suspended food sources. Both species assimilated and respired the suspended bacteria and algae, indicating a niche overlap between these species. Rix et al. (2016) identified a direct trophic link between corals and reef sponges using stable isotope tracer experiments in Red Sea warm-water and north Atlantic CWC reefs and the authors suggest that the presence of this sponge loop in two vastly different reef environments suggests it is a ubiquitous feature of reef ecosystems contribution to the high biogeochemical cycling that may enable coral reefs to thrive in nutrient-limited (warm-water) and energy-limited (cold-water) environments.

Finally, Kazanidis et al. (2018) used on-board feeding experiments to examine the processing of four isotopically-labelled food sources (^{15}N -ammonium chloride, ^{13}C -glucose, $^{13}\text{C}/^{15}\text{N}$ -labelled microalgae and $^{13}\text{C}/^{15}\text{N}$ -labelled bacteria) by *Sponsorites coralliophaga* and its symbiotic bacteria and epibionts from two reefs in the North-East Atlantic. The authors found that *S. coralliophaga* assimilated C and N from all four food sources and this versatile feeding strategy was accompanied by an ability for de novo synthesis of essential and non-essential hydrolysable amino acids (HAAs) and they therefore suggest that metabolic flexibility of *S. coralliophaga* plays an important role in the survival of this massive sponge under food-limited conditions in the deep sea.

3.1.1 Capture rate efficiency for black corals and gorgonians in the Azores

Authors: Maria Rakka, Sandra Maier, Meri Bilan, Antonio Godinho, Dick van Oevelen, Sebastian Hennige, Covadonga Orejas, Marina Carreiro-Silva

Aims and objectives: The aim of this study was to assess the capacity of selected CWC species to capture live zooplankton prey and determine the effect of varying hydrodynamic conditions on this capacity. For this purpose a set of experiments was set for each species in order to estimate prey capture of a predetermined concentration of live zooplankton under different flow rates.

Materials and Methods

Studies on the feeding ecology of habitat-forming CWCs in the Azores focused on one antipatharian and two gorgonian species, which form dense coral gardens in the Azorean infralitoral and deep-sea environments. *Antipathella wollastoni* is a common black coral (order Antipatharia) within the Macaronesia, recorded in the Azores, Madeira, Canaries and Cape Verde Islands (Ocaña et al., 2007). It has a wide bathymetric distribution, since it can be found from 15m to 1400 m of depth. In the Azores *A. wollastoni* is mostly found in the infralitoral of island slopes where it forms dense coral gardens (Fig. 3) below 20m of depth (Tempera et al., 2001; de Matos et al., 2014). It possesses a skeleton exclusively made of organic material (protein and chitin), typical of the order Antipatharia (Goldberg et al., 1991). *Dentomuricea aff. meteor* is a fan shaped octocoral of the family Holaxonia. It is typically encountered in seamounts between 150 and 600 m. *Viminella flagellum* is a whip octocoral, very common in the Azorean EEZ between 100 and 600m. It forms dense coral gardens, very often in coexistence with fan shaped gorgonians such as *D. meteor* and species of the genus *Acanthogorgia*.

The aim of this study was to assess the capacity of selected CWC species to capture live zooplankton prey and determine the effect of varying hydrodynamic conditions on this capacity. For this purpose a set of experiments was set for each species in order to estimate prey capture of a predetermined concentration of live zooplankton under different flow rates.



Figure 3: Coral gardens of the studied species. *Antipathella wollastoni* (A), *Dentomuricea* aff. *meteor* (B), *Viminella flagellum* (C)

Experiments with *Antipathella wollastoni* Coral fragments of *A. wollastoni* were collected in October 2017 at two sites located at the natural parks of Faial and Pico island, namely the reef Baixa da Feteira in Faial and the bay of São Caetano in Pico. A total of 15 colonies with height higher than 40 cm were selected and four fragments with length between 8-10 cm were collected from the apical part of each colony, at depths between 20-40m. Fragments were kept at 1 liter flasks and immediately transferred to aquaria in the DeepSeaLab facilities, IMAR/DOP where they were fixed in bases made of epoxy. All fragments were kept in continuous flow-through open systems in a thermostatic room, in conditions of dim blue light (K) that followed the natural photoperiod while seawater temperature was controlled by cooling systems to match the temperature at the site of collection (19 ± 0.6 °C).

To assess the capture ability of the study species, a series of capture rate experiments were set up using the rotifer *Branchionus plicatilis* as prey. This species was selected as zooplankton food source because of its common use as food for suspension feeders with and animals with small mouth size (Lubzens et al., 1989). Rotifers were cultured continuously in conditions of low salinity (28-30), temperature between 16-18°C, natural light, slight aeration and fed daily with live microalgae of the species *Nannochloropsis gaditana*.

Experimental trials were run in four 33L aquaria that were adapted in order to create conditions of laminar flow (Fig. 4). A series of 8 cm marine propellers (Graupner) attached to heavy duty gear motors (313 rpm, 12V, Servocity) were used to create different flow velocities between 2, 4 and 6 cm/sec. An electromagnetic current meter was used to determine and control the flow velocities created by the motors. The four aquaria were kept in a water bath in order to keep uniform temperature throughout the experimental runs.

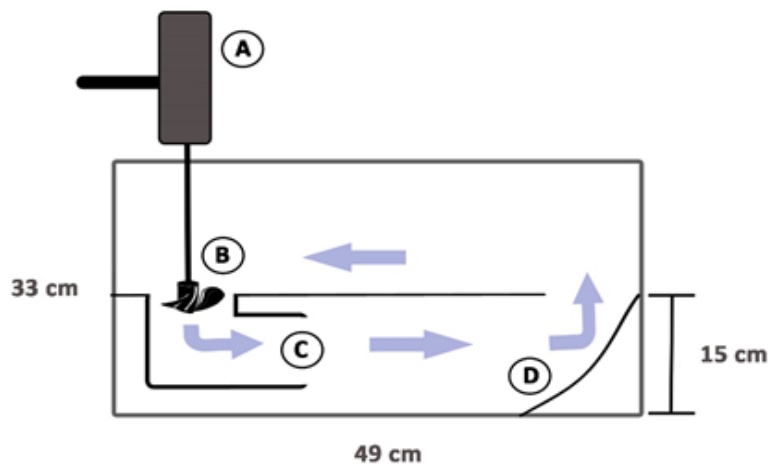


Figure 4: Experimental 33 flume used to determine feeding rates of the species *Antipathella wollastoni* under different flow rates. A: 313 rpm motor; B: 8 cm marine propeller; C: tube facilitating the creation of laminar flow; D: ramp to decrease localized water turbulence. Arrows indicate flow direction.

Three flow velocities were tested: 1.5 cm/sec, 4 cm/sec and 6 cm/sec. In each experimental run, five fragments were randomly chosen and positioned in each experimental flume. Fragments were left for 20-30 minutes to acclimatize in the respective flow velocities. After acclimatization, water renewal was stopped and a predetermined amount of live rotifers was added to the flume, in order to create a target concentration of 2550 prey/L corresponding to carbon concentrations of 17 $\mu\text{mol/L}$. In total, three experimental runs were conducted for each flow regime, with different combination of fragments.

During the experimental trials, four water samples were taken from each aquaria with 10 ml glass pipettes approximately 30 seconds after placing the food, every 15 minutes for the next hour and every hour until completion of 5 hours. The number of rotifers in each pipette was counted using a stereomicroscope. The experiments were repeated by using the skeleton of coral fragments, in order to determine the effect of the flume and flow speed on rotifer concentration. This set of experiments were considered as the control (CTR) treatment. Due to the small polyp size and high density of polyps which complicates the determination of polyp number per fragment, dry weight was used to standardize the capture of each experimental run. In order to obtain dry weight estimates for each fragment, all fragments were dried at 70 °C for 72 hours and weighted with an analytical balance.

Experiments with *Dentomuricea aff. meteor* and *Viminella flagellum* Specimens of the two gorgonian species, *D. meteor* and *V. flagellum*, were collected as by-catch from local long-line fishing vessels during September-November 2018 and transferred to the aquaria in coolers. Colonies were fragmented in fragments of 8-10 cm height and kept in darkness in temperature 14 ± 0.9 °C, corresponding to the annual average temperature at the site of collection of the two species.

The experimental work was performed in flumes with an improved design, with capacity of 13L (Fig. 5) and equipped with 113 RPM motors (12V, Servocity) that can achieve higher flow rates than the initial tanks used for *A. wollastoni* (Fig. 4). Three flow regimes were tested: 3 cm/sec, 6 cm/sec, 9 cm/sec. Temperature was kept constant at 14°C. In each experimental run a fragment was randomly selected, positioned in one of the flumes and left for 15-20 minutes to acclimatize under the selected flow speed. After acclimatization and polyp opening, water renewal was stopped and a predetermined amount of live rotifers was added to the flume achieving a prey concentration of 1500 rotifer/L, corresponding to carbon concentrations of 10 $\mu\text{mol/L}$. Each experiment was repeated four times for each flow regime and each species.

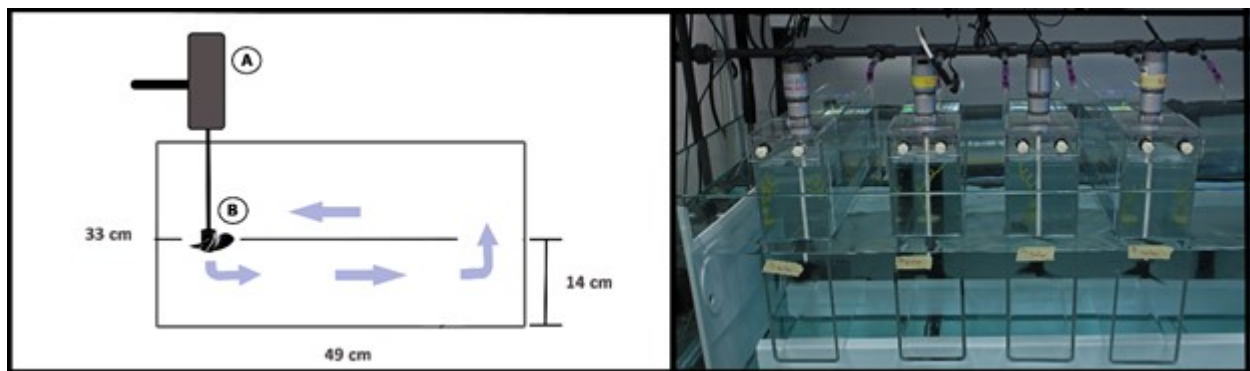


Figure 5: Experimental 13L flume used to study feeding rates of the two gorgonian species under different flow velocities. A: 113 RPM motor, B: 9 cm marine propeller. Arrows indicate flow direction.

At the end of the experimental part, all fragments were photographed from two opposite sides (angles of 0, 180°) and the software image J was used to count the total number of polyps in each fragment. Polyp number was used to standardize the capture of each experimental run.

Statistical analysis Statistical analysis focused on four main independent variables: prey concentration, standardized prey concentration corresponding to the prey available for each standardizing unit (dry weight or polyp), prey capture estimated as a percentage of the provided prey and standardized prey capture. For the case of *A. wollastoni*, only standardized variables were used to account for the high number of coral fragments within each flume. A preliminary statistical analysis was performed to assess the potential decrease of prey concentration due to the designs of the two experimental flumes, by focusing on the experimental runs without coral presence (CTR). This analysis was made by using Generalized Least Squares (GLS), in order to deal with the repeated measures that characterized the experiments. Subsequently, Linear Mixed Models (LMEs) were used to analyze the difference between CTR runs and experimental runs with coral presence (COR), in each flow velocity by examining the effect of Time and its quadratic on prey concentration. LMEs were also used to compare the decrease of standardized prey concentration among the flow velocities. Lastly, non-linear

regression (NLS model) with asymptotic exponential was used to facilitate the comparison of prey capture among the tested velocities.

Results and discussion

Anthipathela wollastoni Prey concentration remained stable throughout the experiment runs of the CTR treatment (Fig.6), which was also confirmed by the GLS models.

A significant decrease in prey concentration was observed in all experimental runs with coral fragments of *A. wollastoni*, under all flow velocities (Fig. 6). In flow velocities of 4 and 6 cm/sec, capture levels were so high so as to diminish prey concentration in values very close to zero and led to negative predicted values by the used models (Fig. 6). Estimated standard deviations between experimental runs of the same flow velocities were high, highlighting differences in capture rates between different coral fragments which can be attributed to coral and polyp position and individual coral behaviour. However, flow velocity had a significant effect on prey concentration with prey concentrations being significantly lower in runs with flow velocity of 4 cm/sec.

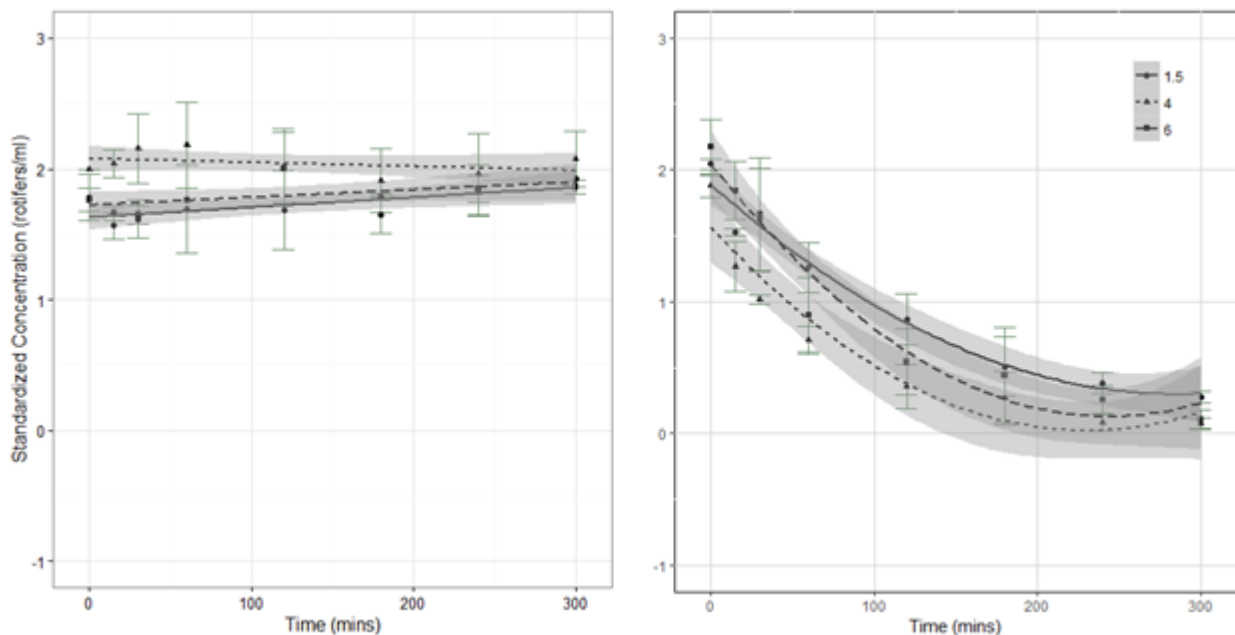


Figure 6: Standardized concentration as the concentration of available prey (rotifers/ml) per DW of tissue of *Anthipathela wollastoni* for the CTR treatment (A) and the coral treatment (B). Estimated means (points) with standard deviations, predicted means from LME models (lines) and 95% confidence intervals (shaded areas) are provided.

Analysis of cumulative prey capture highlighted the high capture capacity of *A. wollastoni*, in the three flow velocities, reaching final capture levels of $86.5 \pm 2.4\%$, $95.6 \pm 2.4\%$ and $95.2 \pm 3\%$ of the available prey quantities in flow velocities of 1.5, 4 and 6 cm/sec respectively (Fig. 7). These estimates

corroborate with the results of the NLS model. However, coral fragments displayed distinct capture rates between the three flow velocities in the first hours of the experimental runs where fragments under 4 cm/sec displayed the higher rate, followed by fragments under 6 cm/sec (Fig. 7).

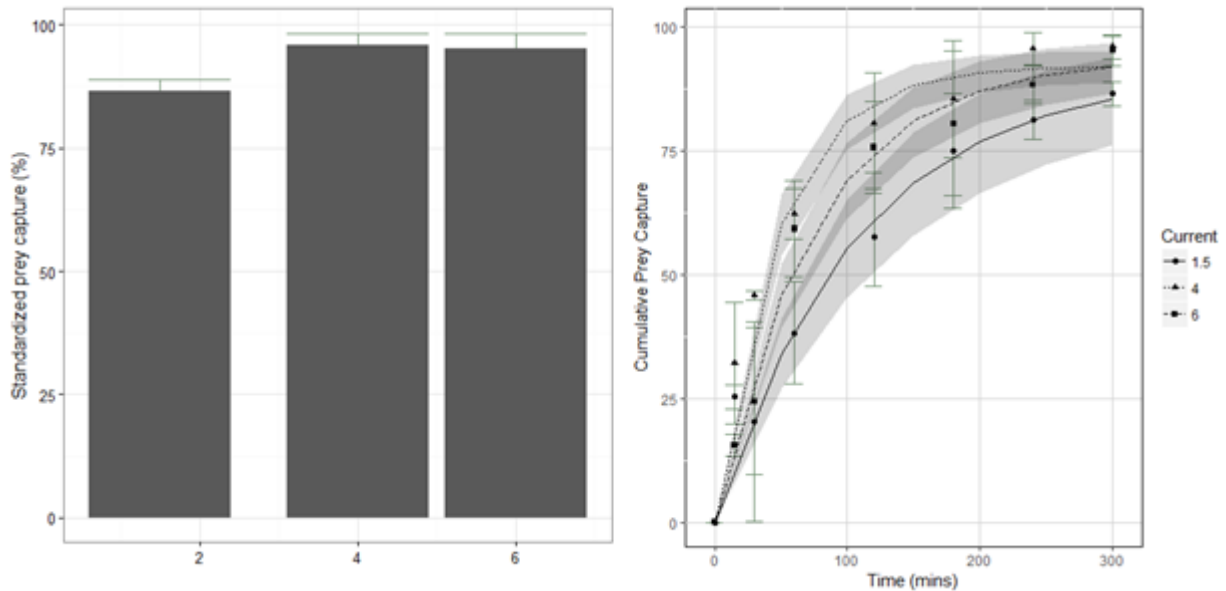


Figure 7: Final standardized prey capture of the species *Antipathella wollastoni* in the end (A) and cumulative prey capture during the course of the experiments including estimated means (points), predicted means from NLS models (lines) and 95% confidence intervals (shaded areas) (B) for three tested flow velocities (1.5, 4, 6 cm/sec).

These results suggest that *A. wollastoni* has the capacity to consume high amounts of prey once it becomes available and this capacity seems to be enhanced in intermediate flow velocities, especially if prey is not available for long time. This can happen during the short duration of tidal currents which are very common in the collection sites of this species. So far, it has been suggested that antipatharians require strong currents to feed (Tazioli et al. 2007; Wagner et al., 2012) and are thus typically found in areas with high accelerated currents such as crests of seamounts, pinnacles and knobs (Wagner et al., 2012). While there is a strong current effect in the collection sites of *A. wollastoni* of this study, the species reaches higher densities in locations protected from strong currents brought by spring tides (see material & methods), which might be a result of more efficient feeding under intermediate flow velocities.

Due to the high number of fragments within each flume, it is unclear whether the similar values of final prey capture among the three flow velocities is a result of the presence of several coral fragments within each flume which can consume high amounts of available prey until its concentration reaches very low values, or the consequence of satiation. Nevertheless, final consumption rates are very high and comparable to those of other suspension feeders (Table 1), suggesting that antipatharians might

play an important role in food webs and benthic-pelagic coupling in the coral gardens they form, as previously observed for coral gardens from other areas (e.g. Ribes et al. 1999; Rossi et al., 2004; Orejas et al., 2003).

Dentomuricea aff. meteor* and *Viminella flagellum Analysis of the collected data for the smaller flumes used for the experimental runs of the gorgonian species revealed a small decrease in prey concentration (<20%) in the CTR experimental runs under 3 cm/sec (Fig. 8). Although this was not highlighted as statistically significant by the GLS models, it might be a result of insufficient prey circulation or entrapment in the lower part of the flume. Further comparisons between COR and CTR runs in flow velocity of 3 cm/sec, revealed that there was no significant difference between the two treatments in none of the two species. In higher flow velocities, there was a significant difference between the CTR and COR runs for both species. This reflects the low capacity of the two gorgonians to capture prey under 3 cm/sec compared to higher flow velocities and can be a result of the low encounter rate with prey (Sebens et al., 1998). Alternatively, it might be due to the ability of prey to avoid coral tentacles under low flow rates (Gori et al., 2015). Due to these results and in order to avoid overestimation of captured prey under 3 cm/sec, this flow velocity was excluded from further analysis.

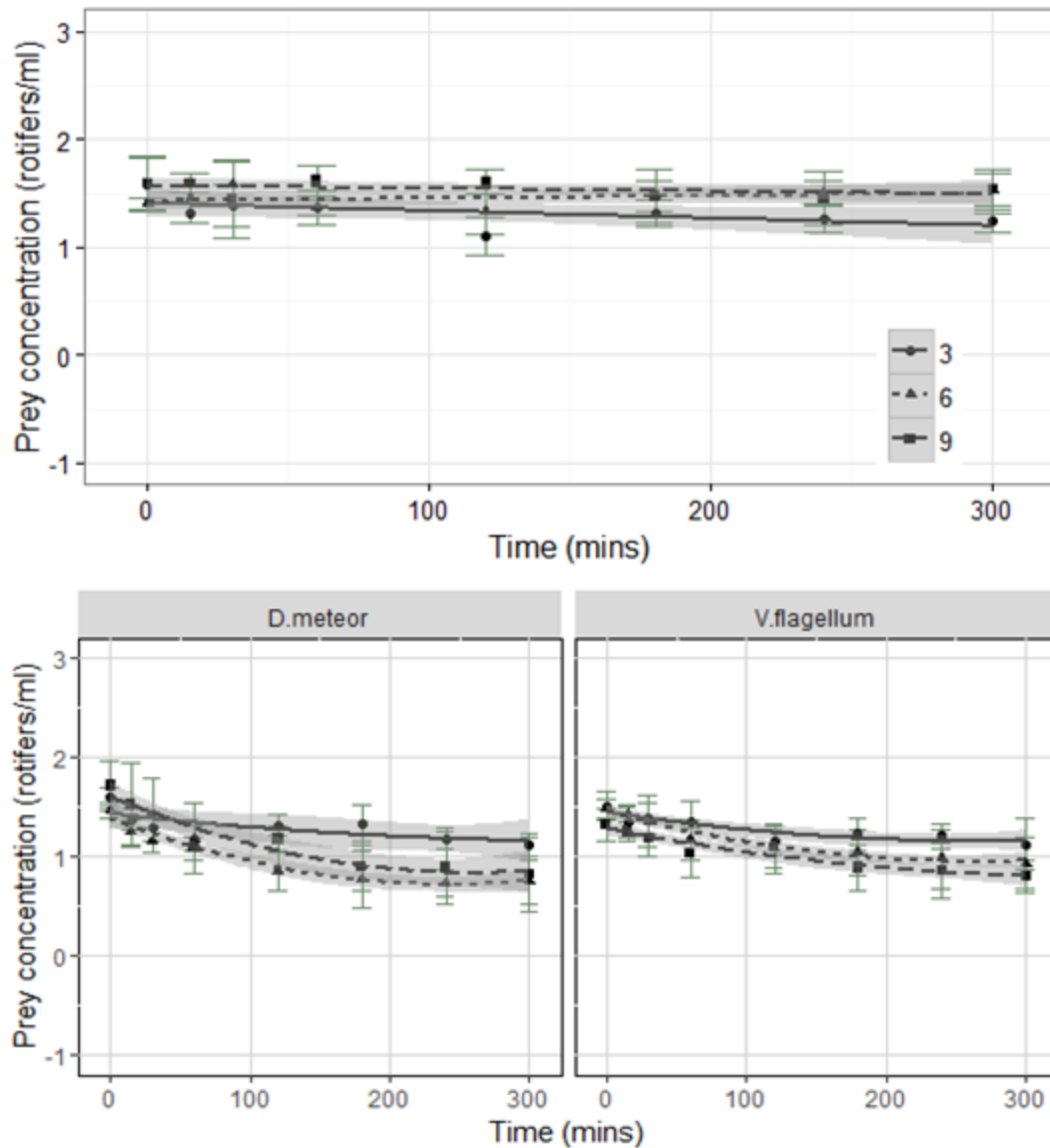


Figure 8: Prey concentration in experimental runs without coral (A) and with coral (B) of the species *Dentomuricea* aff. *meteor* and *Viminella* *flagellum* under three different flow velocities: 3, 6, 9 cm/sec. Estimated means (points) with standard deviations, predicted means from LME models (lines) and 95% confidence intervals (shaded areas) are provided.

Cumulative prey capture was not statistically different between the two remaining flow velocities in both species (Fig. 9). Overall, fragments of *D. meteor* captured higher amounts of prey (Fig. 9), reaching an optimum average capture of 52.47 ± 18 % under 9 cm/sec while *V. flagellum* reached an optimum of 39 ± 8.66 % under 6 cm/sec. Confidence intervals of the LME model in the case of *V. flagellum* were particularly large, suggesting highly variable results among different fragments which might be due to polyp number or polyp and fragment orientation.

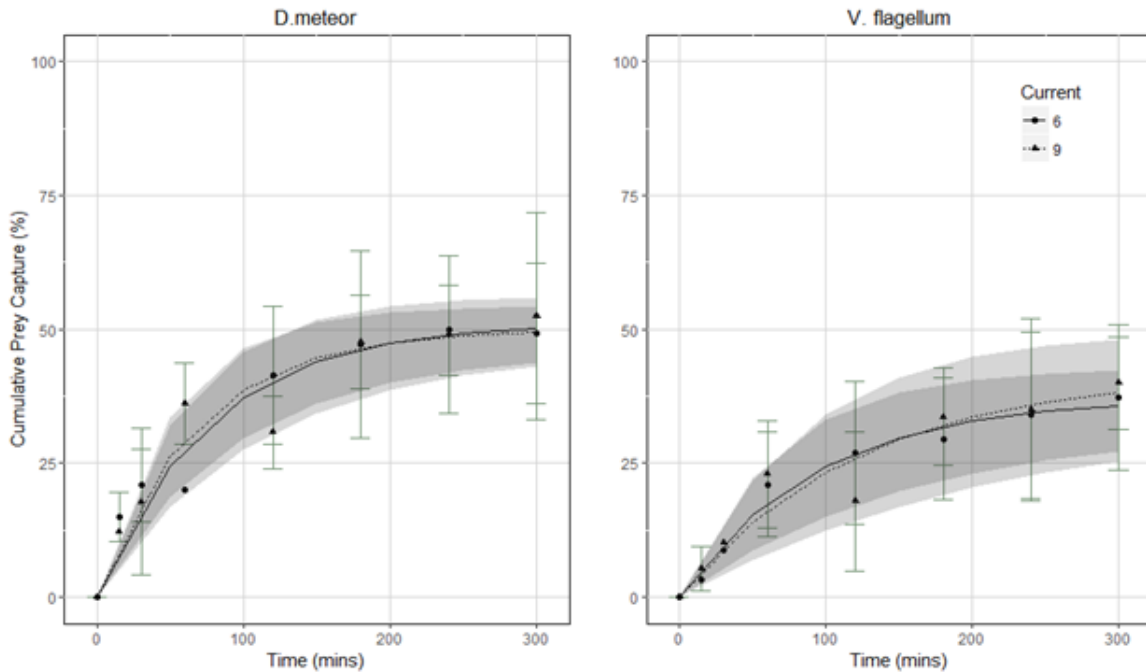


Figure 9. Cumulative prey capture of the species *Dentomuricea* aff. *meteor* and *Viminella flagellum* under two different flow velocities (6 cm/sec, 9cm/sec). Estimated means (points) with standard deviations, predicted means from LME models (lines) and 95% confidence intervals (shaded areas) are provided.

Estimation of standardized prey concentration also revealed high standard deviations for the two gorgonian species for both flow velocities (Fig. 10). Collectively, such high standard deviations are indicative of the highly variable polyp number and polyp density among the used coral fragments and highlights the difficulty in standardizing the data of capture efficiency experiments with gorgonian species in comparison to scleractinians where polyp number can be counted easier and taken into account in order to create similar conditions among experimental runs. Moreover, the available prey concentration per polyp turned out to be much higher for *V. flagellum*, owing to the low number of polyps per fragment comparatively to *D. meteor*. According to the LME models, in both species there was a significant difference in the intercept between the two flow velocities, however their slopes did not vary significantly, which corroborates with the results on cumulative prey consumption (Fig. 7) and highlights the ability of the two species to capture prey in intermediate flow velocities. Similar results have been reported by Chang-Feng & Ming-Chao (1993) who studied the capture efficiency of three tropical gorgonians and found that capture rates were higher at intermediate flow velocities and peaked at 8 cm/sec.

Based on the slopes of the LME models, *V. flagellum* had higher capture rates per polyp than *D. meteor*. This might be due to the bigger size of the polyps of *V. flagellum* and might reflect different feeding strategies by the two species due to their different shape. It is generally accepted that the shape of suspension feeders can affect their feeding capacity and growth (Warner, 1977; Wildish and

Kristmanson, 2005). *V. flagellum*, being a whip coral, can grow to great heights, increasing its polyp number and reaching higher in the water column where prey might be more available. However it has a limited capacity to increase surface and maximize polyp number in different directions. This might be compensated by the large size of its polyps, ensuring that polyps positioned in favourable sides of the colony, for instance in areas where common currents are unidirectional, can capture more prey. Comparatively, *D. meteor*, which is a fan-shape gorgonian, can increase its surface to different directions by expanding its branching pattern and can invest in a larger number of smaller polyps to catch prey. Estimated captured quantities of prey and carbon per polyp were high compared to those reported for cold-water gorgonians in the field (Table 1). However, while overall carbon concentration might be similar in the field, zooplankton concentration is expected to be much lower, explaining such differences. Moreover, as highlighted by Purser et al. (2010), captured prey in these experiments is not necessarily consumed by the polyps. Removed prey quantities in the two species are comparable to those reported in similar experiments with *L. pertusa*, a cold-water scleractinian species (Table 1). However estimated capture per polyp is much lower (Table 1) which is most likely due to the differences in polyp size between members of the two taxonomic orders, with scleractinians having much larger polyps.

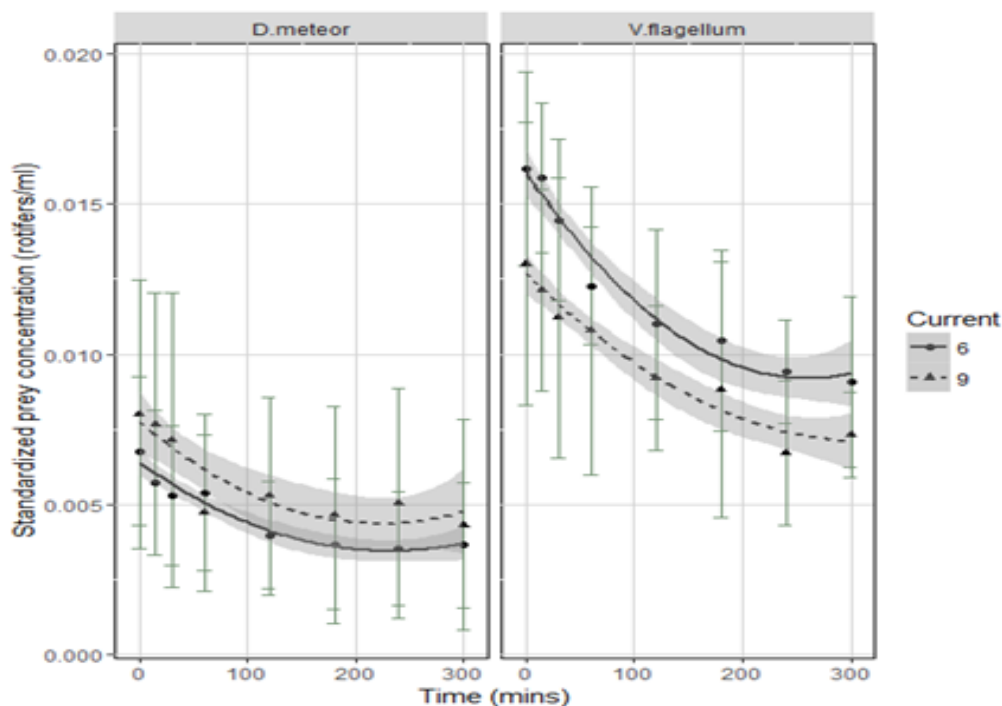


Figure 10. Standardized prey concentration (rotifers/ml available per polyp) for the species *Dentomuricea* aff. *meteor* and *Viminella flagellum* under flow velocities of 6 and 9 cm/sec. Estimated means (points) with standard deviations, predicted means from LME models (lines) and 95% confidence intervals (shaded areas) are provided.

Lophelia pertusa displayed higher capture capacity at lower flow velocities compared to the gorgonian and antipatharian species in this study (Table 1). Such species-specific effects enhance the hypothesis that flow regime can be a very important factor in describing species presence, density and success among different areas. Such knowledge can be crucial to predict species distribution not only under present but also under past and future conditions.

Table 1. Prey capture by some cold-water gorgonians, antipatharians and scleractinians, as reported in this study and in the literature.

	Current (cm/sec)	Prey	Prey concentration prey/L	prey polyp ⁻¹ h ⁻¹	µg C polyp ⁻¹ h ⁻¹	prey fragment ⁻¹	Carbon fragment ⁻¹
<i>A. wollastoni</i>	4	Rotifers		-	-	2376±151	192.46±12.25
<i>V. flagellum</i>	6	Rotifers	1500	17.44±0.84	1.41±0.07	1381.2±6.3	111.2±0.5
<i>D. meteor</i>	9	Rotifers	1500	9.58±2.67	0.77±0.22	1868.7±2.7	151.3±0.2
<i>Lophelia pertusa</i> (Purser et al. 2010)	2.5	Artemia nauplii	1030	73.3± 2	66.4±2	584.9±15.9	655±14.2
	5			20.2±9.5	17.9±10.7	161.20±75.8	143.9±84.9
<i>Lophelia pertusa</i> (Tsounis et al. 2010)	1	Artemia nauplii		283.73±130	462±212		
<i>Leptogorgia sarmentosa</i> (Rossi 2004)		Small zooplankton	natural	0.16±0.02	0.019±0.002		

3.1.2 Capture rate efficiency for scleractinian *Lophelia pertusa*, the bivalve *Acesta excavata* and the sponges *Geodia barretti*, *Stryphnus* sp. and *Phakellia ventilabrum* in Norway

Authors: Stephanie Liefmann, Tina Kutti, Sebastian Hennige, Sandra Maier, Marina Carreiro-Silva, Murray Roberts

Specimen collection Specimens of the sponges *Geodia barretti* and *Stryphnus* sp. were collected from Nakken reef (59°49'53 N, 5°33' 44 E DMS), and Langenuen Fjord (60.00 37° N, 5.19 14° E DMS), South-Western Norway in April 2017. Specimens were collected by the ROV Aglantha. The collected sponges were cut into pieces of ca. 5*5*5 cm to produce explants (small pieces of living tissue cultivated to have more manageable pieces of the massive sponges). *Geodia barretti* and *Stryphnus* sp. explants were cultivated in modified scallop cages at Uggdalsfjorden (60o02' 17N, 05o27' 43E DMS) at 150 m depth. Explants were collected in November 2017, were transported to the Institute of Marine Research (IMR) Austevoll research facilities and placed in 1000 l tank with a flow of 2000 l*h⁻¹. The 7 months 'recovery time' in the field is considered to be sufficient for complete cortex regeneration, re-development of aquiferous systems, for normal pumping and respiration rates to resume, and for representative symbiotic microbial communities to re-establish (Hoffmann et al., 2003, 2006; Kutti et al., 2015). Specimens of the CWC *L. pertusa* and the bivalve *Acesta excavata* were collected from the Nakken reef (59°49'53 N, 5°33' 44 E DMS) during the same cruise as *G. barretti* and *Stryphnus* sp. were collected. The 5 coral colonies and the 30 *A. excavata* individuals were collected using the Remotely Operated Vehicle (ROV) Aglantha from 150-200m depth. Specimens were placed in a 375 l tank until arrival to the Ins IMR Austevoll research station. At the research station the corals were placed in a 1000 l tank with water flowing at and 3000 l*h⁻¹. The bivalves were placed in the same tank as described *G. barretti* and *Stryphnus* sp.

The sponge *Phakellia ventilabrum* was collected from Korsfjorden. (60°9' 46.8N, 05°10.24E DMS) with a trawling net on January 2018 on RV Hans Brattström. The sponges were collected and kept on board on a flow-through system. Upon arrival to IMR Bergen facilities, the sponges were placed in a flow-through 37 l tank before transportation to the Austevoll research facilities where they were put in the same tank with the bivalves and other sponges. The water flowing through all the tanks was unfiltered Seawater from 160 m deep which provided enough food items for all organisms.

Prior to experiments, *L. pertusa* colonies were fragmented into nubbins of 10 polyps each, attached to putty epoxy bases and left to acclimate for 2 weeks. *P. ventilabrum* individuals were cut to 5*5 cm fragments and left to acclimate for 2 months.

Experimental design Each species was submitted to 6 different treatments resulting from the combination of 3 flow speeds and 2 food concentrations (Table 2).

Table 2: Summary of experimental treatments

Flow speed Food Concentration	Low Speed (LS) 18.51±0.63 l h ⁻¹	Medium Speed (MS) 38.75±1.45 l h ⁻¹	High Speed (HS) 60.3±1.82 l h ⁻¹
Natural Food (NF) Natural seston, present on unfiltered deep-sea water (160m deep)	LSNF	MSNF	HSNF
High Food (HF) Extra seston was gathered for 4 days with a 41 µm mesh net	LSHF	MSHF	HSHF

Experiments were conducted in flow-through chambers as described in Strohmeier et al. (2012), where chambers were designed to restrain water recirculation, helping prevent re-filtration. Chamber internal dimensions were: 10.5* 22 * 10 cm (w*l*h). Experiments were run in replicate batches: each batch consisted of 7 replicates of one treatment per species. Specimens were placed in the test chambers (Fig. 11), and one chamber was left with a coral skeleton as a control for particle deposition (the control chamber was left empty when the sponges were being tested). The flow was graduated to the desired value and measured before every experimental run for each chamber. The organisms were left to acclimate until filtering resumed which was verified by visible tentacles for *L. pertusa*, open oscula for the sponges, and open shell for *A. excavata*. For HF treatments (LSHF, MSHF and HSHF) seston was incorporated to the header tank with an IWAKI dosing pump. Water samples were simultaneously taken from the outflow of each chamber (7 with organisms and 1 control). Three subsamples of 10 ml were analysed with a PAMAS S4031 GO (Partikelmess- und Analysesysteme GmbH RUTESHEIM/ GERMANY) particle counter analyser (hereafter referred as PAMAS) with 16 channels. Each channel counted particles of one predetermined diameter from 1 to 16 µm. This range was chosen as preliminary results showed very little particle abundance above that size range. When performing the HF treatments the organisms were left to acclimate to the high food conditions for 2 h before taking the samples. Moreover, a fourth subsample of each seawater sample was transferred into 2 ml cryovials and fixed with 25% Glutaraldehyde (final concentration 0.5 %) to preserve the bacterial and algal populations and frozen at -80° until analysis by flow cytometry. Due to the limited

number of specimens numbers constraints, not all the species and treatments had the same amount of replicate batches and some of the specimens had to be re-used. (Table 3 and 4)

Table 3: Number of experimental batches per species per treatments. Each batch had 7 replicates and one control chamber. LS: low flow speed; MS: medium flow speed; HS: high flow speed; NF: natural food quantity; HF: high food quantity.

Species/ Treatment	<i>L.pertusa</i>	<i>A.excavata</i>	<i>G.barretti</i>	<i>Stryphnus.sp</i>	<i>P.ventilabrum</i>
LSNF	3	4	2	2	2
MSNF	2	4	2	2	2
HSNF	0	4	2	2	2
LSHF	2	1	1	1	1
MSHF	1	2	1	1	1
HSHF	0	1	1	1	1

Table 4: Number of available specimens and their distribution for the experimental batches.

Species	Available specimens	Distribution on the different treatments runs.
<i>L. pertusa</i>	56	Different fragments for each run and treatment
<i>A. excavate</i>	28	Rotated randomly between the runs and treatments
<i>G. barretti</i>	14	The 7 specimens used in the first NF treatments batch were re-used for the HF batches
<i>Stryphnus sp.</i>	14	The 7 specimens used in the first NF treatments batch were re-used for the HF batches
<i>P. ventilabrum</i>	7	The 7 specimens were used for all batches

Lophelia pertusa batches were run between March and April 2018, *A. excavata* batches were run in March April and end of May 2018, and *G.barretti*, *Stryphnus sp.* and *P. ventilabrum* batches were performed between the end of May and the beginning of June 2018. In order to better quantify the amount of POM and Suspended Particulate Matter (SPM) introduced to every batch, 10 l of water were collected from the control chamber and filtered through pre combusted, pre-weighed GF\F filters (WHATMAN). Each filter was rinsed twice with 15 ml ammonium formate to eliminate salts. Filters were subsequently dried for 24h at 60 °C, weighed and burnt for 4.5h at 450 °C and weighed again. Following experiments, Dry Weight (DW) and organic Carbon content of each organism from the different species was determined. *L. pertusa* fragments were individually crushed with a pestle and mortar and placed into pre-weighed tin trays. *Acesta excavata* individuals were scooped out of their shell put into pre-weighed trays *G. barretti* and *Stryphnus sp.* individuals were sliced into small pieces to speed up the drying process. *P. ventilabrum* individuals were placed into pre-weighed trays. All organisms were thereafter weighed in order to obtain wet weight, left to dry at 60°C until weight was stable (2 weeks for *L. pertusa*, 2 days for the sponges, and 3 days for *A. excavata*). The trays were then burnt for 4.5h at 450 °C and weighed again, which to estimate Ash Free Weight (AFW). To obtain organic Carbon content the AFW was subtracted from the DW. Organic content was then standardized to mol C g DW⁻¹.

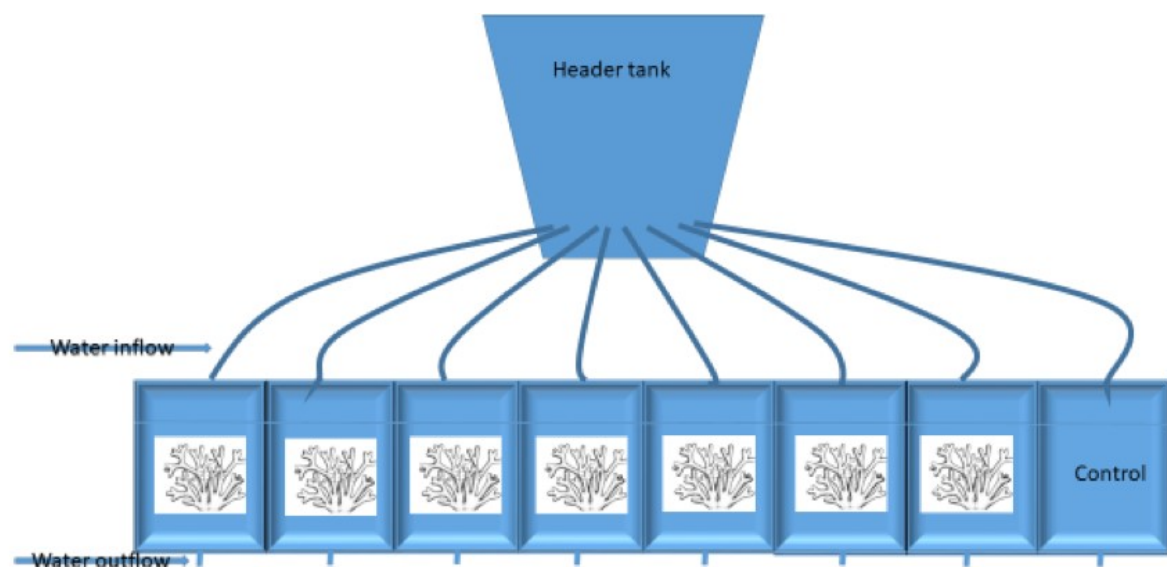


Figure 11: Schematic view of experimental chambers used in Norway

Data analysis: The mean particle counts ml⁻¹ obtained from the three sub samples analysed with the PAMAS were used to calculate size specific Retention Efficiency (RE), for each individual in every batch using the following equation (Cranford et al., 1992):

$$RE=1-(PC_C/PC_B) \quad (1)$$

Where PCC is particle count exiting the control chamber (outflow) and PCB is particle count exiting the experimental chamber (inflow). Multiplying equation 1 by 100 provides estimates of the percentage of particles retained by the organisms. The Clearance Rate (CR) was also calculated for each particle size, for each individual in every batch using the following equation:

$$CR=RE * F \quad (2)$$

Where RE is the previously calculated retention efficiency and F is the flow ($l h^{-1}$) measured for each chamber before each run.

The subsamples placed in the cryovials were analysed with BD LSR FORTRESSA flow cytometer (BD Biosciences New Jersey USA) at the school of biological sciences, Institute of Immunology & Infection Research Flow Cytometry Core Facility, University of Edinburgh. The analyses were performed to account for bacterial and algal cells numbers. Aliquots of 200 μl of each subsample were placed in 96 flat bottom well plates (one sample per well). Each sample was stained with SYBR green (Invitrogen, California USA), final concentration 0.02%. The dye attaches to DNA, making cell fluoresce green, algal and bacterial cells are differentiated because of chlorophyll fluorescence. The filled well plates were put in the auto sampler one by one. The acquisition rate of the auto sampler was 3 $\mu l * sec^{-1}$, total acquired volume per sample was 150 μl . The FITC channel and the PerCP-Cy5-5-A in the flow cytometer were used to detect SYBR-green and Chlorophyll fluorescence respectively. Forward Scatter, (FSC) is used as an estimate for particle size. In order to get a particle size, latex beads of known sizes were analysed through and a regression curve was used to convert the mean FSC values to sizes. The number of SYBR green positive particles (particles containing DNA) were determined by gates. Gates are assigned to distinguish particles of interest in this case defined as particles which fluoresce green and red.

Gating was FSC vs FITC-H to identify negative control profile, the DNA contribution can be determined by a shift in emission intensity. Appropriate gates are applied to the samples to detected DNA content and chlorophyll fluorescence (PerCP-Cy5-5 channel) to discriminate between bacteria and algae. The particles that did not contain DNA were considered silt. For each sample, the flow cytometer provided the total number of particles between 0.3 and 4 μm which was divided into total number of silt, bacterial and algal particles per 150 μl . Using these numbers the RE and CR were calculated using equations 1 and 2 for bacteria, algae, and silt. Calculated CRs were normalized to $mol C^{-1}(CRN)$ (for both results coming from the PAMAS and the flow cytometer).

The results obtained for CRN of particles of 1µm and bigger than 10µm were discarded. Particles of 1 µm around the error zone of the PAMAS S4031 GO instrument. Particles above 10 µm were on a concentration lower than 10 particles ml⁻¹ which is also the detection limit of the instrument. Negative CRN were also excluded from the final analyses since the negative values meant that the analysed samples contained more particles than the control chambers which could be due to particle production/release by the tested organisms.

Statistical analysis Data was analysed using R Studio 1.1.456 version statistical software (RStudio team, 2016) For each specie and treatment, a linear model was used, where the dependent variable was the CRN: average and the independent variable particle size, measured as a categorical variable with n=9 levels: 2 to 10 µm. Due to the high skewedness of the CRN a logarithmic transformation of this variable was done to have a more approximated normal distributed variable. To compare all the multiple factors for each species a Post-hoc tukey adjustments for pairwise comparisons the lsmeans R package (Lenth, 2016) was used.

The log-linear model can be written as:

$$\log(\text{CRN}) = \beta_0 + \beta_1 \text{ParticleS}(3 \mu\text{m}) + \beta_2 \text{ParticleS}(4 \mu\text{m}) + \dots + \beta_8 \text{ParticleS}(10 \mu\text{m}) + \varepsilon \quad (1)$$

A model with independent variables of particle size and treatment with interactions as:

$$\log(\text{CRN.average}) = \beta_0 + \beta_1 \text{ParticleS}(3 \mu\text{m}) + \beta_2 \text{ParticleS}(4 \mu\text{m}) + \dots + \beta_8 \text{ParticleS}(10 \mu\text{m}) + \alpha_9 \text{TreatmentMSNF} + \alpha_{10} \text{TreatmentHSNF} + \dots + \alpha_{13} \text{TreatmentHSHF} + \alpha_{14} \text{ParticleS}(3 \mu\text{m}) \text{TreatmentMSNF} + \dots + \varepsilon$$

Results and discussion

PAMAS Due to natural seston variability the presented results are highly variable. The amount of carbon given to each species is presented in Table 5 in each food treatment, this measurement does not account for OC contained in particles smaller than 0.7 µm. Particle amount decreased with particle size for all treatments (Figure 12). Particle amount differences between NF and HF treatments for each species was statistically significant (p-value < 0.0001) highlighting the success in replicating the two treatments.

High variability was observed among species in the estimated CR for each particle (Table 6). Cases of negative CR were interpreted as particle release from the organisms or attributed to the high variability of the natural seston. Results for each species are presented below.

Table 5: Mean initial organic carbon (OC L⁻¹) given to the organisms per species and food treatment NF: Normal Food, HF: High Food. All values are given as average± SD

	<i>A. excavata</i>	<i>L. pertusa</i>	<i>G. barretti</i> (OC.L ⁻¹)	<i>Stryphnus sp.</i>	<i>P. ventilabrum</i>
NF	0.0004±0.0002	0.0003±0.00021	0.0004±0.0002	0.0003±0.0001	0.0003±0.00009
HF	0.0013±0.0003	0.0006±0.0007	0.0003±0.00007	0.0004±0.00006	0.0004±0.00001

Table 6: Percentage of positive CRN per species and per treatment. LSNF: low speed Normal Food; MSNF: Medium Speed Normal Food; HSNF High Speed Normal Food; LSHF Low Speed High Food; MSHF: Medium Speed High Food; HSHF: High Speed High Food

	<i>A. excavata</i>	<i>L. pertusa</i>	<i>G. barretti</i>	<i>Stryphnus .sp.</i>	<i>P. ventilabrum</i>
LSNF	83.73	92.06	55.55	31.56	46.03
MSNF	76.59	46.03	50	46.03	52.38
HSNF	75	NA	47.62	41.28	26.98
LSHF	34.92	60.32	23.81	25.4	34.92
MSHF	75.40	46.03	25.40	25.40	44.44
HSHF	61.90	NA	11.11	12.70	25.40

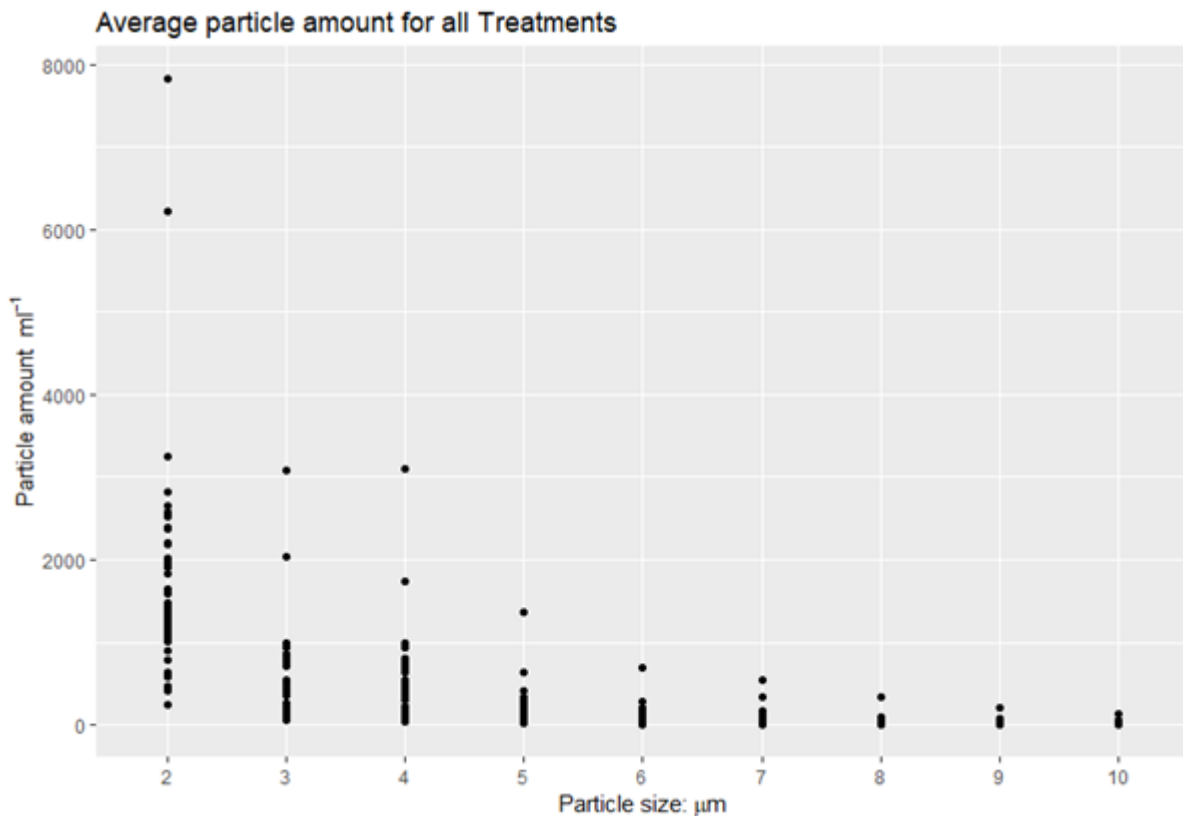


Figure 12: Number of food particles (particles ml⁻¹) for each particle size for all treatments together.

Acesta excavata This species had a higher CR in NF treatments than in HF treatments (143 ± 52 and 78 ± 45 l h⁻¹ mol C, respectively, Figure 13). No interactions were found between CR and flow speed in either the HF and NF treatments, although in HF treatments CR values appeared to be lower at lower speeds (LSHF treatment for all size class particles, Figure 2x). In the treatment HSNF, lower CRN values were observed for particles smaller than 5 μm and the difference was confirmed by the Tukey test which showed that CR values for 2 μm particles were significantly lower than the CR values for particle sizes 6,7,8,9 and 10 μm (p-values:0.00297, 0.0124,0.0019,0.0001). For the treatment MSNF the CR values particles of 2 μm were significantly lower than 10 μm (p-value:0.0437).

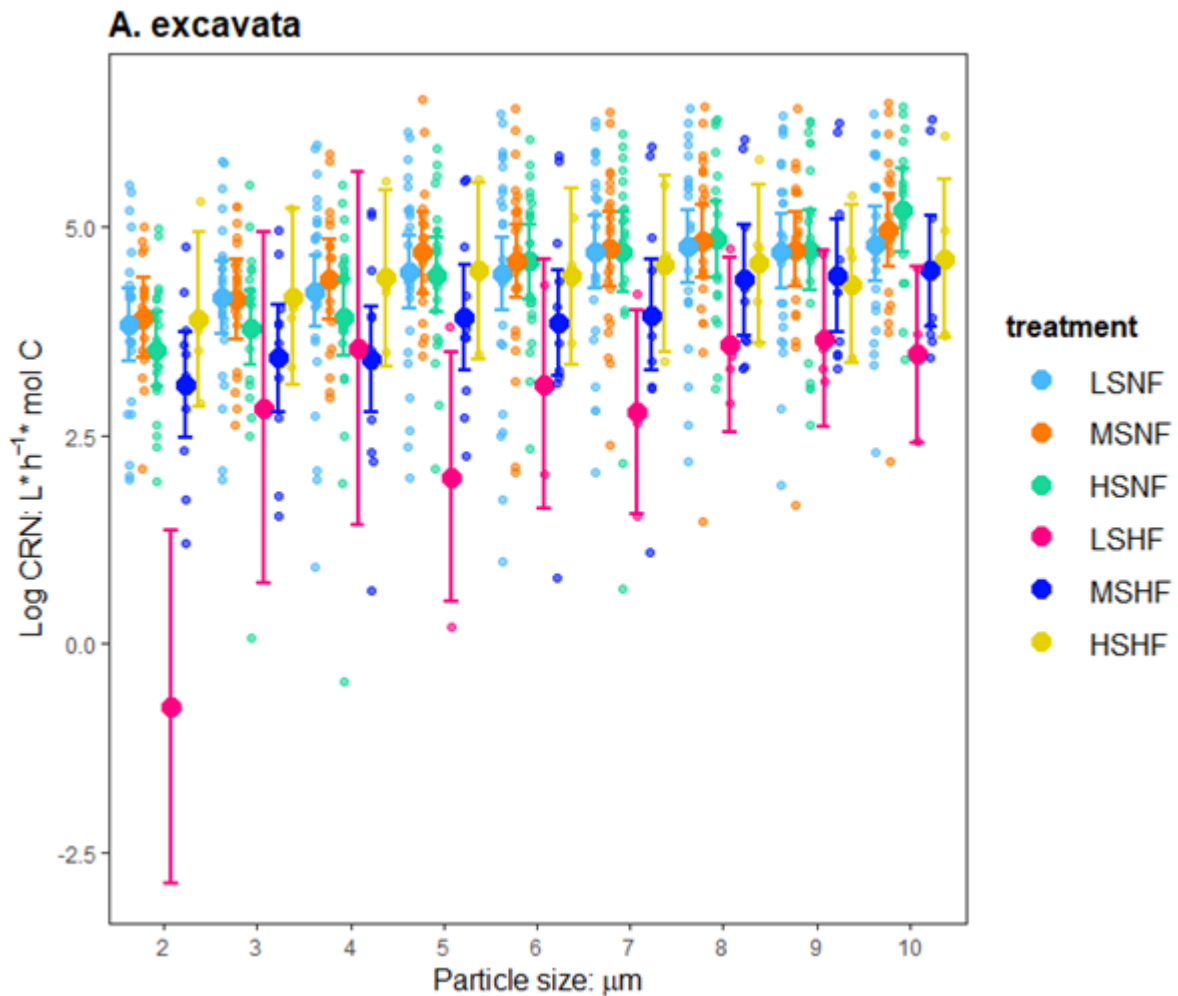


Figure 13: Log-normalized clearance rate (CRN) for *Aesta excavata* for each particle sizes (2-10 μm) and the six experimental treatments. Each colour represents a treatment in each particle size class. The middle of each bar represents the median and the end of the bars the 2 quartiles. The small dots of the same colours represent the amount of positive results. LSNF: low speed Normal Food; MSNF: Medium Speed Normal Food; HSNF High Speed Normal Food; LSHF Low Speed High Food; MSHF: Medium Speed High Food; HSHF: High Speed High Food

Lophelia pertusa CRN seemed to be higher in the NF compared to the HF treatments (118 ± 42 , and 91 ± 50 $l \cdot h^{-1} \cdot \text{mol C}$, respectively, Figure 14). However, the CRN calculated for particles between 8 and 10 μm was higher for LSHF. No interactions were found between food concentration treatments and different flow conditions. In treatment LSNF the estimated CRN for the 2 μm particle was statistically lower from the particle sizes: 5,6,7,8 9, 10 μm , ($0.0001 < p < 0.0056$). In the MSNF treatment, the CRN for particle 2 μm was statistically lower than for particles of 4, 6, 7, 8,9, 10 μm , ($0.0001 < p\text{-values} < 0.0387$) in all other treatments, highlighting that under natural food conditions lower clearance rate was observed for very small particles.

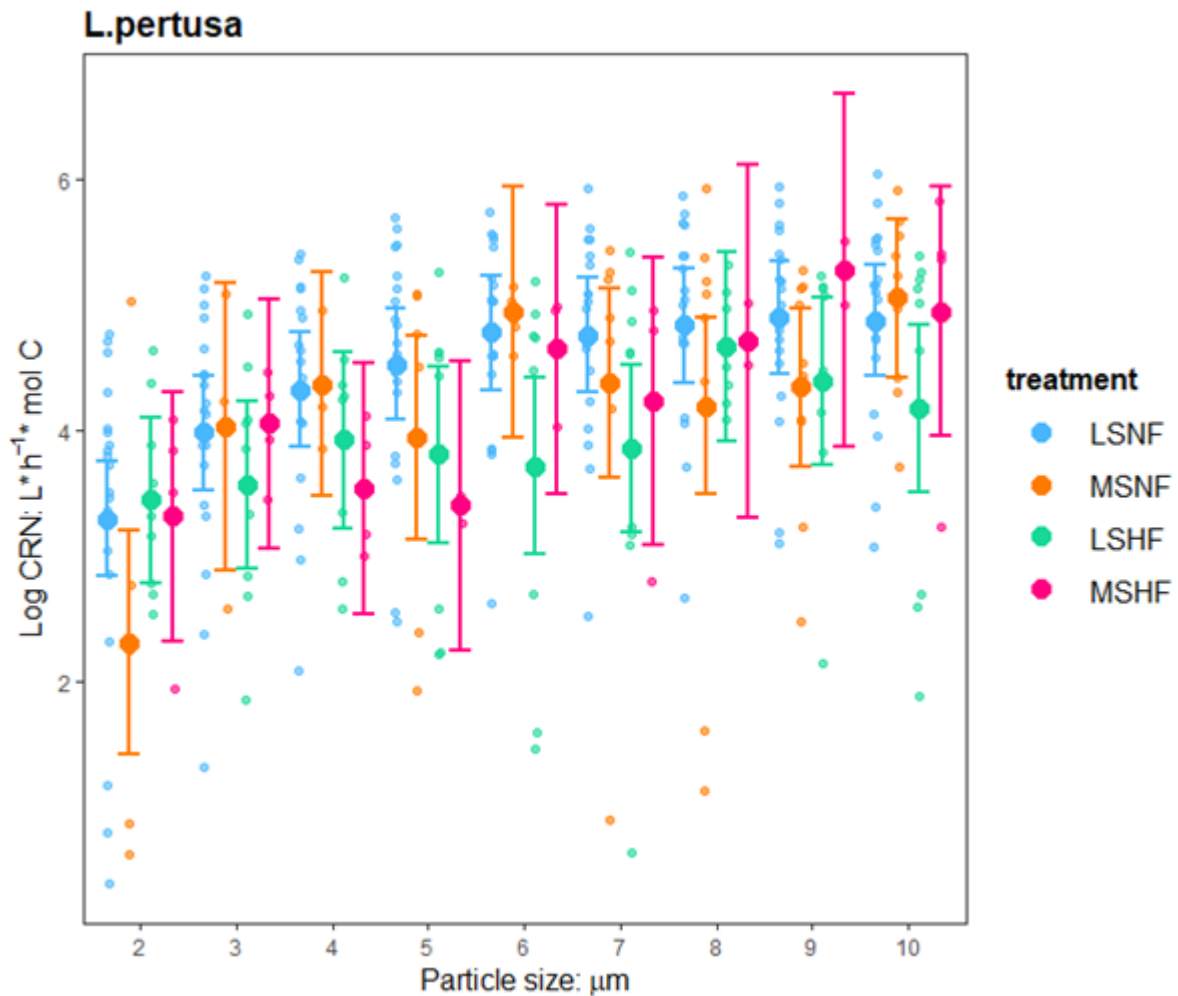


Figure 14: Log-normalized clearance rate (CRN) for *Lophelia pertusa* for each particle sizes (2-10 µm) and the six experimental treatments. Each colour represents a treatment in each particle size class. The middle of each bar represents the median and the end of the bars the 2 quartiles. The small dots of the same colours represent the amount of positive results LSNF: low speed Normal Food; MSNF: Medium Speed Normal food; LSHF Low Speed High Food; MSHF: Medium Speed High Food.

Geodia barretti The calculated CRN suggests that *G. barretti* has a higher CR at MSHF, although this results rely on less than 3 data points for each calculated CRN, hence they are not very representative. The same issue was encountered with the LSHF and HSHF treatments. The CRN values for the HSNF treatments were the highest ($11 \pm 6 \text{ l h}^{-1} \text{ *mol C}^{-1}$). Overall CRN values for NF and HF treatments were 7 ± 5 and $5 \pm 4 \text{ l h}^{-1} \text{ *mol C}$, respectively. No interaction between flow speed and CR was found (Figure 15). In treatment LSNF the CR for particle of 3 µm was statistically different to the CR for 9 µm particles (p-values: 0.0181). In treatment MSNF the CR for the 2µm particle was statistically different to the CR for: 8,9,10 µm particles, ($0.001 < \text{p-values} < 0.0459$).

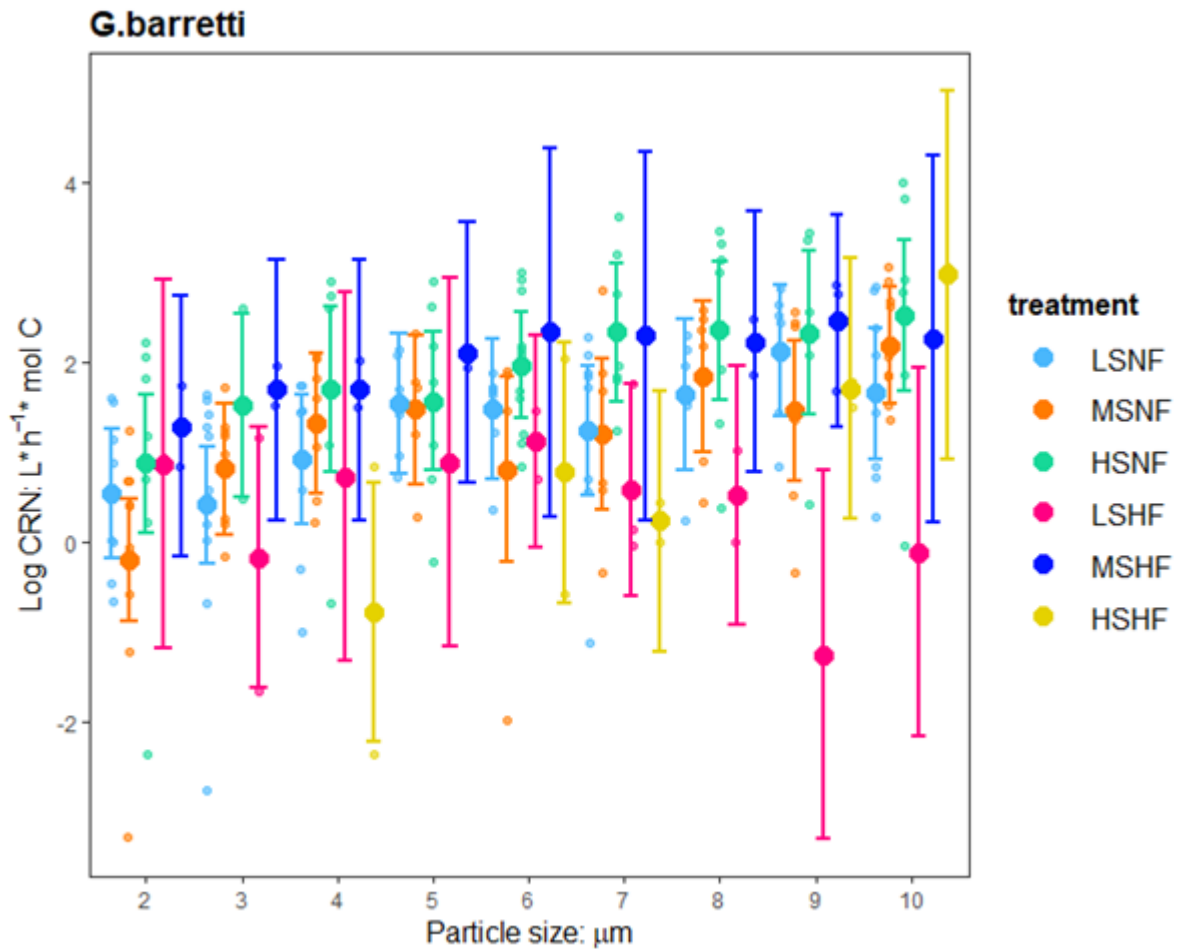


Figure 15: Log-normalized clearance rate (CRN) for *Geodia barretti* for each particle sizes (2-10 μm) and the six experimental treatments. Each colour represents a treatment in each particle size class. The middle of each bar represents the median and the end of the bars the 2 quartiles. The small dots of the same colours represent the amount of positive results. LSNF: low speed Normal Food; MSNF: Medium Speed Normal Food; HSNF High Speed Normal Food; LSHF Low Speed High Food; MSHF: Medium Speed High Food; HSHF: High Speed High Food

Stryphnus sp. For all the particles sizes and treatments *Stryphnus sp.* had the lowest CRN of all the tested species. The results calculated for HF treatments rely on less than 3 positive events per particle size, hence the results are not representative. The CRN values for all the particles sizes were higher for the HSNF treatment except for CR for the 6 μm particle (Figure 16).

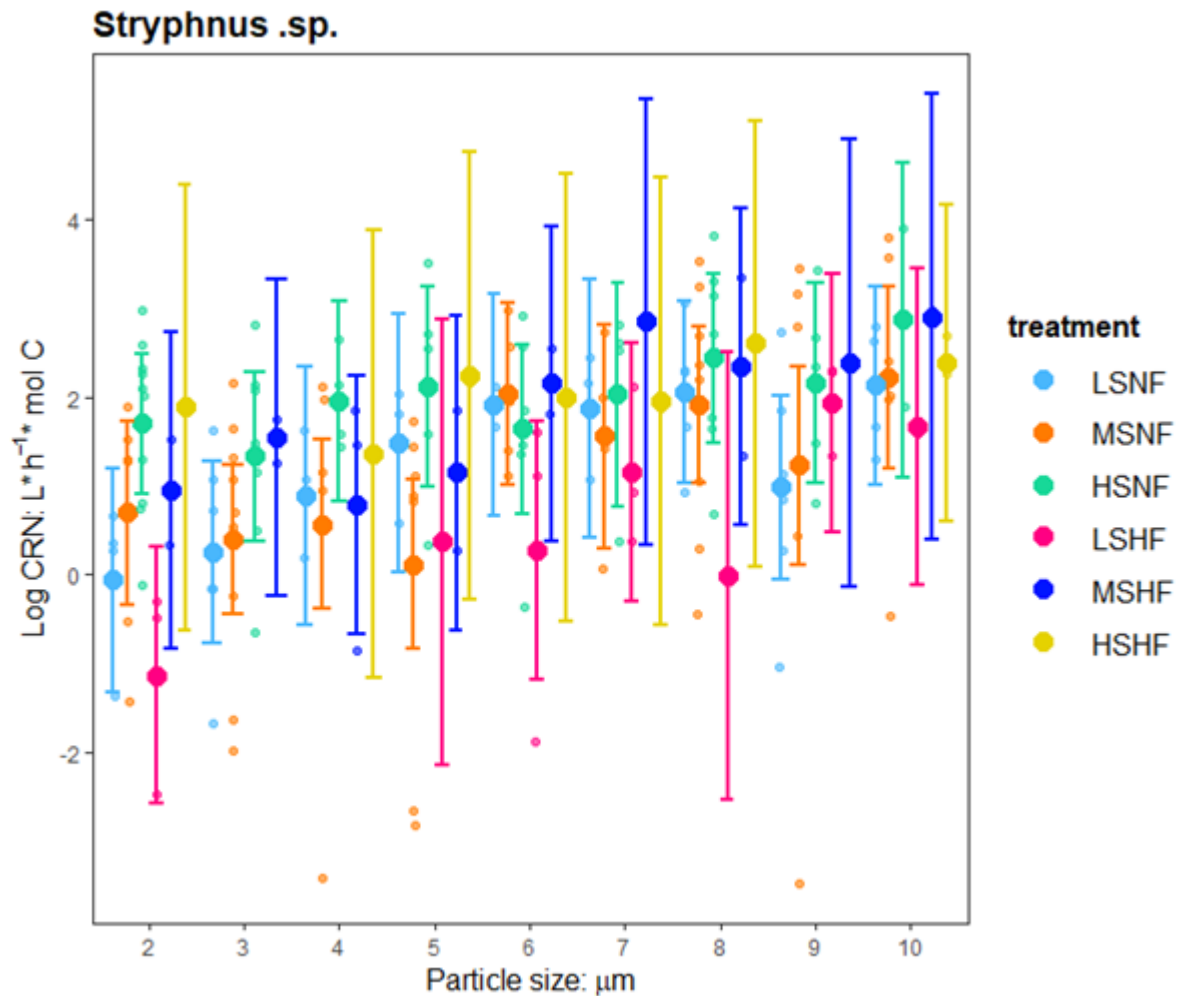


Figure 16: Log-transformed normalized clearance rate (CRN) for *Stryphnus* sp. for each particle sizes (2-10 µm) and the six experimental treatments. Each colour represents a treatment in each particle size class. The middle of each bar represents the median and the end of the bars the 2 quartiles. The small dots of the same colours represent the amount of positive results. LSNF: low speed Normal Food; MSNF: Medium Speed Normal Food; HSNF High Speed Normal Food; LSHF Low Speed High Food; MSHF: Medium Speed High Food; HSHF: High Speed High Food

Phakellia ventilabrum Clearance rates were highest for MSNF, HSNF and MSHF (Figure 17). The CRN values for the treatment HSNF and particles sizes 4, 8 and 10 µm is not representative since it is just based on one data point. In treatment HSNF the CR for the 2 and 9µm particle was statistically different, (p-value: 0.0258).

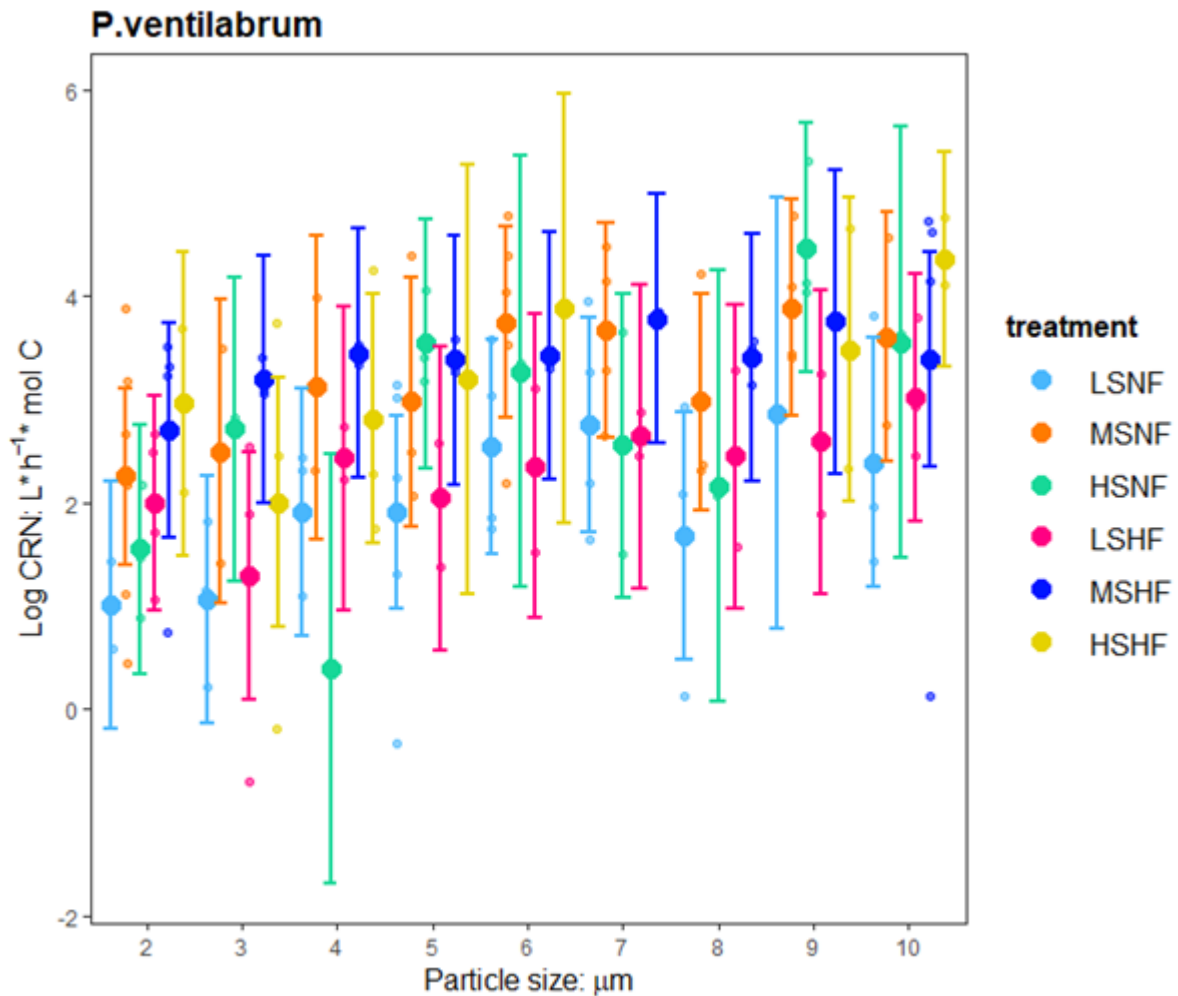


Figure 17: Log- normalized clearance rate (CRN) for *Geodia barretti* for each particle sizes (2-10 µm) and the six experimental treatments. Each colour represents a treatment in each particle size class. The middle of each bar represents the median and the end of the bars the 2 quartiles. The small dots of the same colours represent the amount of positive results. LSNF: low speed Normal Food; MSNF: Medium Speed Normal Food; HSNF High Speed Normal Food; LSHF Low Speed High Food; MSHF: Medium Speed High Food; HSHF: High Speed High Food

Flow cytometry The amount of the different particle types in HF and NF treatments was for the majority statistically significant see (Table 7). Algae had a mean size of $4.39 \pm 0.8 \mu\text{m}$, bacteria had a mean size of $0.52 \pm 0.2 \mu\text{m}$. The particles categorized as silt ranged from 8 to $0.3 \mu\text{m}$ and comprised all the particles that did not have DNA or had chlorophyll fluorescence. Percentage of positive CR can be seen in Table 8.

Table 7: Results of the t test comparing the amount of particle types in Low Food (LF) and High Food (HF) treatments

		<i>A. excavata</i>	<i>L. pertusa</i>	<i>G. barretti</i>	<i>Stryphnus sp.</i>	<i>P. ventilabrum</i>
LSNF LSHF	Silt	0.02	0.0001	0.1	0.9	0.01
	Bacteria	0.06	0.0001	0.0001	0.001	0.001
	Algae	0.001	0.0001	0.0001	0.04	0.45
MSNF MSHF	Silt	0.3	0.0001	0.65	0.0001	0.01
	Bacteria	0.0001	0.0001	0.0001	0.0001	0.16
	Algae	0.0001	0.0001	0.0001	0.0002	0.0001
HSNF HSHF	Silt	0.01		0.85	0.01	0.003
	Bacteria	0.3		0.0001	0.0001	0.45
	Algae	0.0001		0.0001	0.0001	0.0001

Table 8: Percentage of positive CRN per species and per treatment. LSNF: low speed Normal Food; MSNF: Medium Speed Normal Food; HSNF High Speed Normal Food; LSHF Low Speed High Food; MSHF: Medium Speed High Food; HSHF: High Speed High Food

	<i>A. excavata</i>	<i>L.pertusa</i>	<i>G.barretti</i>	<i>Stryphnus .sp.</i>	<i>P.ventilabrum</i>
LSNF	66	22	71	80	57
MSNF	41.	67	73	76	85
HSNF	75	NA	79	76	69
LSHF	32	66	71	89	100
MSHF	64	17	52	42	68
HSHF	53	NA	68	71	80

Acesta excavata Average CR was overall higher in the NF treatment 116 ± 54 vs 66 ± 40 $\text{h}^{-1} \cdot \text{mol C}^{-1}$. For all particle types was higher in HSNF treatment 174 ± 161 $\text{CR l}^{-1} \cdot \text{mol C}^{-1}$ (Figure 18). Average CRN are higher for silt particles (100 ± 67 $\text{h}^{-1} \cdot \text{mol C}^{-1}$) except for the LSHF treatment were just one data point was recorded.

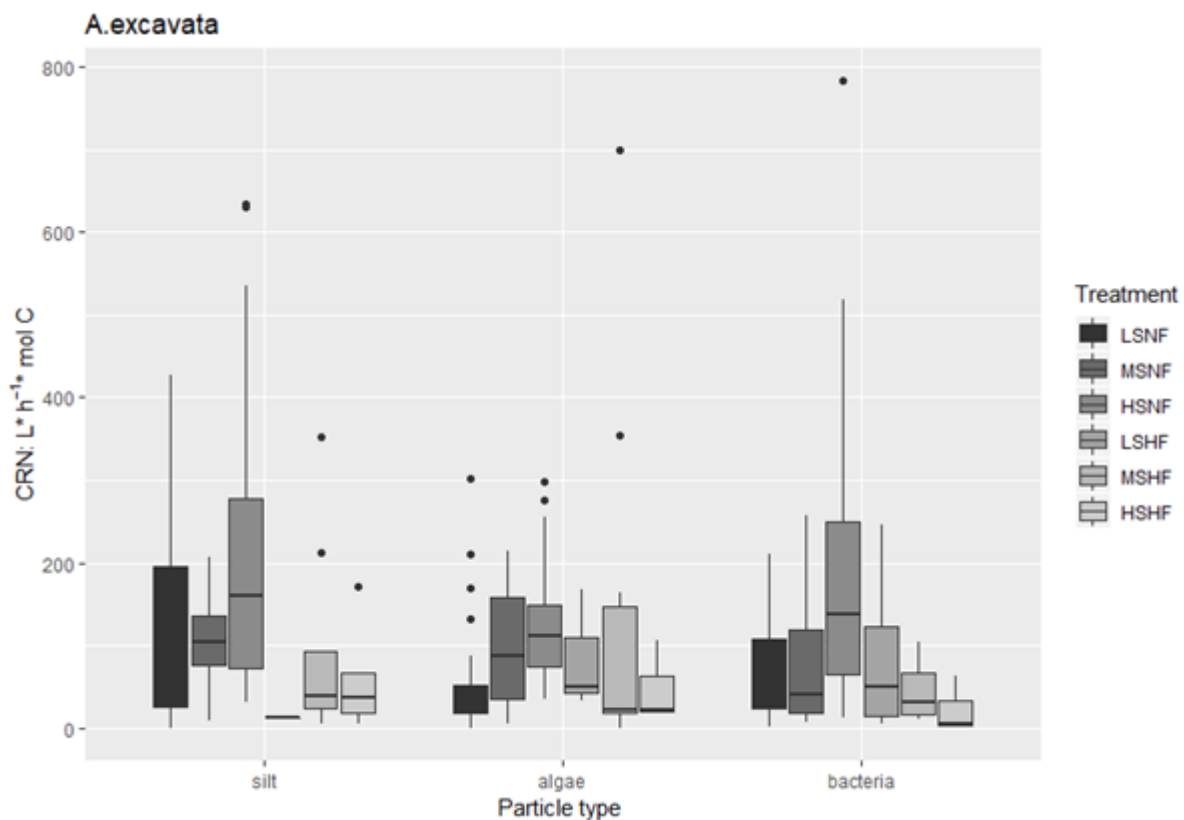


Figure 18: Box plot showing the average CR for each particle type and each treatment.

Lophelia pertusa Average CR are 86 ± 91 and 54 ± 23 $\text{h}^{-1} \cdot \text{mol C}$ respectively. Though the lowest average CR were for LSNF treatment for all particle types 25 ± 10 $\text{h}^{-1} \cdot \text{mol C}$ and they were highest for MSNF 147 ± 98 $\text{h}^{-1} \cdot \text{mol C}$ (Figure 19). In the MSNF treatments the CR for bacteria is significantly higher than for algae, (p-value: 0.00329). The CR for bacteria in MSNF is statistically significantly higher than in treatment LSNF (p-value: 0.0019).

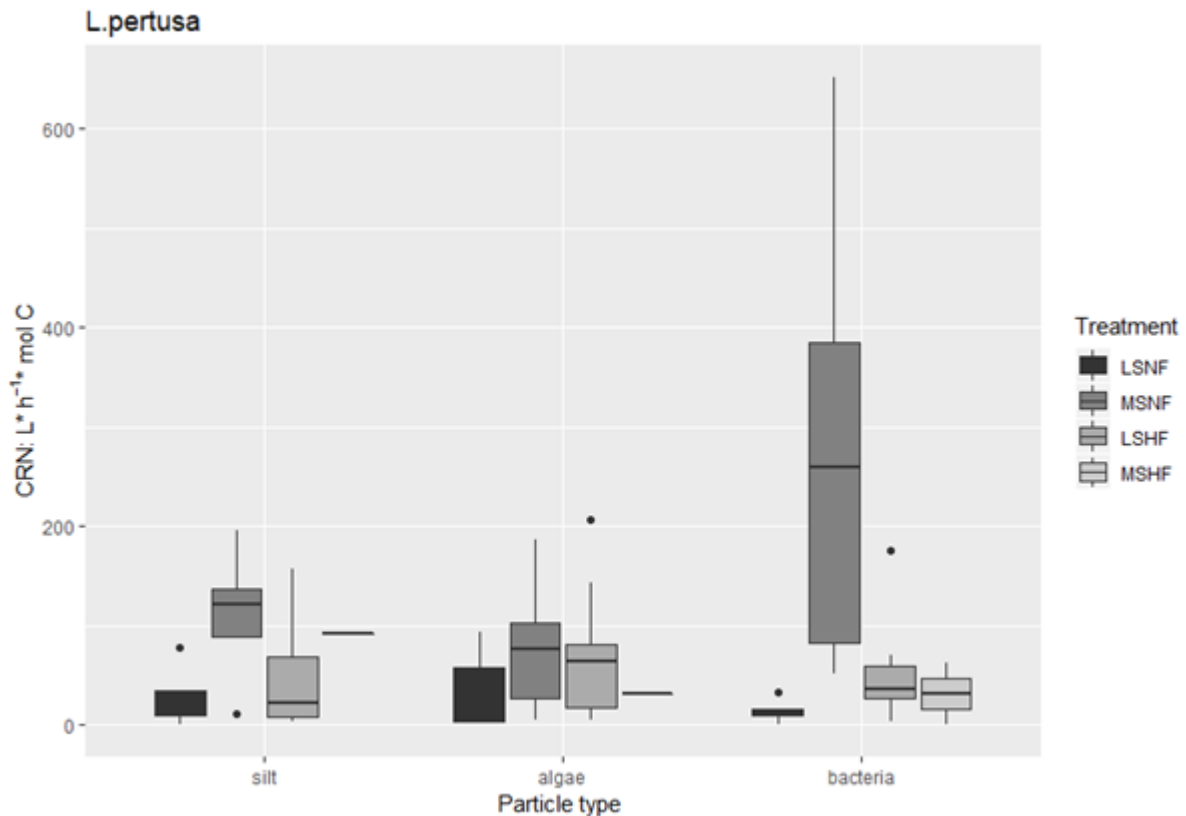


Figure 19: Box plot showing the average CR for each particle type and each treatment.

Geodia barretti Average CR are 26 ± 19 and 15 ± 14 l h⁻¹ * mol C. For all particle types, CR were higher in MSNF with an average of 40 ± 21 l h⁻¹ * mol C (Figure 20). In LSNF the CR for algal particles was significantly higher than for silt, (p-value: 0.0369). For MSNF, CR for bacterial particles was significantly higher than for silt, (p-value: 0.011). In HSNF CR for algal particles was significantly higher than for silt, (p-value: 0.0146). For LSHF treatment the CR for bacterial particles was significantly higher than for silt and algae, (p-values: 0.0004 and 0.0073). The CR for algal particles in HSNF and MSNF was significantly higher than in LSNF, (p-values: 0.004 and 0.04), also the CR for algal particles was significantly higher in MSNF compared to LSHF, (p-value: 0.001). *Geodia barretti* had a CR for silt particles significantly higher in HSNF than in LSNF, (p-value 0.02). The CR for bacteria was significantly higher under MSNF compared to LSNF (p-value: 0.00025), and it was also significantly higher in MSHF than LSNF, (p-value: 0.024).

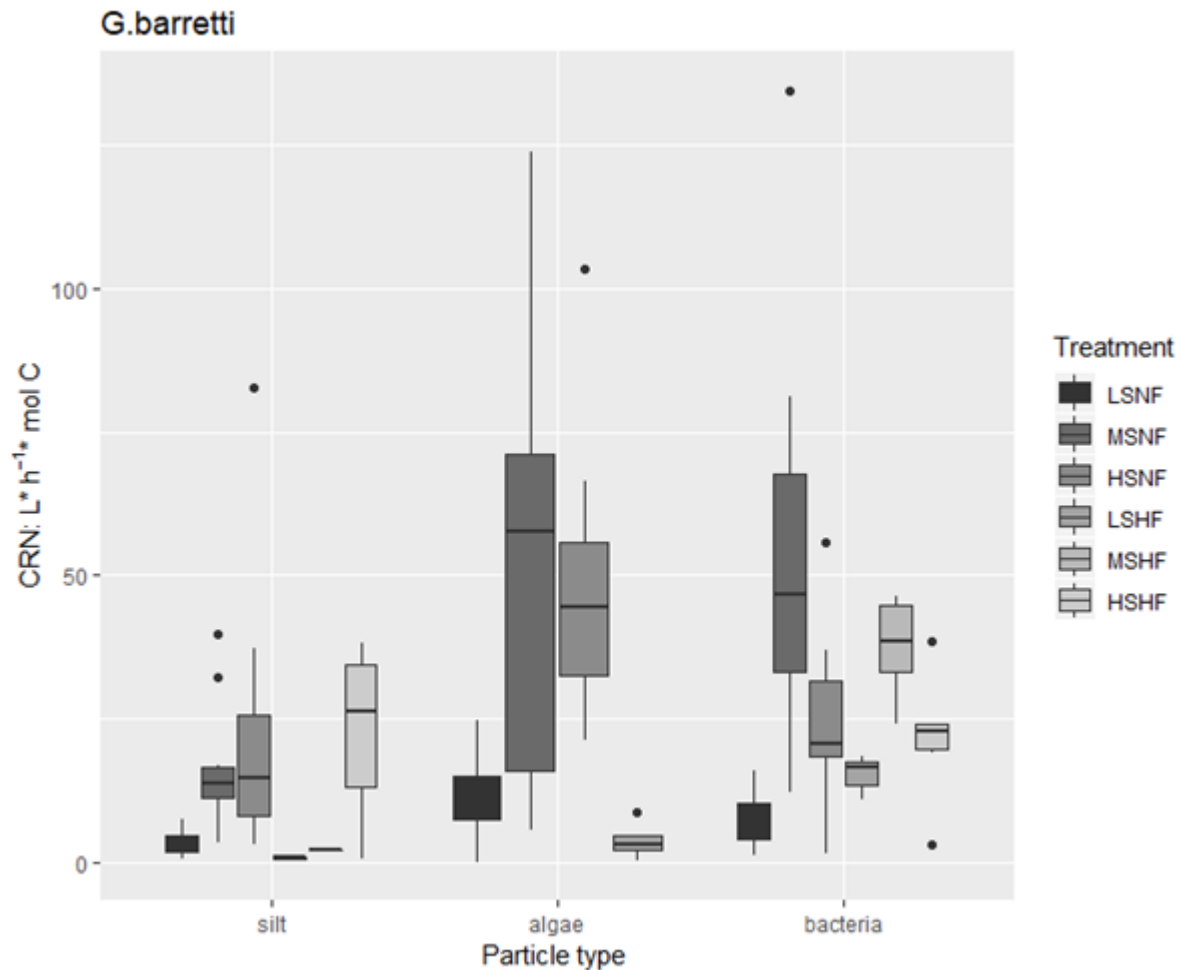


Figure 20: Box plot showing the average CR for each particle type and each treatment.

Stryphnus sp. Mean CR were 18 ± 11 and 8 ± 4 $h^{-1} \cdot \text{mol C}$. The HSNF treatment presented the highest CR for all particles types 29 ± 19 $h^{-1} \cdot \text{mol C}$. In LSHF CR for algae was higher than for bacteria, (p -value:0.0049). For bacteria, the CR in HSNF was significantly higher than in LSHF and MSNF, (p -values: .0.00001 and 0.009) for the same particle type, the CR was significantly higher in HSHF than LSHF, (p -value:0.048).

Phakellia ventilabrum Mean CR were 172 ± 135 and 71 ± 29 $h^{-1} \cdot \text{mol C}$. For all particle types. CR was highest in MSNF 296 ± 71 $h^{-1} \cdot \text{mol C}$ (Figure 21). For MSHF treatment the CR for algae was significantly lower than for silt and bacteria, (p -values: 0.014 and 0.0004). The CR for algae was higher at HSHF than in MSHF, (p -value: 0.016). For silt the CR was statistically higher in MSNF than in MSHF treatments, (p -value: 0.02). *Phakellia ventilabrum* presented a significantly higher CR for bacterial particles under MSNF compared to LSNF, (p -value: 0.013).

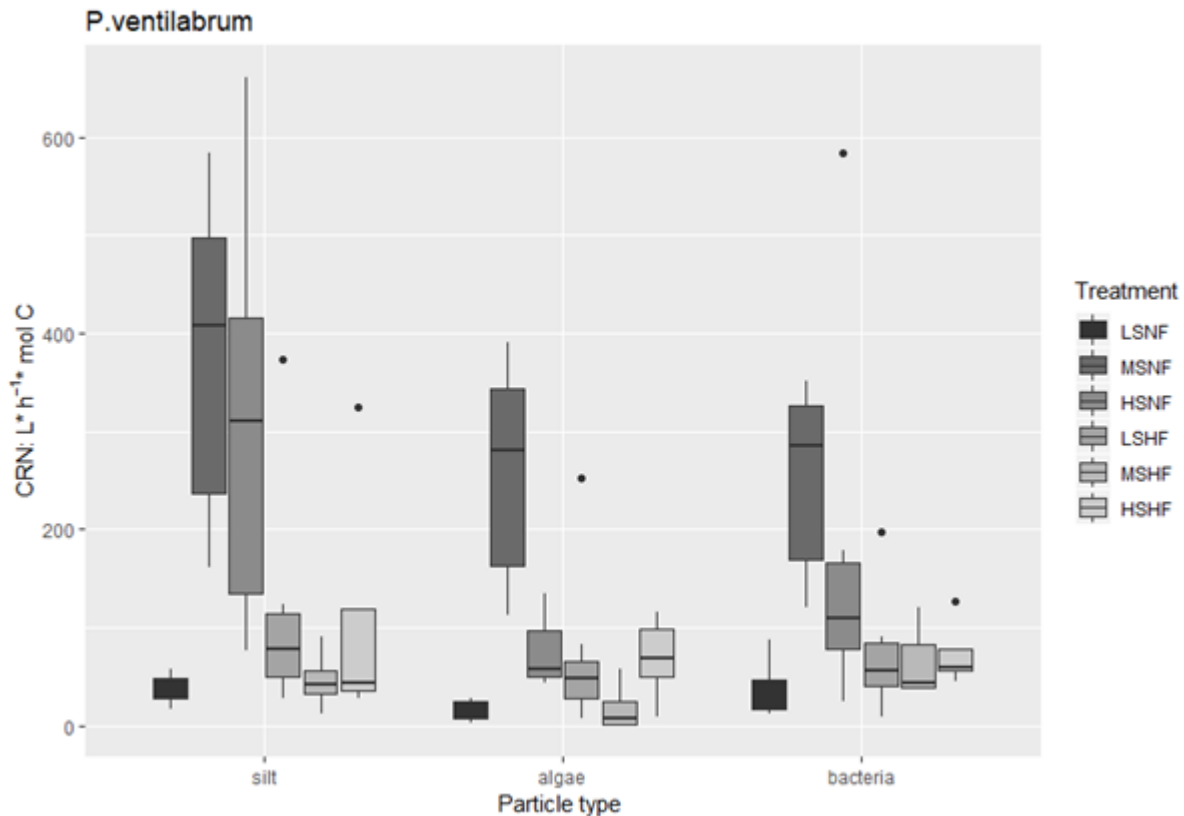


Figure 21: Box plot showing the average CR for each particle type and each treatment.

The PAMAS results revealed increasing CR with increasing particle size for all the species, this trend has to be taken with caution because of the decreasing amount of particles with their size (Figure 12) and variability in particle concentration when using natural water and seston in a flow through system. Hence it is difficult to assess a specifically preference for any given particle size and species, but the particle sizes tested are on the recorded natural spectrum for all the tested species (Järnegren & Altin, 2006; Witte et al., 1997; Mueller et al., 2014).

For all species, HF treatments had an overall lower CR, which suggest that organisms can get stressed or are sensitive to high particle concentration. This phenomenon has been already reported for bivalves (Cahalan et al., 1989) and can be the case of the tested bivalve species *A. excavata*. This argument can be further reinforced by the fact that consistently, for all the species, a lower percentage of positive results were found in HF treatments. The fact that negative results were found suggests that the organisms were releasing particles, pseudo-faeces in the case of *A. excavate*. In the case of sponges, particle release can be explained by cell shedding, sponges have been found to have a high cell turnover (Alexander et al., 2014; de Goeij et al., 2009). In all treatments *L. pertusa* and *A. excavata* (Figures 13, 14) had the highest CR for all treatments without properly characterizing the particles it is very difficult to affirm if they compete and if their competition is exploitative. *L. pertusa* has been

characterized as an opportunistic feeder (Maier et al., 2019; Mueller et al., 2014; van Oevelen et al., 2016), deep-sea bivalves are known to be adapted to low food availabilities and have specific adaptations to food types (Oliver, 1979). Hence if food resources are affected because of global change as predicted (Levin et al., 2015; Sweetman et al., 2017) *L. pertusa* could possibly outcompete *A. excavata*, but is also worth noting that very little information is available on the feeding ecology of *A. excavata* besides its high filtration rate 13 l h^{-1} recorded by Järnegren & Altin, (2006). The results found in this study for *A. excavata* are lower than those calculated in Järnegren & Altin, (2006) which can be due to methodological differences such as the usage of natural seston, and flow through systems. Comparing the obtained CR results for *L. pertusa* in this study is not as straight forward since previous studies quantify its efficiency as capture rate per polyp. The CR for the sponges were lower than for *A. excavata* and *L. pertusa*. Overall *P. ventilabrum* had a higher CR than *G. barretti* and *Stryphnus sp.* (Figure 15, 16, 17). It is difficult to assess if the sponges compete for the same food resources. *Geodia barretti* and *Stryphnus sp* being High Microbial Abundance (HMA) sponges (Schhöttner et al. 2013) are structurally different from *P. ventilabrum* which is a Low Microbial Abundance (LMA) (Schhöttner et al. 2013). This difference can explain the higher CR for *P. ventilabrum*, HMA sponges are recorded to have lower pumping rates compared to LMA sponges (Maldonado et al., 2012; Weisz et al 2008). HMA sponges have also been hypothesized to further complement their diet with their own symbionts and DOM (de Goeij et al., 2008, Leys et al., 2018, Yahel et al., 2007). Sponges are also documented to feed on DOM (Maldonado et al., 2012) the consumed DOM can be converted to detrital POM a process that has been characterized and named the sponge loop (de Goeij et al., 2008; 2009; 2013 Rix et al., 2016). Transformation of DOM into POM can explain how the different studied species are able to co-exist. The POM detritus produced by sponges using DOM from coral mucus has already been observed to be utilized by other detritivores in tropical reefs (Rix et al., 2018).

The results calculated after the Flow cytometry analyses are not going to be directly compared with the results from the PAMAS because they are inherently to very different forms of characterizing particles and counting them. The samples used for this analysis were preserved and frozen.

The results for *A. excavata* and *L. pertusa* suggest that they are opportunistic feeders which is in accordance with the available literature for the former (Mueller et al., 2014). The fact that *A. excavata* feeds on bacteria (Figure 18) suggest that this species is more versatile than previously thought. *Lophelia pertusa* filters more bacteria in HS treatments (Figure 19) is in accordance with previous studies (Orejas et al., (2016) where at higher speeds *L. pertusa* has a higher efficiency capturing small particles. The amount of positive results for *L. pertusa* in LSNF treatments was lower for the results

calculated from flow cytometry data that for PAMAS, this can possibly be explained because of sample degradation. The trend amongst the sponges is the same as in the PAMAS results, CR was overall higher for *P. ventilabrum* than for the other two species (Figures 15-17), again this can be explained by the different morphologies and live strategies, HMA vs LMA as mentioned above (Weisz et al., 2008). Results suggest that *Stryphnus sp.* and *G. barretti* has a preference for algal and bacterial particles evidencing perhaps a more selective feeding strategy in HMA sponges, tropical sponges have been found to have low functional redundancy and to differentiate between different types of bacteria as a food source (Perea-Blázquez et al., 2013). Other studies have also pointed out that sponges can discriminate between particles of similar sizes (Leys, 2006; Maldonado et al., 2010; Yahel, 2006, 2007) hence the sponges are not necessarily in direct competition. Better characterization of the natural seston can be key to better elucidate competition. Characterizing and quantifying the DOM can also give valuable information since sponges are known to feed on it (Maldonado et al., 2012) and one laboratory record suggest that *L. pertusa* can also incorporate carbon from DOM (Mueller et al., 2014). Further investigation of the sponge loop in CWC reefs might elucidate even further C and N processing in the deep-sea, and might explain the niche overlap found between *L. pertusa* and *H. coriacea* found by van Oevelen et al, (2018).

3.1.3 Food preference and assimilation rates of habitat-forming cold-water corals in the Azores

Authors: Maria Rakka, Sandra Maier, Meri Bilan, Antonio Godinho, Dick van Oevelen, Sebastian Hennige, Covadonga Orejas, Marina Carreiro-Silva

Aims and objectives: The objectives of these experiments were (1) to determine the ability of selected habitat forming CWC species to feed on different food substrates such as algae, zooplankton and Dissolved Organic Carbon (DOC); (2) estimate the incorporation of carbon and nitrogen under ingestion of different food sources and (3) assess the metabolic activity of the studied species after ingestion of different food sources.

Materials and Methods

Colonies of the species *A. wollastoni*, *V. flagellum* and *D. meteor* were collected in October 2017 and maintained in aquaria, as described in 2.1.1.1.

Four food treatments were selected, based on the provided food substrate: phytoplankton, zooplankton, DOC and unfed (starved). The diatom *Chaetoceros calcitrans* was chosen as

phytoplankton substrate, since diatoms of the genus *Chaetoceros* are known as basic components of the spring bloom in the area (Santos, 2013). The rotifer *B. plicatilis* (diameter: 80-120 μm) was used as zooplankton substrate. Microzooplankton has been reported to be a main component of the diet of gorgonian species in the Mediterranean (Ribes et al., 2003) and in the Antarctica (Orejas et al. 2003), making rotifers a possible prey for the small polyp size of the two studied species. Lastly, DOC was chosen due to the wide ability of cnidarian species to utilize DOC as food source (Naumann et al., 2011). The phytoplankton and zooplankton substrates were prepared by keeping live cultures under the presence of tracer ^{13}C and ^{15}N . The microalgae *C. calcitrans* and *N. gaditana* were cultured in 2-L Erlenmeyer flasks using artificial seawater and an F/2 culture medium containing 50 % ^{15}N -sodium nitrate (NaNO_3 , Cambridge Isotopes) and 100% ^{13}C -bicarbonate (NaHCO_4 , Cambridge Isotopes) for three weeks. Labelled cultures of the rotifer species were obtained by inoculating starter cultures in filtered seawater (1 μm) under continuous presence of labelled *N. nanochloropsis*, cultured as described above, for 6 days. An algae derived product of dissolved amino-acids (Cambridge Isotopes, U ^{13}C 97–99 %, U ^{15}N 97–99 %, CNLM-452-0.5) was used as DOC source. Labelled cultures were prepared so as to reach the desired concentrations on the day of delivery and were harvested a few hours before provision. Cultures of the species *C. calcitrans* were harvested by light filtering with membrane filters (0.2 μm), rinsed with filtered SW and resuspended in artificial seawater. Rotifer cultures were harvested by filtering (nylon, 40 μm), rinsed and resuspended in artificial seawater. Preliminary analysis was performed to ensure that harvesting did not cause significant decrease in cell concentration. Subsamples of known concentration of labelled cultures of *C. calcitrans* and *B. plicatilis* were harvested, freeze-dried and analyzed for carbon and nitrogen content by elemental analysis. Mean dry weight and carbon content per cell were calculated and used to standardize the amount of carbon provided between the two live food sources and among flumes. During the experiments, cell concentration was used as a proxy of the provided carbon quantity.

Experiments were conducted in 33L flumes described in 2.1.1.1 (Figure 4). A power analysis was used to determine the optimum number of flumes and fragments to be used in each treatment, considering the low number of available flumes. In order to maximize power, multiple fragments were placed in each experimental flume. One fragment from each colony was assigned to each treatment, resulting to three flumes per treatment containing five fragments each for the species *A. wollastoni* and *D. meteor* and four flumes per treatment containing three fragment each for the species *V. flagellum*. Due to logistical constraints experiments on different treatments did not take place simultaneously: three flumes from one treatment were combined with one flume from the starved treatment, leading to three consecutive experimental runs for *A. wollastoni* and *D. meteor*, and four for *V. flagellum*.

Fragments were randomly assigned to the experimental flumes and were left to acclimatize for 6 hours before the start of each experimental run. After the acclimatization period, a flow rate of 4cm/sec was established and left for an hour before pausing water renewal and providing a predetermined amount of carbon to each experimental flume. Flow was kept constant for a total of 12 hours to allow for feeding, a period referred to as food incubation. Upon completion of the food incubation, flow was stopped, flumes were cleaned by siphoning and fragments were left to rest for 12 hours under slight water circulation. Food incubations were repeated five times for *A. wollastoni* and six times for the two gorgonian species. Immediately after the end of the last food incubation, oxygen consumption and excretion measurements took place. Six fragments from each treatment were selected and placed in 450 ml glass respiration chambers filled with filtered (0.2 µm) natural seawater. In each incubation, six chambers were occupied by corals and two were left empty serving as control chambers. All chambers contained glass-coated magnetic stirrers and were placed in a single water bath maintaining temperature at 19 ±0.6 for *A. wollastoni* and 14±0.7 for *D. meteor* and *V. flagellum*. Incubations took place in the dark and lasted for four hours for *A. wollastoni* and 15 hours for *D. meteor* and *V. flagellum*. Oxygen concentration measurements were taken at the beginning and end of each incubation from seven out of the eight chambers, while the chamber containing the largest fragment was continuously connected to an O₂ electrode to allow for continuous monitoring of oxygen saturation. During the respiration incubations, oxygen saturation was never lower than 80 %.

Upon completion of the experimental runs all fragments were freeze-dried and kept at -80 °C until further processing. Fragments of *D. meteor* and *V. flagellum* were dissected to separate the tissue from the skeleton but this procedure was not followed for *A. wollastoni* due to the presence of very dense spines, characteristic of the antipatharian skeleton, that do not allow this separation. Subsequently, tissue was grinded by using mortar and pestle. A subsample of ground material was analyzed for isotopic ratio and C/N content using an elemental analyzer (Thermo Electron Flash 1112) coupled to an isotope ratio mass spectrometer (EA-IRMS, DELTA-V, THERMO Electron Corporation). A second subsample was acidified stepwise with drops of HCl to remove completely the inorganic C fraction, and all remaining material was analyzed on the EA-IRMS for isotopic ratio and organic C content. Calculation of tracer incorporation was performed as described in Maier et al., (2018). Tissue carbon and nitrogen content of each fragment was standardized to dry weight, including tissue and skeleton for *A. wollastoni* and only tissue for *V. flagellum* and *D. meteor*, and expressed as mmol C or N (g DW)⁻¹. In order to calculate tracer incorporation into coral tissue, the heavy/light isotope ratio (e.g. ¹³C: ¹²C) of each coral fragment (R_{sample}) was calculated as $R_{\text{sample}} = ([\delta\text{tracerC}_{\text{sample}}/1000] + 1) \times R_{\text{ref}}$, where $R_{\text{ref}} = 0.0111802$ for organic C and $R_{\text{ref}} = R_{\text{N2}} = 0.0036782$ for organic N. Fractional abundance of ¹³C and ¹⁵N (e.g. F₁₃ = 13C/[12C + 13C])

was expressed as $F_{\text{tracer}} = R_{\text{sample}} / (R_{\text{sample}} + 1)$. Enrichment of each coral fragment was expressed in relation to the fractional abundance of the respective starved fragment or average of starved fragments of the same colony. Final tracer incorporation was estimated by multiplying its fractional abundance with its OC content ($\mu\text{mol }^{13}\text{C fragment}^{-1}$). The total amount of C or N incorporated into coral tissue from the provided labelled food substrate was calculated by dividing the tracer incorporation of each fragment with the fractional abundance (F^{13} or F^{15}) of the respective food substrate. Final tracer C and N incorporation rates were normalized to the OC (moles) of each coral fragment. Independent variables including organic C, organic N, tracer incorporation rate and oxygen consumption were analysed by using Linear Mixed Models (LMEs) with the factors tank and colony being considered as random effects in order to deal with pseudoreplication in the experimental design.

Results and discussion

All food substrates were significantly enriched above background, for the experiments with the three species (Table 2).

Table 9: Tracer fractional abundance (F^{13} , F^{15}) of food substrates provided in the experiments with each studied species.

Experiment	<i>A. wollastoni</i>		<i>D. meteor</i>		<i>V. flagellum</i>	
	F^{13}	F^{15}	F^{13}	F^{15}	F^{13}	F^{15}
<i>C. calcitrans</i>	0.47	0.60	0.58	0.42	0.59	0.41
<i>N. gaditana</i>	0.55	0.70	0.49	0.31	0.58	0.30
<i>B. plicatilis</i>	0.36	0.39	0.21	0.12	0.37	0.15

Fragments of the species *A. wollastoni* had a total C content of 24.29 ± 1.49 mmol C/g DW with organic C representing 29.17 ± 1.79 % of total C. Organic C and organic N content did not change significantly between treatments. All coral fragments fed with labelled food substrates were significantly enriched above background, highlighting the ability of *A. wollastoni* to utilize a variety of food particles. Tracer C incorporation into coral tissue was statistically different among treatments, with fragments fed with zooplankton displaying much higher incorporation, followed by fragments fed with DOC (Fig. 22). The

same pattern was also observed in tracer N incorporation (Fig. 22). Moreover, a large standard deviation was observed in fragments fed with zooplankton in both C and N incorporation, corroborating with the observations made on 2.1.1., that some fragments had higher capacity to capture live zooplankton than others. Tracer C incorporation was significantly higher than tracer N incorporation in all treatments. Oxygen consumption was also significantly higher in fragments fed with zooplankton compared to the rest of the fragments (Fig. 23). The ability of antipatharians to capture and feed on live zooplankton has been reported before (Lewis, 1978; Warner, 1981; Wagner et al., 2012). However to our knowledge this is the first study that highlights the selective feeding strategy of an antipatharian species. In addition, the higher tracer incorporation and oxygen consumption of fragments offered zooplankton food substrate, suggest that zooplankton is of high importance for the growth and metabolism of this species, as it has been already documented for CWC scleractinian species (Naumann et al., 2011).

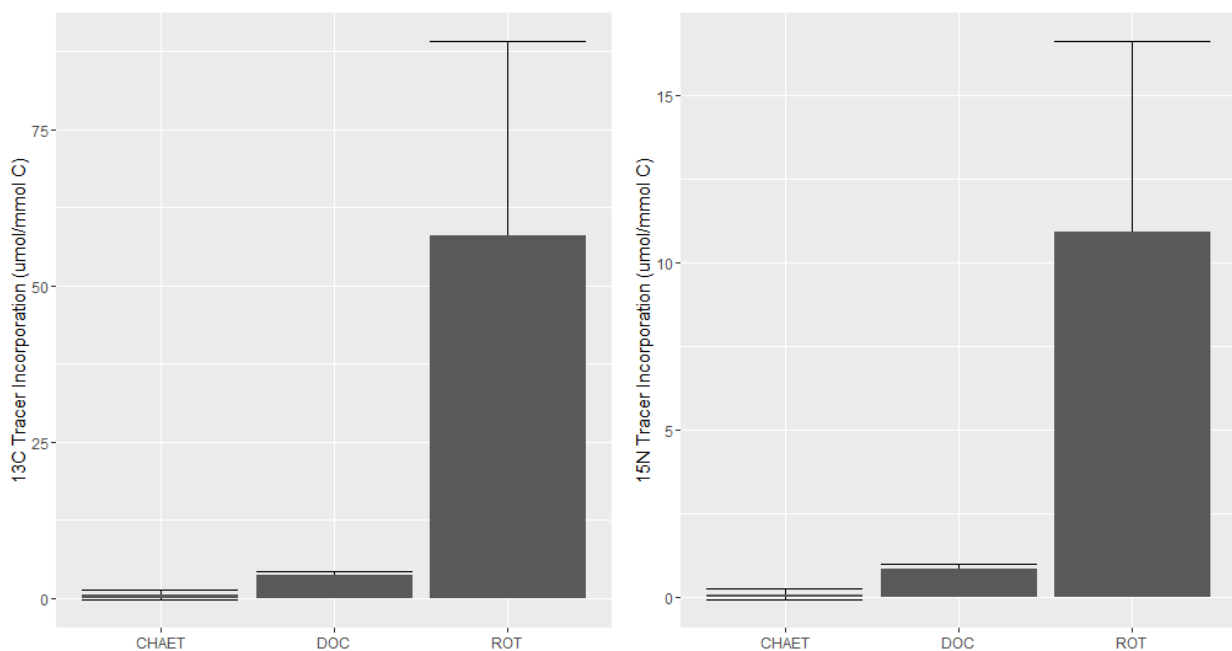


Figure 22: ^{13}C and ^{15}N tracer incorporation in tissue of the species *Antipathella wollastoni* for three food substrates: diatom *Chaetoceros calcitrans* (CHAET), Dissolved Organic Carbon (DOC) and rotifer *Branchionus plicatilis* (ROT).

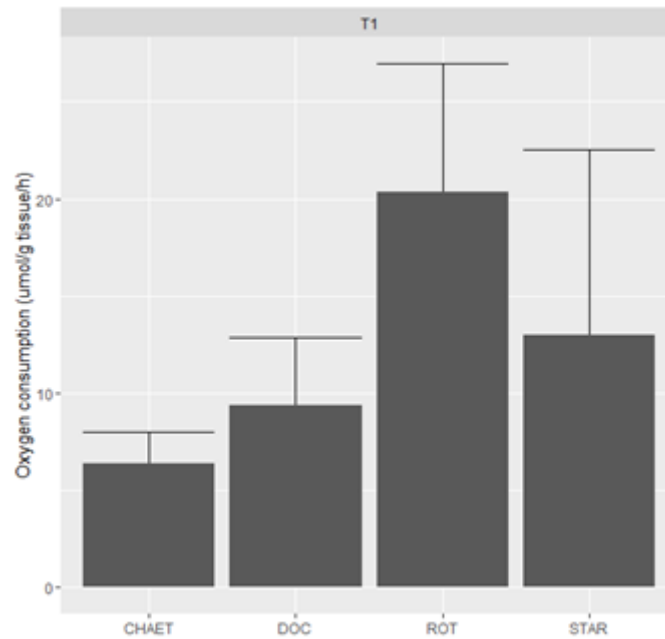


Figure 23: Oxygen consumption of fragments of the species *Antipathella wollastoni* under four different food treatments: CHAET: phytoplankton substrate; DOC: Dissolved Organic Carbon substrate; ROT: Zooplankton substrate; STAR: no food substrate (starved).

Dentomuricea aff. meteor and *V. flagellum* displayed a C content of $7.10 \pm 1.77\%$ and $8.00 \pm 1.48\%$ of total C respectively. Neither organic C nor organic N content varied significantly among treatments. At the end of the experiment, however, tracer C and N incorporation was significantly different among treatments and species. Fragments fed with zooplankton had higher tracer C and N incorporation, followed by fragments fed with DOC, for both species (Fig. 24, 25). In *D. meteor*, oxygen consumption was significantly higher in fragments fed with zooplankton and DOC, compared to the rest of the treatments (Fig. 26). In *V. flagellum*, oxygen consumption was higher in the zooplankton treatment, followed by the DOC and phytoplankton treatment, while the starved treatment displayed the lowest values (Fig. 26). Similarly to the case of *A. wollastoni*, these results demonstrate the ability of the two gorgonian species to feed on a variety of food sources. In the field, it is possible that feeding of the two gorgonian species displays seasonal patterns with colonies opportunistically feeding on available food sources, which has been also reported for other cold-water octocorals (Ribes 1999; Orejas et al., 2003). The higher values of tracer incorporation and oxygen consumption for fragments fed with the zooplankton food substrate emphasize their selective capacity and preference for zooplankton food sources. Also, it provides an indication of the importance of zooplankton for major physiological and metabolic processes of the two gorgonian species as it has already been demonstrated by CW scleractinians corals (Naumann et al. 2011). Considering the seasonal patterns of zooplankton dynamics in temperate, as well as in high latitude ecosystems, it is likely that zooplankton can also

control life history processes which are highly energy dependent and also display seasonal patterns such as gametogenesis and reproduction.

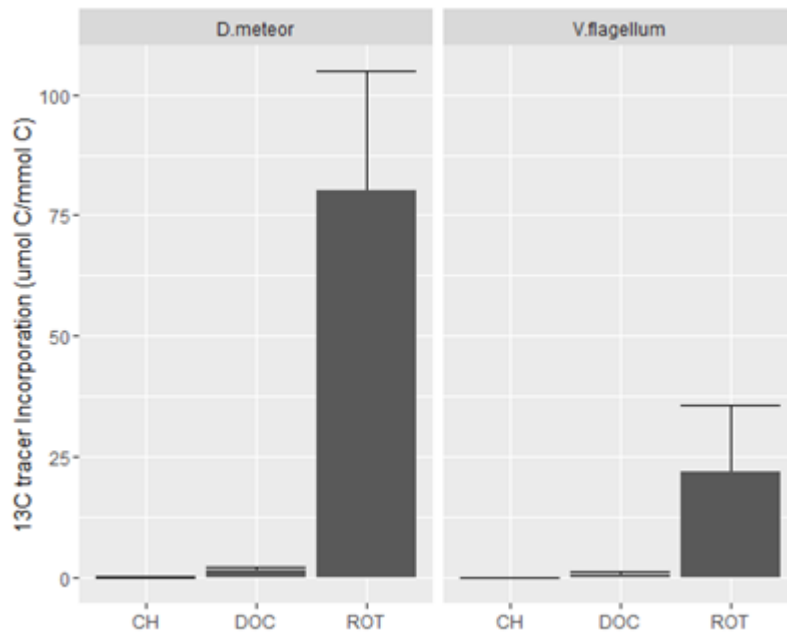


Figure 24: ^{13}C tracer incorporation in tissue of the gorgonian species *Dentomuricea* aff. *meteor* and *Viminella* *flagellum* under three food substrates: diatom *Chaetoceros calcitrans* (CHAET), Dissolved Organic Carbon (DOC) and rotifer *Branchionus plicatilis* (ROT).

Another emerging aspect from the collected data is the higher values of tracer incorporation and oxygen consumption displayed by *D. meteor* in all treatments (Fig. 24, 25, 26). Such results are indicative of different metabolic strategies between the two species. While fragments of *D. meteor* appeared to be more efficient in removing prey (section 2.1.1.) under similar flow velocities, further studies are needed to examine whether the lower values displayed by *V. flagellum* can be attributed to lower capture and ingestion of prey or if ingested prey was used for other metabolic processes such as excretion, calcification or growth of the main skeletal axis which was not considered in this study.

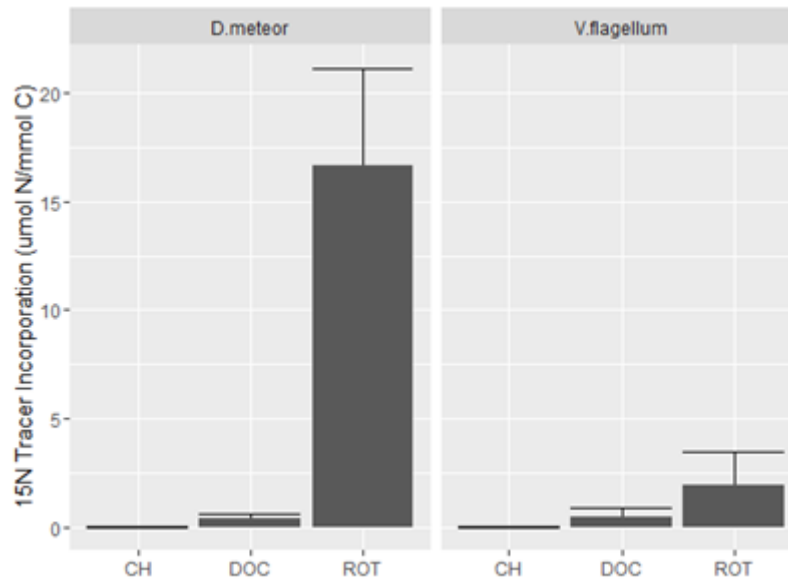


Figure 25: ^{15}N tracer incorporation in tissue of the gorgonian species *Dentomuricea* aff. *meteor* and *Viminella* *flagellum* under three food substrates: diatom *Chaetoceros calcitrans* (CHAET), Dissolved Organic Carbon (DOC) and rotifer *Branchionus plicatilis* (ROT).

The three coral species, despite their taxonomical differences, ingested higher quantities of zooplankton compared to other food substrates. Zooplankton has been suggested as a major food source that can sustain major physiological processes in scleractinians (Kiriakoulakis et al., 2005; Naumann et al., 2011). However, similar studies with *L. pertusa* (Mueller et al., 2014) reported a more flexible capacity of the species to ingest and utilize different food substrates. The results presented herein suggest that zooplankton derived energy can be of great importance for the survival of octocoral and antipatharian species. Moreover, since the three studied species are habitat-formers, physiological processes on the colony level can affect whole communities by altering their biogeochemical cycles and growth dynamics. It is therefore becoming evident that zooplankton dynamics can be a crucial driver for the distribution, and ecosystem function of coral gardens.

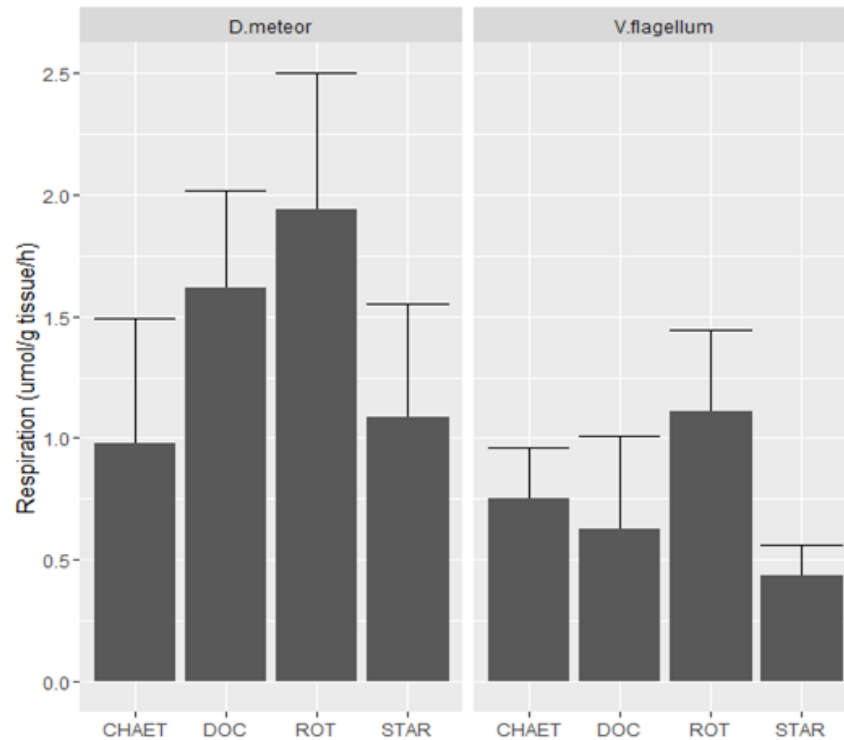


Figure 26: Oxygen Consumption for the species *D. meteor* and *V. flagellum* under four different food treatments. CHAET: phytoplankton substrate; DOC: Dissolved Organic Carbon substrate; ROT: Zooplankton substrate; STAR: no food substrate (starved).

3.1.4 Competition for food between two coexistent species in Azores coral gardens, *Dentomuricea aff. meteor* and *Viminella flagellum*

Authors: Stephanie Liefman, Marina Carreiro-Silva, Maria Rakka, Sandra Maier, Sebastian Hennige, Murray Roberts

Aims and objectives: Understand competition interactions of two co-occurring octocoral species *D. meteor* and *V. flagellum* under different water flow conditions by assessing bulk ^{13}C and ^{15}N incorporation.

Materials and methods

Specimen collection and maintenance Specimens of *V. flagellum* and *D. meteor* specimens were collected were obtained from bycatch material caught during scientific longline fishing cruises (ARQDAÇO monitoring programme, University of the Azores) on the Condor Seamount (38°08'N, 29°05'W) onboard of the RV "Arquipélago" in November 2018 from a depth ranging from 179 to 384 m. After collection, the colonies were transported to the DeepSeaLab Facilities IMAR /DOP where they

were fragmented into nubbins of 5 to 10 cm and maintained as described in 2.1.1.1 until used in experiments.

Isotopically labelled food production *Nannochloropsis* microalgae were cultivated in Artificial Sea Water (ASW) enriched with f/2 media where 100% of the NaHCO_3 was replaced by 99% $\text{Na}^{13}\text{CO}_3$ (Sigma-Aldrich) and 50% of the NaNO_3 by 99% $\text{Na}^{15}\text{NO}_3$ (Sigma-Aldrich). Each liter of culture media consisted of 800 ml of ASW and 200ml of natural sea water filtered through a Gf/F filter (WHATMAN). The algal cultures were cultivated for 3 weeks at a temperature of 14°C and a light cycle of 16h light and 8h dark. The algal cells were harvested at a mean concentration of 2.9×10^7 cells ml^{-1} , (a total of 54 l of algal culture were produced).

Stock cultures of rotifers *B. plicatilis* at a concentration of 87 individuals ml^{-1} were fed the isotopically labelled algae. Each 12 l stock culture was fed twice daily for 4 days with 0.8 l of the isotopically labelled micro algae suspension at a concentration of 2.9×10^7 cells ml^{-1} . After the incubation time, *B. plicatilis* cultures were separated into equal portions of 500 ml aliquots containing 0.002683 mol C, filtered through 41- μm mesh, rinsed with filtered seawater packed into plastic containers and frozen at -18°C until used.

Experimental design To assess competition under different flow regimes, one specimen of each species were placed together on a 33 l flume (Figure 4). Two water speeds were tested: 4 cm s^{-1} and 2 cm s^{-1} and named hereafter as Treatment 1 (T1) and Treatment 2 (T2) respectively. Four experimental runs of each treatment were performed. After the nubbins were transferred to the experimental flume, they were left to acclimate for 24h before the commencement of the experiments with a flow of 12 l h⁻¹. After the acclimation period the propellers attached to a rotating 12V engine (Servocity), were introduced to the flumes to create water movement at the desired speeds for T1 and T2, corals were left to acclimate to the water speeds for 1h. Following that period the water circulation was closed and the frozen isotopically labelled rotifers, in a predefined quantity of 0.002683 mol C, were added to each flume. The system was left with the predefined flow speed for 12 h. Food incubations lasted just for 12 hours so to avoid a large drop in pH, which had been previously noted for *D. meteor* and *V. flagellum* in closed systems. Subsequently 5 l water samples were taken, the propellers were removed, water circulation was opened and the flume was vacuumed to remove food residuals. Water samples were filtered through Gf/F filters dried at 60°C for 24h, weighed then burned at 450°C for 4h and re-weighed in order to assess the amount of carbon left in the water. This process was repeated for 6 consecutive days, with 12 hours intervals in between each food incubation period. Between each incubation period 5 l samples were collected from each flume, samples were filtered through a Gf/F filter dried at 60°C for 24h, weighed then burned at 450°C for 4h and re-weighed, to estimate the

background amount of C present in the seawater. As a control treatment for competition for food resources, each species was tested individually by placing a single individual in the flume and expose it to the 2 different water speeds, C1 and C3 were the control treatments for *V. flagellum* at 4 and 2 cm s⁻¹ respectively, C2 and C4 were the controls for *D. meteor* at 4 and 2 cm s⁻¹ respectively. The same process as described above was performed for the control treatments, with each control treatment having 4 replicates in total. Only four flumes were available hence the experiments had to be performed in batches.

Sample processing After the six incubation periods were finished for each batch the specimens were collected and frozen at -18 °C. When all the experimental batches were finished all the samples were freeze-dried and, weighed to obtain DW. The dry samples were then shipped to the University of Edinburgh.

Coral tissue was separated from the skeleton, weighed; and homogenized with a pestle and mortar. For ¹³C analysis, aliquots of 4 mg of each sample were weighed into silver capsules and were subsequently acidified stepwise with 5% HCl to eliminate inorganic carbons. Acidification process was repeated until no bubbling was observed. The samples were dried over night at 50 °C between acidification episodes. For ¹⁵N analyses 2 mg of each sample was weighed in a tin capsules. All samples analysed for isotopic ratio using EA-IRMS (Elemental Analysis - Isotopic Ratio Mass Spectrometer) HS20-22E (Sercon). Stable isotope data are presented as a per mille (‰) deviation from a standard as $\delta X (\text{‰}) = ((R_{\text{sample}} - R_{\text{reference}}) / R_{\text{reference}}) \times 1000$, where (X) is ¹³C or ¹⁵N, R_{sample} is the isotope ratio (¹³C/¹²C or ¹⁵N/¹⁴N, respectively) in the sample and $R_{\text{reference}}$ is the isotope ratio of the reference material ($R_{\text{reference}} = 0.0111797$ for C and $R_{\text{reference}} = 0.0036765$ for N). The atomic fraction (F) of ¹³C and ¹⁵N in specimens was calculated with $F = R / (R + 1)$. Excess values (E) are calculated as $E = F_{\text{sample}} - F_{\text{background}}$, so that positive excess values indicate uptake of the isotopically-labelled food. Total ¹³C and ¹⁵N assimilation was calculated as the product of excess (E) and the biomass of the specimen (Moodley et al., 2005). The biomass was expressed in C and N units and calculated by multiplying the specimen's dry weight (DW) with C and N content (as % of specimen's DW). The normalization of total C and total N assimilation to specimen's biomass was carried out through the division of total C and total N assimilation by biomass (in C or N units, respectively). The total amount of tracer incorporated from the food source into each fragment (tracer C incorporation, μmol tracer fragment⁻¹) was calculated by dividing each ¹³C assimilation by the fractional abundance (F^{13} and F^{15}) of the labelled food normalized C and N incorporation was expressed as [μmol tracer (mmol OC)⁻¹].

Statistical analysis Data was analysed using R Studio 1.1.456 version statistical software (RStudio team, 2016) Assimilation of C and N values did not have a normal distribution hence Kruskal-Wallis

non-parametric test was used to analyse the data. After the Kruskal-Wallis test Multiple comparison test between treatments or treatments versus control was done using the R package *pgirmess* (Giraudoux et al 2018).

Results and discussion

Between the start and the end of each incubation, the pH of the aquaria dropped on average 0.065 ± 0.03 units and the temperature decreased on average for all aquaria $1.14 \pm 0.17^\circ$ C. All the tested corals incorporated tracer C and N into their bulk tissue (Table 10). The data suggest *V. flagellum* incorporated more C and N tracer at high speeds either when in competition or in control treatments but no statistical difference was found. The incorporation was higher when in competition than in control treatments (Figure 27). *Dentomuricea meteor* also incorporated more tracer C and N on high speed treatments (C2 and T1), under competition conditions. Fragments of *D. meteor* under higher speed displayed the highest incorporation rate for this species (Figure 28). Competition experiments revealed a statistically significantly higher incorporation of C and N tracers by *D. meteor* under T1 (p-value: 0.02), (Figure 28).

Table 10: Average ^{13}C and ^{15}N bulk tracer incorporation in corals for each treatments

Species/treatment		C tracer incorporation [$\mu\text{mol C (mmol OC)}^{-1}$]	N Tracer incorporation [$\mu\text{mol N (mmol N)}^{-1}$]
<i>V. flagellum</i>	T1	12.24 \pm 8.01	14.53 \pm 9.92
	T2	12.74 \pm 12.46	10.44 \pm 9.63
	C1	8.32 \pm 8.57	8.69 \pm 8.69
	C3	5.57 \pm 4.49	5.16 \pm 3.96
<i>D. meteor</i>	T1	68.89 \pm 53.83	65.94 \pm 38.13
	T2	18.25 \pm 14	17.84 \pm 8.9
	C2	28.48 \pm 15.69	28.23 \pm 20.56
	C4	26 \pm 24.39	19.21 \pm 19.41

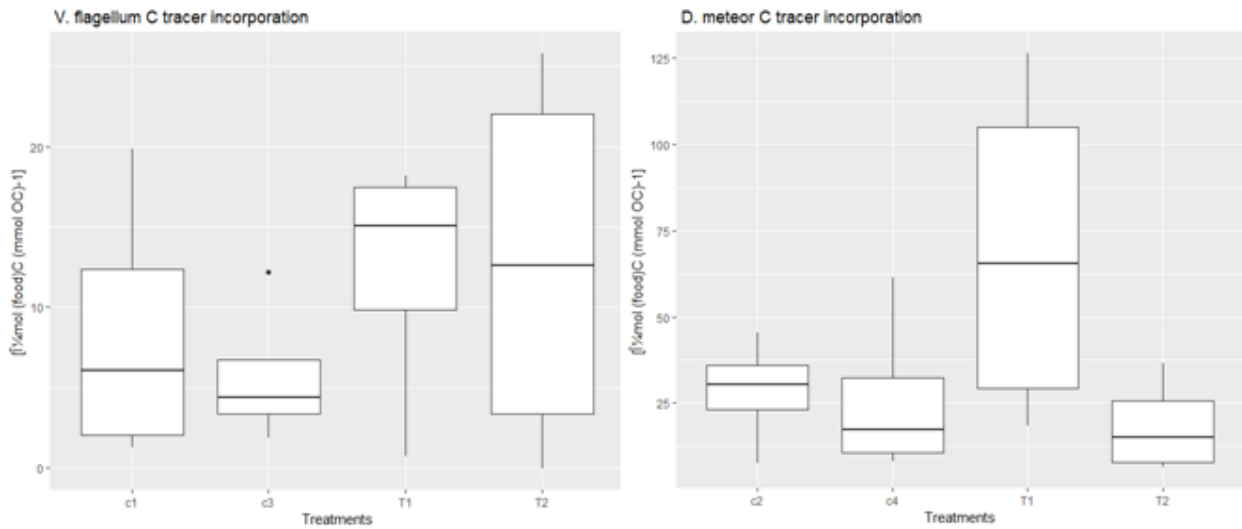


Figure 27: Average tracer incorporation for the octocorals *Viminella flagellum* and *Dentomuricea* aff. *meteor*. Note the different scales in the y axes. (trends for N tracer were the same hence graphs are not shown). C1: individual *V. flagellum* at 4 cm s⁻¹; C3: individual *V. flagellum* at 2 cm s⁻¹; T1: both species at 4 cm s⁻¹; T2: Both species at 2 cm s⁻¹; C2: individual *D. meteor* at 4cm s⁻¹; C4: individual *D. meteor* at 2 cm s⁻¹

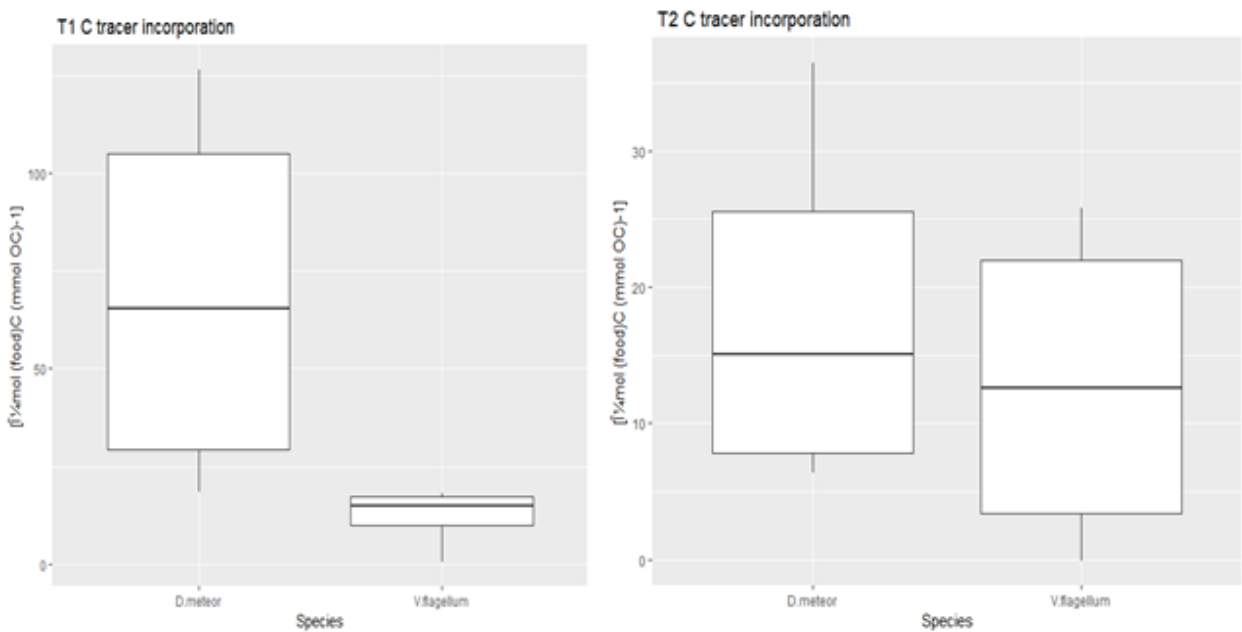


Figure 28: Tracer incorporation per species per treatment, note the difference in scale in the 2 graphs. ¹⁵N incorporation showed the same trend. T1: both species at 4 cm s⁻¹; T2: Both species at 2 cm s⁻¹

Both species have a higher incorporation under 4cm s⁻¹ most likely due to higher prey encounter rate (Sebens et al., 1998). Moreover, flow speed at 2cm/sec could have not been sufficient to keep enough food in suspension. *D. meteor* had a higher incorporation of C and N tracers for all treatments when

compared to *V. flagellum* (Figures 27, 28), which suggest that the former has the possibility to outcompete the latter when found in mixed coral gardens if food resources become scarce.

Higher food uptake by *D. meteor* can also be due to it being a branching/fan shaped coral (Fig (picture above) which can create eddy turbulence around the branches increasing the possibility of prey encounter, similar to the documented fact that coral colonies at that are found at higher densities feed more efficiently at higher water speeds (Sebens et al., 1984; 1997). Polyp morphology differences can also explain the possible niche overlap when found in mixed gardens suggested by the present results. *Viminella flagellum* has larger and longer polyps than *D. meteor*. The larger sized polyps may be deformed at higher velocities, and this can reduce the speed range at which this species is more effective at catching prey compared to the range of corals having smaller polyps (Chang-Feng & Ming-Chao 1993) such as *D. meteor*. Other studies comparing polyp sizes in the anemone *Metridium seneli* also found that smaller polyps were more efficient at higher speed flow (Anthony, 1997). This can point that perhaps the tested speeds were not the ideal for the species, as reinforced by the fact that differences in incorporation rates for the different species are not as big in the 2 cm s^{-1} speed treatment. The present study assessed competition based on one food source, which was the preferred experimental food source for both of the species (Rakka et al in preparation). Different zooplankton sources might be available in the Condor Seamount. Selectively preying in different zooplankton can be a possible explanation on how these two species co-exist in mixed coral gardens. *Viminella flagellum* rises higher up in the water column hence it most likely get access first to food items in the water column, which could also offset possible resource exclusive competition. The findings of this study suggest that both of the species when in competition (T1 and T2) have a higher incorporation rate when compared to the respective controls (Figure 27), though this is less marked for *D. meteor* in T2 and C4 (2 cm s^{-1}). This can perhaps be explained by the fact that two organisms in one aquarium create more eddy turbulence in the water flow increasing particle encounter with the polyps

3.2 Assessing the impact of ocean acidification under variable food supply on the octocoral *Viminella flagellum*

Authors: Maria Rakka, Sandra Maier, Meri Bilan, Antonio Godinho, Ines Martins, Dick van Oevelen, Sebastian Hennige, Patricia Puerta, Covadonga Orejas, Marina Carreiro-Silva

The deep Atlantic Ocean is an area already experiencing significant environmental changes and is predicted to continue to be heavily impacted by global changes over the next 100 years (Sweetman

et al., 2017). Projections for 2100 suggest temperature (T) increases between 1-4°C, a decrease in pH of up to 0.4 pH units (OA), declines in oxygen concentrations up to 3.7%, and 40% loss of the food supply to the ocean seafloor (2) which are predicted to reduce the habitat suitability of fish and CWC in the North Atlantic (Gehlen et al. 2014; Sweetman et al 2017, see DL 3.3).

Experimental studies with the reef-building CWCs from NE Atlantic and Mediterranean to date have showed the ability of scleractinian CWCs to calcify and grow under OA and warming predicted for 2100 and even under undersaturated conditions (Form & Riebesell, 2012; Maier et al., 2012, 2013; Hennige et al., 2014; Hennige et al., 2015; Movilla et al., 2014; Büscher et al., 2017, Maier et al., 2018). In contrast, studies using the same species in the Gulf of Mexico and California margin suggested a great susceptibility of the same CWC species to OA alone or in combination with warming and deoxygenation with decreased calcification rates, increased skeletal dissolution, and induced mortality (Brooke et al., 2013; Lunden et al., 2014; Georgian 2016; Kurman et al., 2017; Gómez et al., 2018) potentially related to genotypic variability between CWC populations (Kurman et al 2017). Despite these differing physiological responses, coral framework supporting live reefs are susceptible to corrosive waters and will suffer chemical and biological dissolution (Hennige et al., 2015; Schönberg et al., 2017), possibly resulting in reef structure collapse under the predicted shoaling of the aragonite saturation horizon as a consequence of OA (Davies and Guinotte, 2011; Yesson et al., 2012; Perez et al., 2018).

Furthermore, because of the short-term nature of the experimental work, it remains unclear whether CWC can be sustained indefinitely, as OA has been shown to affect coral metabolism (Hennige et al., 2015; Gori et al., 2016) and up-regulate genes related to stress, immune responses, energy production and calcification (Carreiro-Silva et al., 2014). A key question has been the ability of CWC to resist OA under the reduced food conditions predicted for 2100. Records of CWC occurrences in undersaturated waters have been associated with areas of high primary productivity, leading to the hypothesis that increased food supply may compensate the extra necessary energy for CWC to survive under these undersaturation conditions (Thresher et al 2011; Baco et al 2017). Indeed, reduced food availability has been linked with reduced physiological performance (e.g. calcification and respiratory metabolism) and condition of CWCs (Naumann et al., 2011; Larsson et al., 2013; Büscher et al., 2017), although it has not been shown to increase calcification in carbonate undersaturation conditions (Maier et al., 2016; Busher et al., 2017). Nevertheless it is plausible that the metabolic costs of calcifying in extremely low carbonate conditions may become prohibitively expensive compromising coral survival (Carreiro-Silva et al 2014; Hennige et al., 2015; Maier et al. 2016).

In contrast to scleractinian CWCs, the impact of reduced calcite saturation states on octocorals has been little studied, but the limited experimental evidence suggests reduced calcification and growth of temperate octocoral *Corallium rubrum* (Cerrano et al., 2013) and reduced metabolism in the deep-sea octocoral *D. meteor* (Carreiro-Silva et al unpublished information) suggesting that octocorals may be negatively affected by OA. To better understand the impacts of OA on coral garden forming octocorals in Azores, we performed an experiment testing the interactive effects of OA and food availability. Specific objectives of this experiment were to determine if and how food concentration alters the impacts of OA on the physiology of the tested species; and to assess the impact of OA on food uptake and food assimilation.

The initial plan included testing the effect of predicted change OA using three scenarios, including a present day and two elevated CO₂ levels; a median and the projected CO₂ scenario in accordance with IPCC RCP8.5, the current CO₂ trajectory for 2100. However, due to the limited laboratory space to accommodate for the high number of experimental tanks necessary for this experimental design and limited number of coral fragments available, it was decided to exclude the median OA scenario as it was considered more important to test for the "business as usual scenario" IPCC RCP8.5 to test for the interactive effects of OA and food availability affecting coral garden communities in the future.

Materials & Methods

Sample collection Colonies of the octocoral *V. flagellum* were obtained from bycatch material caught during scientific longline fishing cruises (ARQDAÇO monitoring programme, University of the Azores) at Condor Seamount onboard of the RV "Arquipélago" in October-November 2018 from a depth ranging from 179 to 384 m. A total of 19 colonies were collected, fragmented and maintained as described in 2.1.1.1.

Data collected during field work missions in July 2018 to measure oxygen fluxes and total community OM mineralization of coral gardens in the Condor Seamount as part of D2.3 (WP2 Task 2.2) were used to simulate natural habitat conditions of *V. flagellum* in aquaria. Five water samples were collected with a 5L niskin bottle deployed at seabed using a hand held cable. Subsamples of 100 ml were collected in borosilicate flasks to determine total alkalinity (TA) while the rest of the collected seawater was filtered with 0.2 µm GFF filters (Whatman Glass microfiber filters) to estimate concentrations of particulate organic carbon (POC) in the coral garden. A CTD attached to the niskin bottle recorded data on Temperature (T) and salinity (S) which corresponded to 14 ± 0.6 °C and 36 ± 0.214 respectively (full set of data provided in DL 2.3). Additional results for daily temperature

fluctuations obtained through the deployment of eddy correlation for DL 2.3 were also taken into account. These data were used to replicate environmental conditions in the aquaria experiments and estimate the pH values corresponding to the two experimental pCO₂ scenarios.

Experimental design A fully crossed factorial experimental design was used to test the interactive effect of OA and food availability. Two treatments manipulating pCO₂ conditions were used: present day (~385 atm) and IPCC RCP8.5 scenario (1000 atm; IPCC, 2014), in combination with three food treatments (starved, low food availability, high food availability), resulting in 6 treatment combinations (Figure 29).

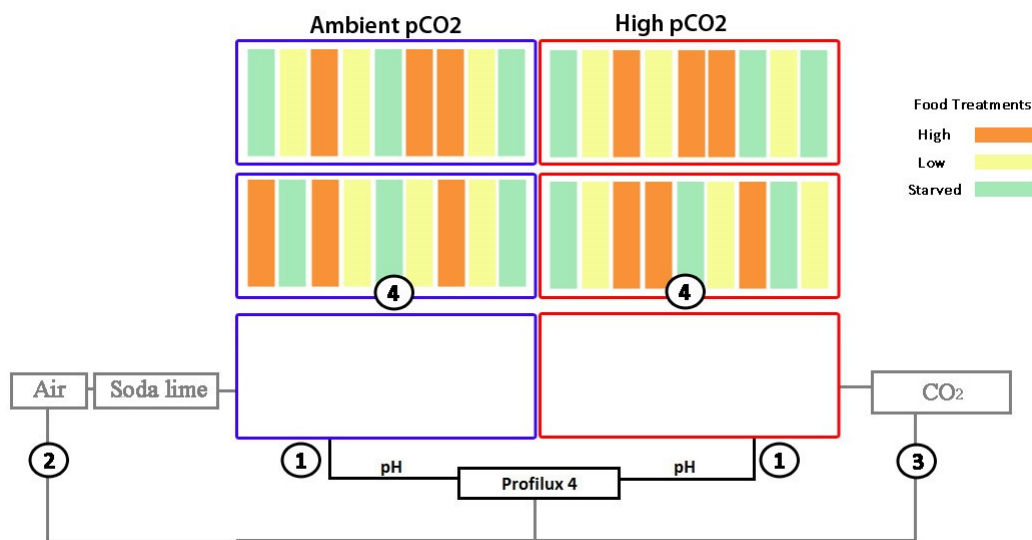


Fig. 29: Experimental setup. (1) Continuous monitoring of pH conditions in storage tanks by Profilux 4; (2) Controlled addition of air filtered through soda lime in storage tank to increase pH in the low pCO₂ treatment; (3) Controlled addition of CO₂ in storage tank to decrease pH in the high pCO₂ treatment; (4) Four water baths, two for each pCO₂ treatment with 9 experimental aquaria each. Each experimental aquaria is assigned to one food treatment adding up to 6 experimental aquaria per crossed treatment.

The experimental systems included two storage 150L tanks, which were constantly supplied with seawater pumped from 5m depth and passed through an ultraviolet filter system and subsequently through 1µm nylon filters. The two tanks were used to simulate two OA scenarios referred above with two pCO₂ levels ~385 atm 1000 atm, corresponding to pH values of 7.85 and 8.21 respectively (NBS scale). In order to achieve the two pCO₂/pH values, the control tank was bubbled with CO₂-free air, created by an air pump connected to soda-lime filters while the high pCO₂/low pH tank was bubbled with pure CO₂ (Figure 29). Bubbling in both tanks was controlled by a central controller (Profilux 4, GHL) connected to glass electrodes which continuously monitored the pH values in the two storage tanks. Each tank provided water continuously to 18 experimental aquaria, similar to the ones used in 2.1.1 (Figure 5), which were placed in a total of four water baths, keeping temperature stable at 14.5 ± 0.5 °C for each replicated aquaria per treatment.

A total of 36 fragments of *V. flagellum* were fragmented as described in 2.1.1.1 one month before the beginning of the experiment and were distributed to the 36 experimental aquaria. Seawater pH was gradually adjusted to the required levels within a week, time referred to as acclimatization week (W_{ac}) and kept stable for another six weeks (W_0 - W_6). During this period, conditions of the three food treatments referred above were recreated 5 days per week in the different aquaria: (1) In the starved treatment no food was provided; (2) in the Low Food treatment prey was provided in a concentration of 250 live rotifers/L and (3) in the High Food treatment, prey was provided in a concentration of 1500 live rotifers/L. The low rotifer concentration treatment corresponds to carbon concentration of $1.60 \mu\text{mol C/L}$, which is close to the values of natural carbon levels estimated at Condor seamount ($1.55 \pm 0.68 \mu\text{mol/L}$; D.L. 2.3) while the high concentration treatment corresponds to $10.12 \mu\text{mol/L}$ which is the highest value of carbon that could be achieved under laboratory conditions.

Once every week, the provided prey was enriched with ^{13}C and ^{15}N , as described in 2.1.2.1. Water circulation was paused before prey provision and remained closed for approximately 6 hours, period which was considered as a food cycle. During prey provision a continuous laminar flow with speed of 6 cm/sec was created in each aquaria by using 113 heavy duty motors (see 2.1.1.1). After the end of the food cycle, all aquaria were cleaned by siphoning and water replacement of least 2/3 of the initial volume in order to remove any non-consumed prey.

Temperature pH and salinity in all aquaria were measured manually every day using a Mettler-Toledo S8 glass electrode and S30 SevenEasyTM conductivity meter which were calibrated every other day. Water samples for TA were collected once per week and analyzed using a spectrophotometric method (Dionísio et al., 2017; adapted from Sarazin et al., 1999) with an estimated error of 0.8 - 4%. Levels of phosphorus (P), Silica (S) and Nitrite (NO_3) were also monitored by taking water samples once a week. Seawater carbonate chemistry parameters (Table 2) were calculated from the measured TA and pH at the average experimental water temperature and salinity using the program CO2SYS (Lewis and Wallace 1998) with the thermodynamic constants of Mehrbach et al. (1973) as refitted by Dickson and Millero (1987).

In order to assess the physiological response of the target species to the experimental treatments, the following rationale was adopted: coral activity was assessed to determine if fragments were able to actively feed on the provided prey, prey capture was used to monitor the amount of captured prey and subsequently oxygen consumption, Dissolved Inorganic Carbon excretion (DIC), nutrient excretion, and growth were determined to assess the fate of the ingested prey under the different pCO_2 treatments. Coral activity was measured twice per day, 1h after feeding and 1h before the end of the feeding cycle. Fragments were considered open if at least one polyp was extended and closed

if all polyps were retracted. Prey capture was estimated by counting prey in water samples that were taken at the beginning and at the end of the feeding cycle in three aquaria from each crossed treatment twice a week. Only aquaria with open fragments were used for the prey capture estimates. Samples were taken and counted as described in 2.1.1.1. Measurements of oxygen consumption, DIC excretion and nutrient excretion were performed in closed-cell incubations at the end of each experimental week, right after the end of the feeding cycle, following procedures described in 2.1.2.1. Determination of bulk DIC fluxes, i.e. the amount of carbon respired, was not possible as DIC concentrations did not change significantly between the beginning and end of incubations. However, the samples were used to estimate tracer C respiration, which corresponds to the amount of carbon ingested through the isotopically enriched prey and subsequently respired, by multiplying DIC by its relative enrichment in ^{13}C according to Maier et al., (2019). To estimate potential growth, images were taken at four sides of each fragment with a scale and processed with the software Image j in order to provide estimates of polyp number and surface. Moreover, at the end of the experiment fragments were collected, freeze-dried and processed in order to assess tracer incorporation. Calculations for tracer incorporation and tracer C respiration were made as described in 2.1.2.1. Herein, we present results on coral activity, prey capture, oxygen consumption as well as preliminary results on C tracer respiration, with the rest of the variables pending further analysis.

Statistical analysis Generalized Linear Models (GLMs) were used following the procedure described in 2.1.1.1. Two approaches were followed: the first approach focused on general means of all experimental weeks, in order to examine overall effects of the experimental treatments, and the second approach focused on data within food treatments, to study time trends without compromising statistical power.

Results & Discussion

Parameters of seawater carbonate chemistry during the course of the experiment pooled for the different food treatment levels are presented on Table 11.

Table 11: Seawater carbonate chemistry parameters (mean \pm sd) determined for each experimental week in the two pCO₂ treatments (control: 400 ppm; high: 1000 ppm) pooled for the different food treatment levels. Temperature, salinity, pH (pH_{NBS}) and Total alkalinity (TA) were monitored during the experimental period and all the other parameters (Dissolved Inorganic Carbon (T_{CO2}) and Aragonite saturation (Ω_{AR}) were calculated. Temperature was kept constant at 14.5 ± 0.5 and salinity at 36 ± 0.4

Experimental Week	pH _{NBS}		TA($\mu\text{mol}/\text{kg}^{-1}$)		T _{CO2} ($\mu\text{mol}/\text{kg}^{-1}$)		Ω_{AR}	
	400 ppm	1000 ppm	400 ppm	1000 ppm	400 ppm	1000 ppm	400 ppm	1000 ppm
W ₁	8,19 \pm 0 .01	7,85 \pm 0 .01	2386.5 \pm 54	2412.9 \pm 29	2143.17 \pm 44.6	2316,31 \pm 24	2,66 \pm 0 ,12	1,36 \pm 1 .41
W ₂	8,17 \pm 0 .02	7,86 \pm 0 .03	2228.6 \pm 58	2318.8 \pm 72	2006.15 \pm 43.7	2220,85 \pm 58	2,38 \pm 0 ,14	1,34 \pm 1 .47
W ₃	8,18 \pm 0 ,02	7,86 \pm 0 .01	2337.4 \pm 34	2508.7 \pm 59	2102.68 \pm 21.5	2406,14 \pm 53	2,55 \pm 0 ,14	1,45 \pm 1 .51
W ₄	8,18 \pm 0 .02	7,86 \pm 0 .01	2388.6 \pm 54	2463.7 \pm 88	2150.33 \pm 39.4	2362,23 \pm 81	2,62 \pm 0 .16	1,42 \pm 1 .50
W ₅	8,20 \pm 0 .01	7,85 \pm 0 .01	2445.4 \pm 33	2495.1 \pm 58	2192.58 \pm 25.4	2396,61 \pm 52	2,78 \pm 0 .09	1,41 \pm 1 .48
W ₆	8,20 \pm 0 ,01	7,85 \pm 0 .01	2402.6 \pm 43	2481.4 \pm 42	2152.84 \pm 34.8	2383,23 \pm 36	2,73 \pm 0 .1	1,40 \pm 1 .46

Under the control pCO₂ treatment, significantly higher proportion of fragments were closed in the starved treatment compared to the other two food treatments (Figure 30). Under the high pCO₂ treatment, however, no statistically significant difference was observed among food treatments. Within the high and low food treatments, more closed fragments were observed under the high pCO₂ treatment (Figure 30). The inverse pattern was observed under the starved treatment, with the percentage of closed fragments with closed polyps being significantly higher in the control pCO₂ treatment. Overall, there was high variability in all the experimental treatments, as highlighted by the large standard deviation in Figure 30.

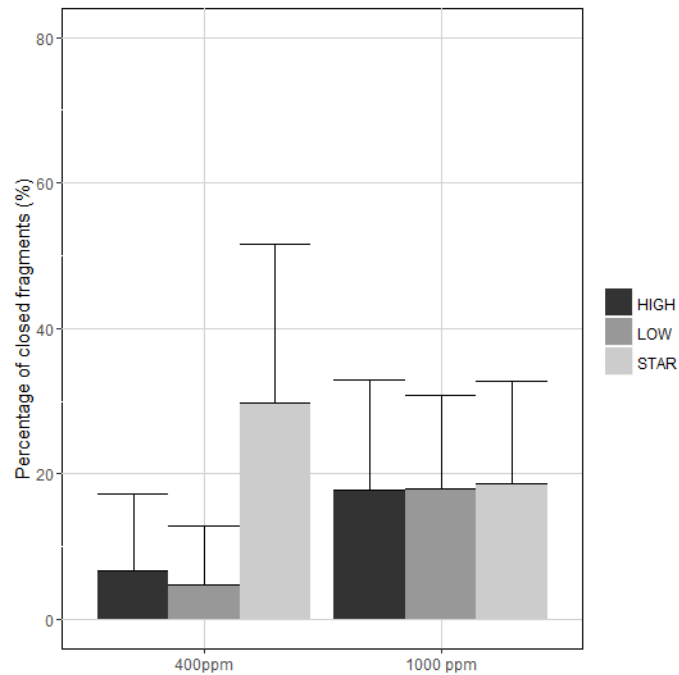


Figure 30: Coral activity of fragments of the octocoral *Viminella flagellum* expressed as percentage of fragments with closed polyps under two pCO₂ treatments (control: 400 ppm; acidified: 1000 ppm) and three food treatments (High food concentration: HIGH, low food concentration: LOW; starved: STAR)

Great variability was detected in the time patterns among the three food and pCO₂ treatments. Within the high food treatment, the percentage of closed fragments was significantly higher under the high pCO₂ treatment except on week 4 where the opposite pattern was observed (Figure 31). Under the low food treatment, there were no statistical differences among the two pCO₂ treatments, except for week 3 when the percentage of closed fragments was much higher under the high pCO₂ treatment. Lastly, under the starved food treatment there were fluctuations with the percentage of closed fragments reaching a maximum in week 4 for the control pCO₂ treatment and in week 2 for the high pCO₂ treatment, after which it started decreasing again (Figure 31).

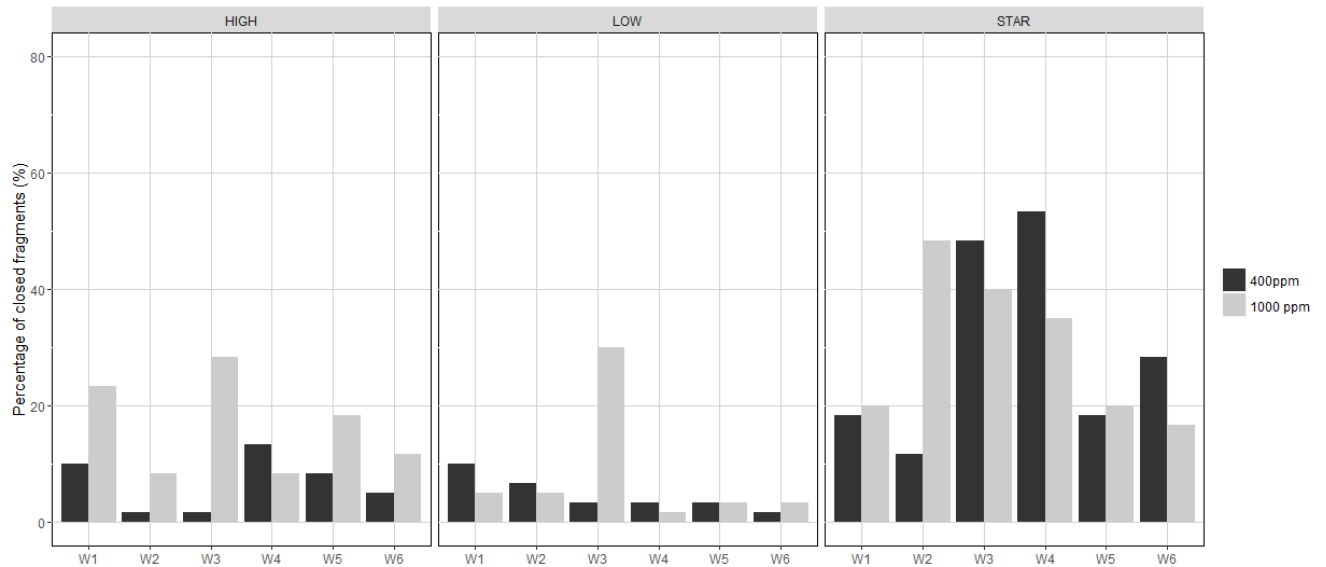


Figure 31: Coral activity of fragments of *Viminella flagellum* expressed as percentage of closed fragments under two $p\text{CO}_2$ treatments (control: 400 ppm; acidified: 1000 ppm) and three food treatments (High food concentration: HIGH, low food concentration: LOW; starved: STAR) for each of the experimental weeks (W1-W6).

The average initial concentrations for the high food treatment were $17780,6 \pm 3932$ prey/L and 17700 ± 4995 prey/L in the high and control $p\text{CO}_2$ treatment respectively while for the low food treatment they were 2595 ± 803.6 prey/L and 2561 ± 643.7 prey/L respectively. The error in recreating the desired food concentration was higher in the high food treatment, reaching levels of 20% in comparison to the low food treatment where the error was on average 8%. However, the initial concentrations did not differ significantly between the two $p\text{CO}_2$ treatments. Fragments consumed on average 38.85 ± 18.13 % of the provided prey in the high food treatment and 75.91 ± 18.21 % of the provided prey in the low food treatment in both $p\text{CO}_2$ treatments. However, standardized captured prey (i.e. capture divided by fragment dry weight, Fig. 32) was significantly higher for the high food treatment compared to the low food treatment. As a result, fragments in the high food treatment captured on average 27.8 % more prey than fragments in the low food treatment.

Standardized prey capture, reached 2286.12 prey/g coral DW/h corresponding to 14.73 $\mu\text{mol C/g DW/h}$ in the high food treatment compared to 747.17 prey/g coral DW/day corresponding to 4.81 $\mu\text{mol C/g DW/day}$ in the low food treatment. High variation in the amount of captured prey was observed among coral fragments, especially when standardized with coral DW (Fig. 4). Although capture seemed to increase for fragments under high food and high $p\text{CO}_2$ conditions over the experimental time period (Fig. 32), percentage capture was not significantly different among $p\text{CO}_2$ treatments and fluctuations in standardized capture throughout time in both $p\text{CO}_2$ treatments (Fig. 32) were also not statistically significant. Both statistical results might be due to the very high variation observed among coral fragments.

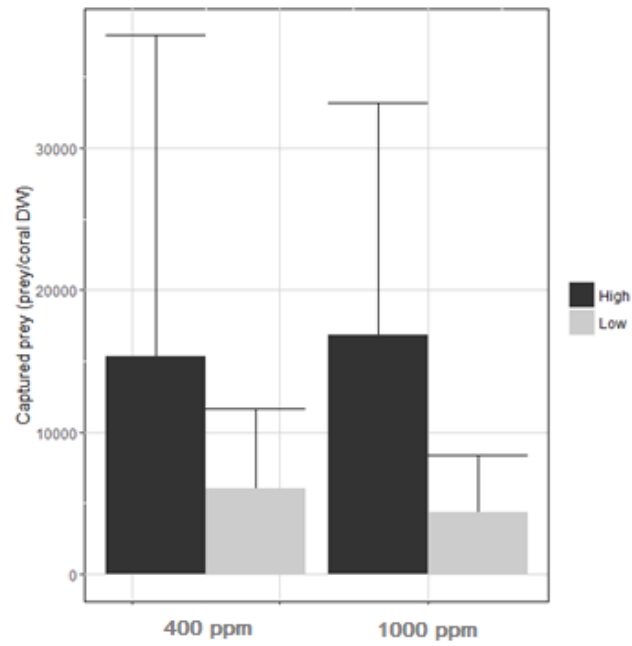


Figure 32: Standardized captured prey (prey/coral DW) of fragments of Viminella flagellum under two pCO₂ treatments (control: 400 ppm; high:: 1000 ppm) and two food treatments (High food concentration: HIGH, low food concentration: LOW).

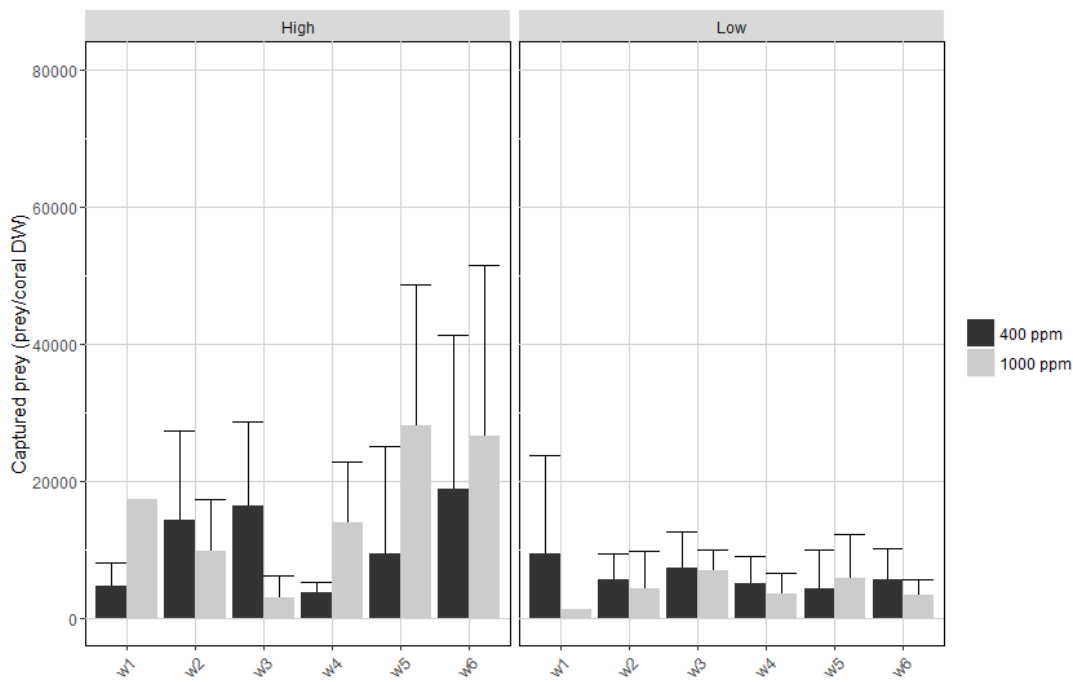


Figure 33: Standardized captured prey (prey/coral DW) of fragments of Viminella flagellum under two pCO₂ treatments (control: 400 ppm; acidified: 1000 ppm) and two food treatments (High food concentration: HIGH, low food concentration: LOW) for each of the experimental weeks (W1-W6).

Oxygen consumption was higher in the high pCO₂ treatment under low food and starved conditions, but it was not statistically significant between pCO₂ treatments under high food conditions (Fig. 34). Although a peak in oxygen consumption was observed in week 5 in all treatments (Fig. 35), statistical analysis revealed that oxygen consumption fluctuations over time within each food treatment were not statistically significant, owing to the large observed variability.

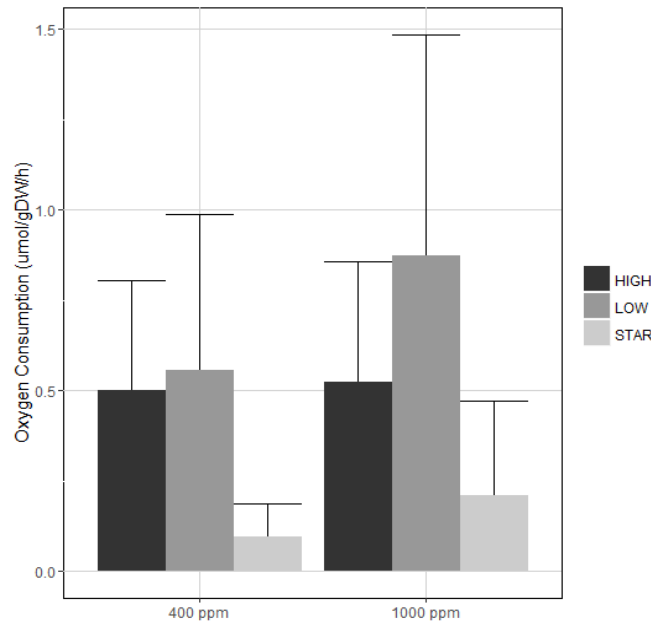


Figure 34: Oxygen consumption of fragments of *Viminella flagellum* under two pCO₂ treatments (control: 400 ppm; acidified: 1000 ppm) and three food treatments (High food concentration: HIGH, low food concentration: LOW; starved: STAR).

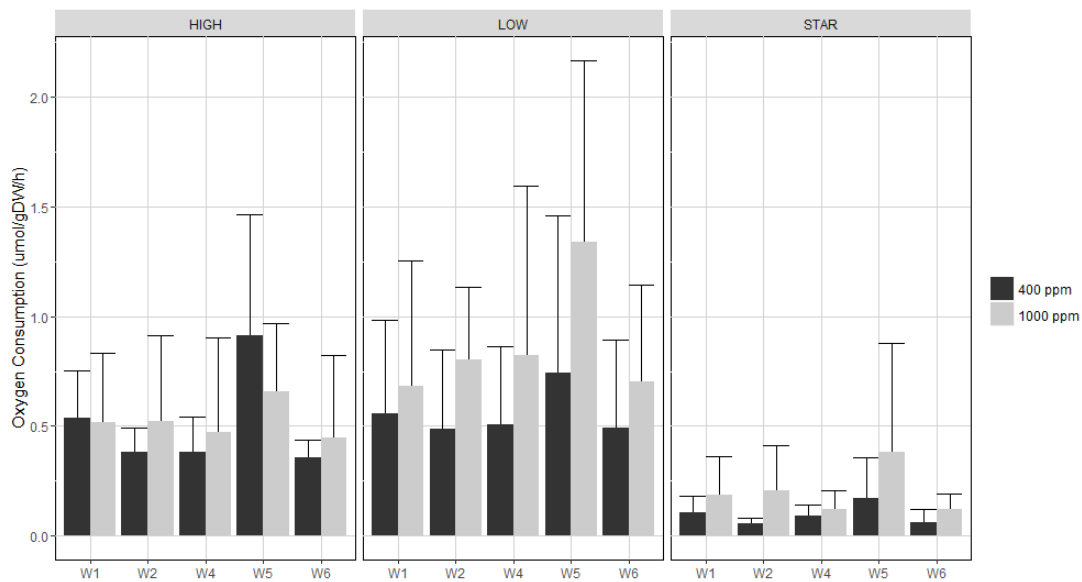


Figure 35: Oxygen consumption of fragments of *Viminella flagellum* under two pCO₂ treatments (control: 400 ppm; high: 1000 ppm) and three food treatments (High food concentration: HIGH, low food concentration: LOW; starved: STAR) for each of the experimental weeks (W1-W6).

Tracer C respiration displayed overall higher levels in the high pCO₂ treatment (Figure 36) which were more pronounced and statistically significant in the high food treatment. Fragments under the low food treatment displayed higher values of tracer C respiration in comparison to the high food treatment, especially in the control pCO₂ treatment (Figure 36). However, under the high pCO₂ treatment this difference was not statistically significant. No significant trend in tracer C respiration was detected over time (Figure 37).

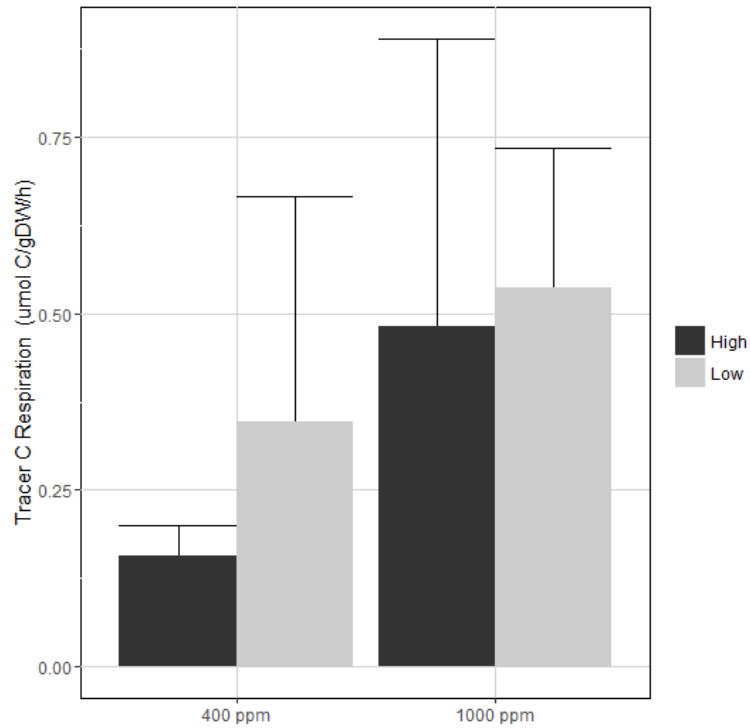


Figure 36: Tracer C Respiration of fragments of *Viminella flagellum* under two pCO₂ treatments (control: 400 ppm; acidified: 1000 ppm) and three food treatments (High food concentration: HIGH, low food concentration: LOW).

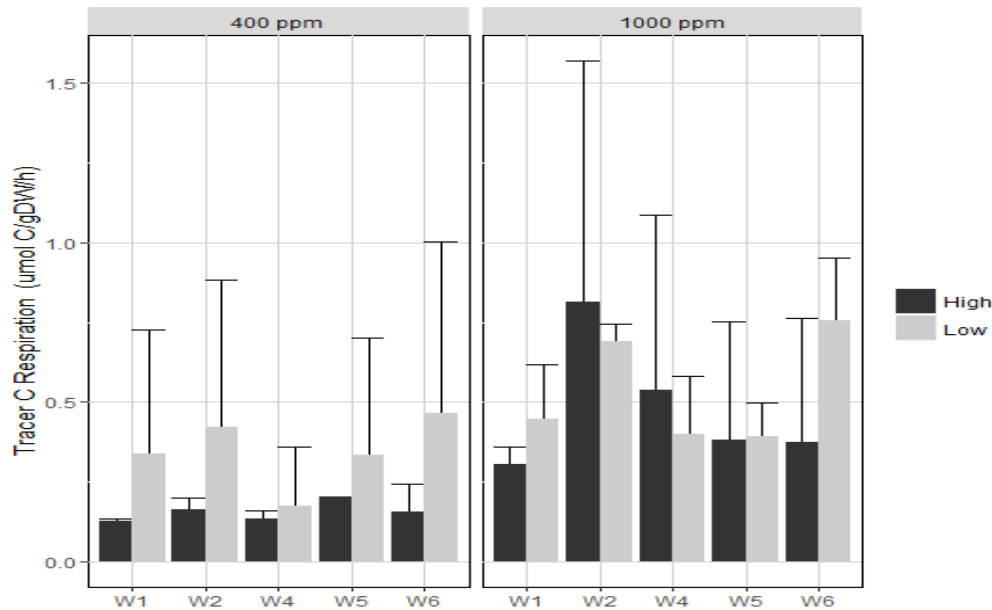


Figure 37: Tracer C respiration of fragments of *Viminella flagellum* under two pCO₂ treatments (control: 400 ppm; acidified: 1000 ppm) and three food treatments (High food concentration: HIGH, low food concentration: LOW for each of the experimental weeks (W1-W6)).

Polyp expansion in cnidarians facilitates prey capture and handling, increases oxygen and waste product diffusion and exposes potential symbionts to light, e.g. in the case of symbiotic corals (Bell et al., 2006). Contraction, on the other side, is used as a protection against predators and as a mechanism to reduce oxygen, waste product diffusion and overall metabolic rates (Swain et al., 2015). Therefore, polyp activity is a vital process for the survival and metabolic function of octocoral species. A number of studies report increased contraction of anthozoans under non-optimal environmental conditions. In the case of octocorals, examples include Mediterranean octocorals which displayed increased polyp contraction under low pH (Cerrano et al., 2013) and high temperature (Previatti et al., 2010). Similarly to the species in these studies, it is likely that *V. flagellum* displayed higher percentages of closed fragments in the high pCO₂ treatment as a defensive response or in an attempt to lower its metabolic rates, as it is also suggested by the provided data on oxygen consumption. Moreover, the behaviour observed in fragments in the starved treatment may be indicative of an energetic trade-off between the processes of retraction and expansion: the absence of food during W1 forced more and more fragments to choose retraction, possibly reducing their metabolic rates, while during the last three weeks of the experiment an increasing percentage of fragments returned to expansion, possibly in search for food or due to accumulation of metabolic byproducts.

Exposure to acidification has been shown to cause a variety of impacts on the metabolism of marine invertebrate species (Pörtner et al., 2004). Invertebrates subjected to suboptimal environmental conditions such as lower pH are expected to display high metabolic energy demands in order to

maintain vital processes such as the acid-base regulation in extracellular and intracellular fluids (Lannig et al., 2010). One way to compensate for such demands is to increase food intake which was clearly not the case for the fragments of *V. flagellum*. Another strategy is to enter metabolically slower or depressed stages, which decreases physiological performance and can be reflected in lower oxygen consumption and growth rates (Pörtner 2004; Lannig et al., 2010). Moreover, acidification not only can cause metabolic depression but also shifts in metabolic processes such as protein synthesis (Pörtner et al., 2004) and protein catabolism (Zhao et al., 2017).

Viminella flagellum displayed a decrease in coral activity under acidified conditions which can consequently lead to lower energy input, however main metabolic rates such as oxygen consumption and tracer C respiration remained stable or even increased under acidified conditions. The increased oxygen consumption and tracer C respiration observed under acidified conditions are indications of increased metabolic demands. Moreover, changes in oxygen consumption and tracer C respiration were uncoupled: tracer C respiration increased in both food treatments (Figure 36) under acidified pH but oxygen consumption increased only in the low food treatment (Figure 34). The ratio of CO₂ to oxygen production, known as respiratory quotient, can be considered as an index of the substrate used to produce energy (Hatcher, 1989). When aerobic respiration oxidizes carbohydrates, it results in an equal ratio of CO₂ release and oxygen consumption but when proteins or lipids are used to produce energy, less CO₂ is released for the same volume of consumed oxygen, leading to lower ratios of respiratory quotient. Estimates of oxygen consumption can consist an overall sum of various energy consuming processes, complicating precise estimates and interpretation of the respiratory quotient (Lannig et al., 2010). In addition, in the present study it was not possible to determine bulk DIC respiration (see materials and methods). Nevertheless, the uncoupling between the patterns in tracer C respiration and oxygen consumption in the case of *V. flagellum* fragments under acidified conditions is a strong indication of a change in metabolic processes among fragments in the two food treatments. Further analysis of the collected data is needed to provide insights to these changes.

Responses to OA seem to be case-specific, depending on the taxa, species, life history stage, location, or even depth (Kroeker et al., 2010; Kroeker et al., 2013; Georgian et al., 2016). A number of studies have investigated the impacts of OA on cold-water scleractinians, reporting decrease in respiration rates (Hennige et al., 2014), up-regulation of stress and immune related genes (Carreiro-Silva et al., 2014) and differential responses regarding growth (Movilla et al., 2014) and calcification (Buscher et al., 2017; Maier et al., 2009). Only a few studies have focused on cold-water octocorals, including mainly work on the red coral *C. rubrum* in the Mediterranean (Cerrano et al., 2013; Bramanti et al.,

2013). To our knowledge, this is the first study providing detailed insights to the combined effects of OA and food availability on the metabolism and growth of a cold-water octocoral.

Cold-water octocorals are fundamental players in deep-sea communities in the North Atlantic and especially in the Azores Archipelago where coral gardens constitute the major CWC habitat (Braga-Henriques et al., 2013). In these communities cold-water octocorals increase habitat complexity which has been marked as a fundamental element in marine communities with high biodiversity (Levin et al., 2001) and therefore high level ecosystem functioning (Danovaro, 2008). Negative impacts of acidification on the species physiology, such as the one described for *V. flagellum*, may not directly affect their survival but are expected to impact other processes such as long-term growth and reproduction with possible detrimental effects on the population level (Portner et al., 2004). Furthermore, such impacts are expected to affect the ecological performance of the species which in the case of habitat formers can lead to cascading negative effects on the whole community.

3.3 Ecotoxicological studies on the sponge *Halichondria panicea*

Authors: Johanne Vad, Theodore B. Henry, Murray Roberts

Little is known about the capacity of sponges to cope with environmental stressors such as chemical pollution. Sponges high filtration rates mean that they can bioaccumulate a range of chemicals including polycyclic aromatic hydrocarbons (PAHs) (Batista et al., 2013; Mahaut et al., 2013), polychlorinated bisphenyls (Gentric et al., 2016) and metals (Olesen and Weeks, 1994; Berthet et al., 2005). While this has led to research on sponges for biomonitoring purposes (Châtel et al., 2011; Batista et al., 2013; Mahaut et al., 2013; Gentric et al., 2016), the biological impacts of contaminants in sponges, including petroleum hydrocarbons, have remained poorly understood. PAHs have been shown to inhibit sponge *Crambe crambe* larvae settlement (Cebrian and Uriz, 2007). Furthermore, exposure to the PAH Benzo[a]Pyrene (BaP) induced DNA damage in *Tethya lyncurium* (Zahn et al., 1981, 1983). Activation of the mitogen-activated protein kinases (MAPK) cell signalling pathway has also been detected in *Suberites domuncula* exposed to diesel contaminated seawater (Châtel et al., 2011). However, further studies are needed to better understand the physiological impacts in sponges of petroleum hydrocarbons that can occur, at high concentrations, during an accidental spill.

To study the impact of oil and dispersants on sponges in a laboratory environment, water accommodated crude oil fractions (WAFs) and chemically enhanced WAFs (CEWAFs) should be used. WAF is defined as a laboratory solution produced by mixing crude oil and seawater with limited energy (slow stirring speed without the formation of a vortex) (Aurand and Coelho, 2005). The resulting

solution should be free of visible oil droplets (Aurand and Coelho, 2005). CEWAF is defined as a laboratory solution obtained by mixing crude oil, chemical dispersant and seawater with medium energy (medium stirring speed with small vortex formation) (Aurand and Coelho, 2005). The resulting solution can contain small oil droplets in suspension (Aurand and Coelho, 2005). No study to date has yet investigated the impact of crude oil WAF and CEWAF on sponges.

Amongst temperate shallow-water sponges, *Halichondria panicea* is a species that has been more widely studied. Early publications have described *H. panicea* seasonal growth rate, silica uptake, reproduction and physiology (Barthel, 1986, 1988; Riisgard et al., 1993; Thomassen and Riisgaard, 1995; Frøhlich and Barthel, 1997; Schönberg and Barthel, 1997; Osinga et al., 1999) while later work focussed on the bacterial community associated with this sponge species (Althoff et al., 1998; Wichels et al., 2006; Schneemann et al., 2010). The relationship between *H. panicea* and its environment and how the sponge interacts with other organisms such as mussels and nudibranchs have also been investigated (Knowlton and Highsmith, 2005; Khalaman and Komendantov, 2016; Khalaman et al., 2017). More recently *H. panicea*'s diet, filtration rate and dynamic osculum behaviour have also been researched (Riisgård et al., 2016; Kumala et al., 2017). Some information on the sponge tissue organisation is also available (Erkes-Medrano et al., 2015). Furthermore, the impact of cadmium pollution on *H. panicea* physiology has been studied (Olesen and Weeks, 1994). Widely present in Scotland at intertidal depth (Ackers et al., 2007), *H. panicea* is easy to sample and therefore constitutes an ideal model sponge species to use in experimental work. The objective of the experimental work presented here was therefore to determine the physiological impacts of WAF and CEWAF on the marine shallow-water sponge *H. panicea*.

Materials and Methods

Sample collection *H. panicea* samples were collected at Coldingham bay, located 80 km to the south of Edinburgh, Scotland. *H. panicea* can easily be found in the bay, at low tide, colonising rocks underneath kelps where it grows in a yellow-green encrusting/cushion morphotype (Figure 38ABC). Sponges were carefully removed with a scalpel from the rocks and placed into sampling bags filled with freshly collected seawater. Upon return to the University of Edinburgh, samples were kept in retention tanks in a cold-room at 10° C, for up to three weeks, prior to the. Surface seawater were also collected at Coldingham bay to be used for the preparation of treatment solutions. Upon return to the University of Edinburgh, the seawater samples were also kept in a cold-room at 10° C and aeration was provided until the samples were needed.



Figure 38: *Halichondria panicea* from Coldingham bay. (A) *H. panicea* colonising a rock collected from Coldingham bay (B) Sample in incubation chamber (C) Close-up of healthy *H. panicea* with three oscula.

Experimental apparatus To conduct exposure experiment with *H. panicea*, bespoke incubation chambers in a flow-through experimental apparatus were used. In total, 16 chambers of 750 mL of volume were manufactured. The chambers were made of a beaker of 80 mm in diameter in tempered glass while the lid was constructed of PTFE (Figure 39A). Each subset of four incubation chambers could be placed onto a holding plate and the lids could be locked onto the chamber by tightening a metal panel with bolts placed above the lid (Figure 39B). A water-proof magnetic rotor column was attached to the centre of each holding plate. This magnetic rotor column enabled the magnetic stirrers attached to the lids of the four chambers placed around the column to move (Figure 39B). Each lid was also equipped with a Presens sensor spot (Presens Precision Sensing GmbH, Germany) enabling direct respiration measurement without the need to transfer the sponge into respiration chambers as well as inflow and outflow valves. The inflow valves were fitted with inner PTFE tubing so that inflow water entered from the lower half of the chamber (Figure 39AB).



Figure 39: Incubation chambers and experimental apparatus. (A) Incubation chamber with (1) locking system, (2) inflow PTFE tube and (3) magnetic stirrer. (B) Holding plate with four incubation chambers. At the centre of the plate, a waterproof magnetic rotor column controls the magnetic stirrers in the four adjacent chambers. (C) Experimental apparatus with (1) Duran® bottles containing the treatment solutions, (2) Marine Color™ peristaltic pumps, (3) incubation chambers on holding plates and (4) used seawater collection bucket.

Chambers were connected through PTFE tubing to three six-channel Marine Color™ peristaltic pumps (Figure 39C). Each channel of the peristaltic pumps was itself connected back to a one litre Duran® bottle containing the relevant treatment solution (Figure 39C). Air bubbling was provided into the Duran® bottle through PVC tubing connected to glass Pasteur pipettes so that the treatment solutions were only in contact with the glass pipette. Flow was set at 750 mL per 24 h to allow replenish the chamber every day.

Experimental design To investigate the impact of WAF and CEWAF on *H. panicea* physiology, two types of experiments were conducted: a single concentration experiment and two dose-response experiments. In the single concentration experiment, sponge samples were exposed to WAF (1 g/L of oil), CEWAF (1 g/L of oil with dispersant) and BaP (10 ppb as described in Zahn et al., 1983) dissolved in DMSO for 48 h (three replicates per treatment). Sponge samples were also kept in two control conditions: seawater and DMSO (three replicates per condition). Sponges were placed in the incubation chambers described above and left to acclimatise for 48 h before starting the exposure.

Sponges were then exposed for 48 h to the relevant treatment solution. Clean seawater was pumped back into the chambers for another 48-hour period before the end of the experiment. Dose-response experiments were also conducted during which sponges were exposed to increasing nominal concentrations of crude oil (WAF dose-response) or crude oil and dispersants (CEWAF dose-response) for 48h. For both treatments, the nominal oil loading ranged from 0.01 g/L to 10.0 g/L of oil. Sponges were placed in their chambers and left to acclimatise for 48 h before exposure, as for the single concentration experiment. The sponges were then exposed to their treatment for 48 h after which the experiments were terminated.

Treatment preparation In all experiments presented in this thesis, Schiehallion crude oil (BP) and dispersant Slickgone NS (Dasic International) were used. Schiehallion crude oil is produced at Schiehallion oil field in the Faroe-Shetland channel and was provided by BP. The crude oil is characterised by an American Petroleum Institute gravity of 25.2, a sulphur content of 0.46 % and a viscosity of 67 centistokes (cST) at 20°C (BP, 2017). Slickgone NS, provided by the Oil Spill Response Limited, is one of the dispersants approved for use by the United-Kingdom Marine Management Organisation and is listed for potential use in the Faroe-Shetland channel in the case of a spill (BP, 2014; Marine Management Organisation, 2018).

The chemical response to oil spills ecological research forum (CROSERF) protocol, which allows for the preparation of WAF and CEWAF at different nominal oil loadings, was followed (Aurand and Coelho, 2005). For the single concentration experiment, WAF at 1 g/L of oil loading and CEWAF at 1 g/L of oil loading were prepared. For the dose-response experiments, WAFs and CEWAFs at 0.01, 0.03, 0.05, 0.1, 0.5, 1.0, 2.5, 3.5, 5, 7.5 and 10.0 g/L oil loadings were prepared. The amount of crude oil added to seawater was first weighed. A glass syringe was used to sample and transfer the crude oil to a Duran® bottle filled with one litre of seawater. The glass syringe was weighed before and after the transfer to determine the exact weight of oil added to the seawater. When preparing CEWAF, dispersant was applied after the addition of the oil to the seawater at a volume ratio of 1:10 as advised by the manufacturers (Dasic International OSD Limited, 2018). The mixture was then mixed for 18 hours using a magnetic multi-plate stirrer at low (for WAF) or medium speed (for CEWAF). At the end of the 18 h mixing time, solutions were left to settle for three hours and the water fraction was then carefully removed and used in the experiments.

BaP (positive control) and dimethyl sulfoxide (DMSO) (negative control along with seawater) solutions were also prepared for the single concentration experiment. A stock solution of BaP in DMSO at a concentration of 0.1 g/L was first prepared. For the BaP treatment solution, 100 µL of stock solution was then added to 999.9 mL of seawater prior to the use in the experiment (no mixing time was

allowed for this treatment). The same volume of DMSO only was also added to seawater in the DMSO only treatment.

Sponge volume determination The volume of each sponge sample, to be used for the normalisation of the respiration and clearance rate, was determined at the end of each experiment. The thickness of the sample was measured directly with a calliper. A photography was then taken of each sample and the freely available software Fiji was used to determine the surface area of the sample (Schindelin et al., 2012). Surface area was then multiplied by the thickness to determine the sponge volume. For this technique to be precise, the thickness of the tissue needs to be homogenous throughout the sample. *H. panicea* present at Coldingham Bay are of an encrusting morphotype, with little variation in the layer thickness. Standardisation to the volume is therefore here applicable and was chosen even though standardisation to other parameters, such as carbon content, could have also been considered.

Respiration rate measurements Respiration rate was determined by analysing the decrease in O₂ over time in each chamber. Concentration of O₂ in each chamber was measured every 15 seconds during two hours using Presens sensor spots connected to Oxy-4 optodes (Presens Precision Sensing GmbH, Germany). A two-hour time period was enough to detect a significant change in O₂ concentration in the respiration chamber. Stirring in the chambers was kept active during the measurement time but the inflow and outflow were closed so no fresh input of seawater was added. To account for microbial respiration in the seawater, blank measurement of respiration in seawater and treatment solutions were also determined in empty chambers. %O₂ was converted to µmol/L using the R package presens (Birk, 2016). Sponge respiration rate were then determined using the following formula:

$$\text{Respiration rate} = (\text{Resp}_{\text{Chamber}} - \text{Resp}_{\text{blank}}) / V_{\text{sponge}}$$

where Resp_{chamber} is the respiration rate determined in the chamber with a sponge, Resp_{blank} is the respiration rate determined in the blank chamber without a sponge and V_{sponge} the volume of sponge tissue (determined at the end of the experiment).

Clearance rate measurements Clearance rate is an estimation of the amount of water filtered by the sponge per unit of time and per unit of sponge volume and can be used as a proxy for filtration rate. To determine clearance rate, Isochrysis Instant Algae® (Reed Mariculture, California) diluted solution was added to each chamber and the sponges were left to filter for two hours. Stirring in the chambers was kept active during the measurement time but the inflow and outflow were closed so no fresh input of seawater was added. Water samples were collected every 20 minutes and algae cell

concentrations were determined through total absorbance measurements. Clearance rates for each sample was calculated as follows (De Goeij et al., 2008):

$$\text{Clearance rate} = ((V_{\text{water}}/t) \ln(C_0/C_t)) / V_{\text{sponge}}$$

where V_{water} is the volume of water in the chambers, t the time of incubation, C_0 and C_t the initial and final concentration of algae in the chamber and V_{sponge} the volume of sponge tissue.

Statistical analysis To determine if treatment influenced respiration and clearance rates during and after exposure in our single concentration experiment, a repeated-measure Analysis of Variance (ANOVA) was carried out with Rstudio (R Core Team, 2017). Using the R package lme4 (Bates et al., 2015), a linear mixed-effect model was fitted to each data set with treatment, time, treatment*time as fixed explanatory factors and individual sponge as a random effect. Residual normal distribution and sphericity was checked graphically. To determine the effect of increasing oil loading in WAF and CEWAF solutions on respiration and clearance rate (dose-response experiments), a dose-response analysis was performed using the package drc (Ritz et al., 2015). A dose-response model was fitted to each dataset (respiration and clearance) using a Weibull 1 three parameter (upper asymptotic limit, slope and ED50) function with treatment as a grouping factor. As controls from WAF and CEWAF experiments did not statistically differ from each other, the model was constrained to a single asymptotic limit while slope and ED50 were estimated independently for each treatment. A lack-of-fit test and no effect test were then carried out to determine if the models were significant. Further comparison of significant parameters between treatments was also carried out using the package drc (Ritz et al., 2015).

Results and Discussion

Gross observations All *H. panicea* samples kept in control conditions survived the experiments, appeared healthy and still displayed their natural sharp yellowish green colours at the end of the experiments. Furthermore, all *H. panicea* samples survived the 48 h exposure to DMSO, BaP and WAF during the single concentration experiment and the 48 h exposure to WAF in the dose response experiments (at all oil loadings). These samples also appeared healthy as no signs of external tissue damage could be detected, and their colour remained unchanged until the end of the experiments. When considering the CEWAF treatment, all sponges survived the exposure in the single concentration experiment (1g/L of oil with dispersant). However, some samples exposed to the highest oil loading in the CEWAF dose response experiment showed significant rapid external tissue decay, displaying patches of dark tissue and died within the first 24 h of the total 48 h exposure. Specifically, sponges

exposed to 3.5 g/L, 7.5 g/L (one of the two replicates survived) and 10 g/L of oil with dispersant did not survive the exposure.

Single concentration experiment Respiration rates between individuals across the single concentration experiment varied greatly. Overall, respiration rate ranged from 0.6 (BaP ind. 1 after exposure) to 35.3 $\mu\text{mol cm}^{-3} \text{ hour}^{-1}$ (Control ind. 3 during exposure) (Figure 40). No clear pattern could be determined (Figure 40) and no statistical differences between treatment (p-value=0.34), time (p-value =0.53) or time*treatment (p-value =0.89) were detected by the repeated-measures ANOVA (Table 12). Clearance rates also varied between individuals and throughout the single concentration experiment, but a clear pattern could be detected in these data (Figure 40).

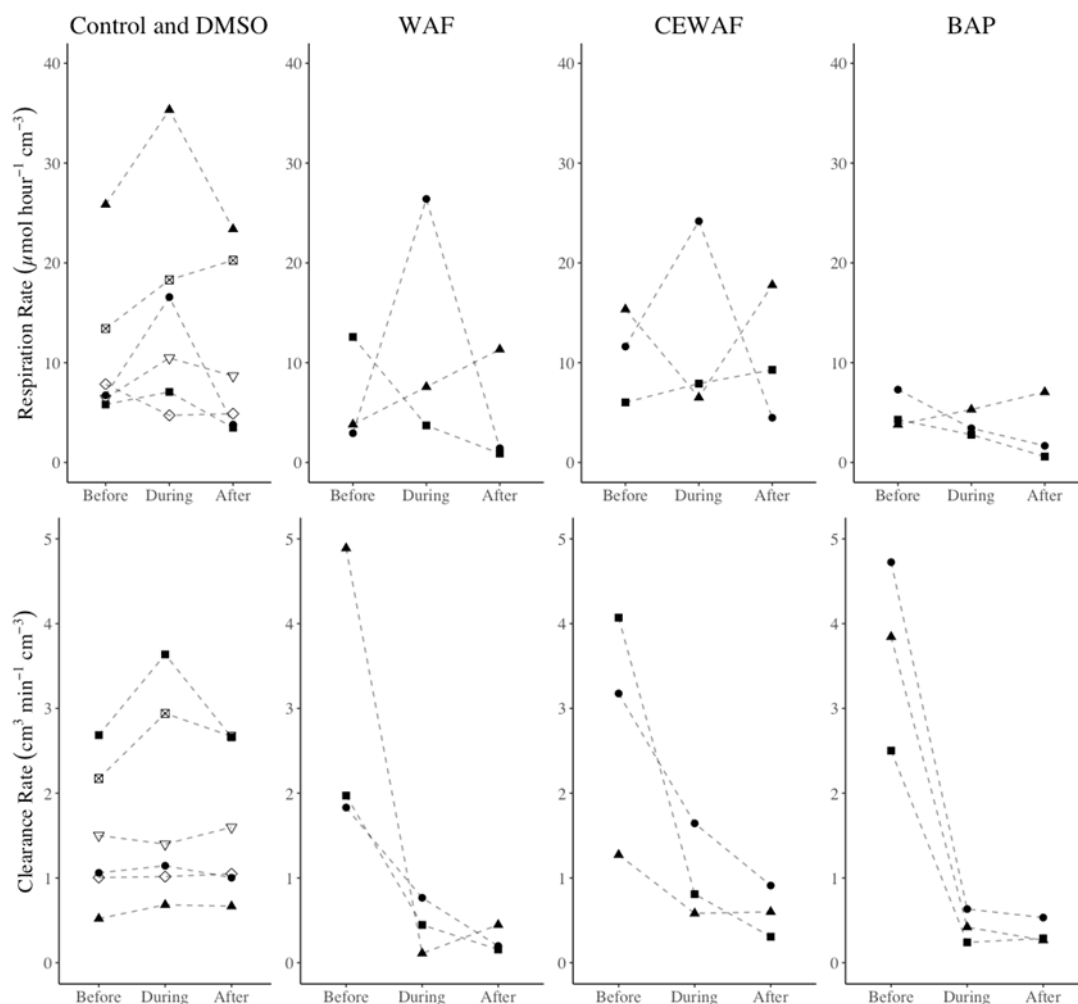


Figure 40: Physiology results of the single concentration exposure experiment. In the first panel, full symbols represent control sample measurements whereas empty symbols represent DMSO sample measurements

A sharp decrease in clearance rate was measured in all samples exposed to WAF, CEWAF and BaP during the exposure and the clearance rate remained low 48 h after the end of the exposure (Figure

40). All values measured in samples in control and DMSO conditions across the experiment as well as in samples before exposure in hydrocarbon treatments ranged between 0.5 (Control ind. 3 before exposure) and 4.9 $\text{cm}^3 \text{cm}^{-3} \text{min}^{-1}$ (WAF ind. 3 before exposure). In the hydrocarbon treatment conditions (WAF, CEWAF and BaP) during and after exposure, clearance rate decreased to a minimum of 0.1 $\text{cm}^3 \text{cm}^{-3} \text{min}^{-1}$ (WAF ind. 1 after exposure). Time (p -value=1.61e-08) and Treatment*Time (p -value=3.01e-05) appeared as strongly statistically significant in the repeated-measures ANOVA (Table 12).

Table 12: Results of the repeated-measures analysis of variance (ANOVA) on respiration and clearance rates from the single concentration exposure experiment. Element in bold highlight statistical differences

Response Variable	Explanatory variable	χ^2	Degrees of Freedom	Pr(> χ^2)
	Treatment	4.4808	4	0.3448
Respiration rate	Time	0.3949	1	0.5298
	Treatment*Time	1.1318	4	0.8892
	Treatment	0.8513	4	0.9314
Clearance rate	Time	31.9094	1	1.615e-08
	Treatment*Time	26.1080	4	3.010e-05
	Treatment	0.8513	4	0.9314

Dose-response experiments Physiological data gathered in the dose-response exposure experiments were in accordance with the data collected during the single concentration experiment. Respiration rate varied across individuals in both the WAF and CEWAF experiments and ranged from 1.1 (7.5 g of oil/L with dispersant) to 22.9 $\mu\text{mol cm}^{-3} \text{hour}^{-1}$ (1 g of oil/L) (Figure 41). No clear pattern was detected in the data (Figure 41) and no dose-response models appeared to fit the data or to detect any effect of oil loading on respiration rate. Clearance rate rapidly decreased with increasing oil loading in both the WAF and CEWAF dose-response experiments (Figure 41). Clearance rate in control conditions varied from 0.3 to 5.5 $\text{cm}^3 \text{cm}^{-3} \text{min}^{-1}$ across WAF and CEWAF experiments. The lowest clearance rate in the WAF exposure only reached 0.3 $\text{cm}^3 \text{cm}^{-3} \text{min}^{-1}$ (at 10 g of oil/L) while the lowest clearance rate measured in the CEWAF experiment dropped to 0.01 $\text{cm}^3 \text{cm}^{-3} \text{min}^{-1}$ (at 5 g of oil/L with dispersant).

Overall clearance rates in samples exposed to CEWAF were lower than those measured in samples exposed to WAF at the same oil loading. All coefficients of the Weibull 1 log-logistic dose response model (slope, upper asymptotic limit and ED50) were statistically significant (Table 39). The model fitted the data well (lack of fit test p -value=0.84) and a dose effect on clearance rate was statistically significant (p -value=6.4e-07) (Table 32). CEWAF ED50 (0.04 g/L of crude oil with dispersant) differed statistically from WAF ED50 (1.56 g/L of crude oil), however the slopes for each dataset did not differ significantly (Tables 12 and 13).

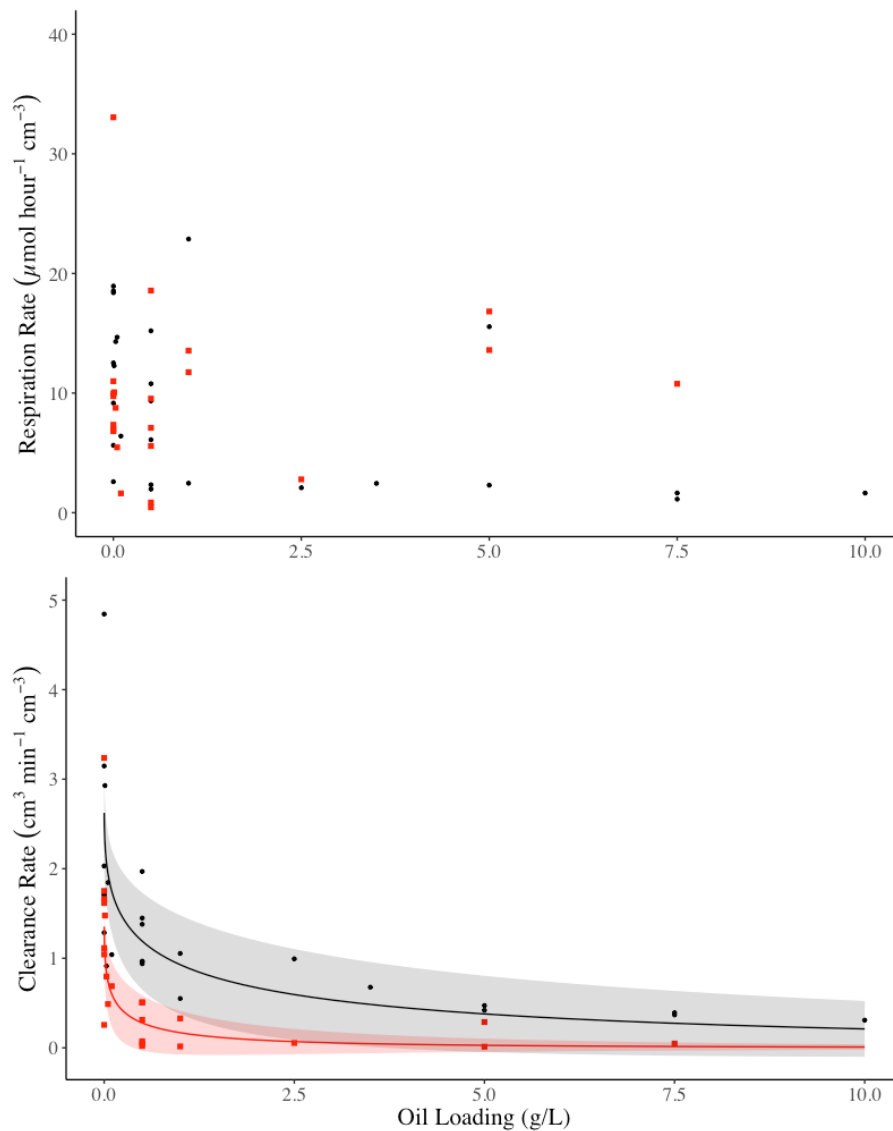


Figure 41: Dose-response physiology measurements. WAF measurement are in black dots and CEWAF measurements are in red squares. The clearance rate dose-response model is plotted in black for WAF samples and in red for CEWAF samples. Ribbons around each curve represent the confidence intervals

Table 13: Results of the dose-response model applied to clearance rate from the dose-response experiments. Elements in bold highlight statistical differences

Parameters estimates				
	Estimate	Std Error	t-value	p-value
Slope WAF	0.369172	0.120051	3.0751	0.000104
ED50 WAF	1.560996	0.482497	3.2458	0.003609
Slope CEWAF	0.326211	0.076470	4.2659	<2.2e-16
ED50 CEWAF	0.043311	0.018123	2.3910	0.021145
Upper Asymptote	2.229147	0.070923	31.4304	0.002242
Lack Of Fit Test				
Model Degrees of Freedom	RSS	Degrees of Freedom	F-value	p-value
44	31.901	17	0.6226	0.8446
No Effect Test				
	χ^2 test	Degrees of Freedom	p-value	
	3.431826e+01	4	6.411789e-07	

Table 14: Results of parameter comparison tests between dose-response model estimates. Elements in bold highlight statistical differences.

Parameter compared	Estimate	Std Error	t-value	p-value
ED50	0.027668	0.045363	-21.434	<2.2e-16
Slope	0.88363	0.87114	-0.3458	0.7311

Implication for future work

Both respiration rate and clearance rate were measured during the exposure experiments conducted in this study but only clearance rate was impacted by exposure to hydrocarbons. Respiration rates from the single concentration experiment and the dose-response experiments were highly variable and did not seem to change with exposure to hydrocarbons. The high variability seen in these measurements is, however, in accordance with the literature available for *H. panicea* (reviewed in Osinga *et al.*, 1999). Clearance rates measured in both the single concentration experiment and in the dose-response experiments also displayed high inter-individual variability, which is in accordance with literature available for other encrusting sponges (De Goeij *et al.*, 2008). However, in contrast to respiration rate, clearance rate decreased sharply in sponges exposed to WAF or CEWAF, even at low oil loading. A decrease in filtration rate was also observed in *H. panicea* exposed to cadmium (Olesen and Weeks, 1994), showing that this appears to be a typical physiological response to pollutants in *H. panicea*. Concentration of cadmium over 100 µg/L led to longer term filtration loss with filtration rate remaining low for several hours after exposure (data only available for 4 h in the study) (Olesen and Weeks, 1994). This is also in accordance with observations made in the single exposure experiment where sponges exposed to hydrocarbon treatments (WAF, CEWAF and BaP) displayed lowered clearance rate even 48 h after the end of the exposure. It is likely that stopping its filtration activity for extensive periods of time will strongly impact survival of *H. panicea*. The capacity of sponges to survive longer exposure periods should therefore be investigated.

4 Physiological model of cold-water corals and sponges under different scenarios of environmental change (flow velocity and food supply)

Authors: Evert de Froe, Dick van Oevelen, Karline Soetaert

Deep-water sponges and CWCs are key biotic components of the deep Atlantic Ocean ecosystem, as they form structurally complex habitats that sustain high biotic abundance and biodiversity at the seafloor (Hogg *et al.*, 2010; Roberts *et al.*, 2006). Although these reef-forming systems are increasingly recognized as important deep-sea habitats, our capacity to predict their occurrence, let alone biogeochemical activity, relies solely on statistical models in which sponge (e.g. Knudby *et al.*, 2013) or coral (Davies and Guinotte, 2011; Rengstorf *et al.*, 2014; Tittensor *et al.*, 2010) occurrence is related to environmental variables such as temperature, salinity, seafloor rugosity, aragonite saturation state and surface productivity.

Another approach to predicting CWC reef or sponge ground occurrence is by developing models that are stronger rooted in mechanisms. A recent study showed that sponge grounds and CWC reefs jointly process almost 30% of the flux of OM to the seafloor via benthic-pelagic coupling on the Norwegian shelf, a contribution which has hitherto been missed in budget estimates (Cathalot et al., 2015). The enhanced OM processing rates have been confirmed in several studies conducted at ATLAS case study areas (Deliverable 2.3, in prep) The high rates of OM processing by these reefs, however, imply that sponges and corals manage to 'circumvent' the food limitation that is characteristic for life at the deep seafloor (Wei et al., 2010), indicating that OM availability is an important predicting factor in the occurrence of sponge or coral ecosystems. In addition, recent reports suggest that living CWCs and DWS are the main contributor to benthic respiration in their respective habitats (de Froe et al, in prep; D2.3.; Cathalot et al., 2015). These results suggest that we can use CWC and DWS biomass as a proxy for the environmental status of the ecosystem. Another consideration is including the hydrodynamics at the site, which is responsible for downslope transport of surface waters (Duineveld et al., 2007; White et al., 2005), downward convection over reefs (K. Soetaert, pers. comm.) and enhanced particle transport over a reef ecosystem through accelerated currents and elevated turbulence (Mienis et al., 2007; Soetaert et al., 2016; Van Haren et al., 2014, D2.4, in prep). Also, from a geological perspective, Hebbeln et al. (2019) (Deliverable 1.4) identified food availability and hydrodynamics as key and consistent explanatory factors describing the rise and demise of CWC reefs at geological time scales. In their analysis, also other factors such as oxygen concentration, salinity and temperature were considered and although these factors were deemed relevant for individual reef systems, the factors food availability and hydrodynamics (albeit both quite loosely and qualitatively defined) explained coral at all studied reef systems.

Hence, a more mechanistic approach to predict CWC and sponge biomass should at least include the factors food availability and hydrodynamics. Soetaert et al. (2016) developed a method to predict OM in the water column based on export from the photic, degradation, sinking and advective transport by local hydrodynamics, with the latter forcing received from a local high-resolution hydrodynamic model. The current velocity and OM concentrations in the bottom layer predicted by such a model may then set limits on the growth of coral and sponge biomass. A classic way to model the development of faunal biomass in aquaculture (Stigebrandt, 2011) or natural settings in through the use of carrying capacity. The carrying capacity sets the maximum amount of biomass that can be sustained by the environment, while limiting factors can be included that determine how much of the carrying capacity can be realized. The limiting factors that need to be included differs between sponges and corals. Both taxa are opportunistic organisms, which feed on a variety of OM sources that are suspended in the water column (Mueller et al., 2014; Yahel et al., 2007), with one crucial

difference. Sponges actively filter large amounts of seawater through their internal aquiferous system (Leys et al., 2011). Hence, the feeding rate of sponges is proportional to the food concentration in the water column. In contrast, CWC are 'passive' suspension feeders that 'catch' organic resources with tentacles and therefore depend on the flux of food particles (i.e. current velocity x food concentration) that passes at a given location (Shimeta and Jumars, 1991). At the same time, too low food concentrations or fluxes prohibits the development of extensive sponge or coral reefs in the deep ocean due to energy limitation. A recent paper suggests that these differences in feeding mode was responsible for the higher food uptake of sponges in incubation experiment (Van Oevelen et al., 2018).

Other physiological parameters that feature in the carrying capacity modelling include assimilation efficiency and respiration rates, which we have compiled from the literature in D2.1 and are estimated for other species in this Deliverable. The carrying capacity model can also be easily extended to predict consequences of increasing temperature (e.g. Dodds et al., 2007; McClain et al., 2012) or OA (McCulloch et al., 2012) on biomass development by increasing respiration or maintenance rates accordingly. Deliverable 2.1 provides a compilation of experiments have assessed how respiration was affected by warming and OA.

An important goal of WP2 is to link biomass development of CWC and DWS to environmental forcing. In this section, we develop physiological models for passive (i.e. CWC) and active (i.e. sponges) suspension feeders based on literature and experimental data (see section 3) on physiological parameters such as respiration and assimilation efficiency. For illustrative purposes, we here also link the respective physiological models to theoretical trajectories of variable food supply. Results reported here will be followed in Deliverable 2.5, where the physiological models will be linked to realistic food supply predictions from the coupled hydrodynamic (D2.4) and biogeochemical (D2.5) models. Hence, our goal here is to develop comparatively simple physiological models that are based on parameters from the literature (D2.1) and data from recent experiments reported here, which will eventually be implemented in the computational heavy biogeochemical-hydrodynamic models in D2.5.

Materials and methods

Model set-up The physiological models for passive (PSF) and active (ASF) suspension feeders consists of the state variables PSF and ASF benthic biomass (mmol C m^{-2}). As detailed below, the main difference between the model formulations for PSF and ASF is that the former depends on the organic matter *flux* for the uptake of food particles from the water column, while ASF depend on the organic matter *concentration* for their food uptake (Van Oevelen et al., 2018).

The physiological model for PSFs is given by:

$$\frac{d\text{PSF}}{dt} = AE_{\text{PSF}} \cdot NGE_{\text{PSF}} \cdot v_{\text{bb1}} \cdot OM_{\text{bb1}} \cdot A_{\text{PSF}} \cdot \left(1 - \frac{\text{PSF}}{CC_{\text{PSF}}}\right) - m_{\text{PSF}} \cdot \text{PSF}$$

in which AE_{PSF} is the assimilation efficiency of PSF (-), NGE_{PSF} the net growth efficiency of PSF (-), v_{bb1} is the current velocity (i.e. $\sqrt{u_{\text{bb1}}^2 + v_{\text{bb1}}^2}$) in the benthic boundary layer (m d^{-1}), OM_{bb1} is the OM concentration in the benthic boundary layer (mmol C m^{-3}), A_{PSF} is the carbon-specific surface area for PSF ($\text{m}^2 \text{mmol}^{-1} \text{C}$), CC_{PSF} is the carrying capacity of PSF biomass on the seafloor (mmol C m^{-2}) and m_{PSF} is maintenance respiration (d^{-1}).

The physiological model for ASF (i.e. sponges) is similar to that of PSF, although uptake of OM is not dependent on bottom flow, as active filter feeders maintain their own current velocity for OM uptake:

$$\frac{d\text{ASF}}{dt} = AE_{\text{ASF}} \cdot NGE_{\text{ASF}} \cdot FR_{\text{ASF}} \cdot OM_{\text{bb1}} \cdot \left(1 - \frac{\text{ASF}}{CC_{\text{ASF}}}\right) - m_{\text{ASF}} \cdot \text{ASF}$$

in which AE_{ASF} is the assimilation efficiency for ASF (-), NGE_{ASF} is the net growth efficiency for ASF (-), FR_{ASF} is the mass-specific filtration rate ($\text{m}^3 \text{mmol}^{-1} \text{C d}^{-1}$), CC_{ASF} is the carrying capacity for ASF (mmol C m^{-2}) and m_{ASF} is the mass-specific maintenance respiration rate for ASF (d^{-1}).

Values for v_{bb1} and OM_{bb1} will later be generated by the coupled hydrodynamic-biogeochemical model (D2.5) and will be given theoretical trajectories here for illustrative purposes (see below). The other physiological parameters, below for *L. pertusa* being a representative PSF of the Rockall Bank case study area and *Geodia* sp. as representative ASF for Davis Strait, are based on experiments conducted within ATLAS (see above) or on literature report (D2.1) (Table 155; Table 1616).

Table 15: Model parameters for the Passive Suspension Feeders (PSF)

Passive suspension feeders			
Parameter	Value	Unit	Source
AE_{PSF}	0.8	-	Fraction of ingested food particles available for digestion. No data available for <i>L. pertusa</i> . Estimated for tropical corals by (Anthony, 1999; Anthony et al., 2002)
NGE_{PSF}	0.3	-	Fraction of assimilated food particles that is incorporated into the coral tissue. Estimated from data reported in (Maier et al., 2019)
A_{PSF}	7.05e-05	$m^2 mmol^{-1} C$	Polyp surface per mmol C biomass. Based on data on number of polyps per weight of coral (Gori et al., 2014) and surface area per polyp (Purser et al., 2010)
CC_{PSF}	6000	$mmol C m^{-2}$	Maximum coral biomass on Rockall Bank. Estimated based on D2.3 and video survey.
m_{PSF}	0.00267	d^{-1}	Respiration after 28 weeks of starvation, reported by (Larsson et al., 2013).

Table 16: Model parameters for the Active Suspension Feeders (ASF).

Active suspension feeders			
Parameter	Value	Unit	Source
AE_{ASF}	0.80	-	Set to value for PSF
NGE_{ASF}	0.15	-	(Koopmans et al., 2010; Thomassen and Riisgard, 1995; Van Oevelen et al., 2018)
FR_{ASF}	3.6e-05	$m^3 mmol^{-1} C d^{-1}$	(Kutti et al., 2013a)
CC_{ASF}	30,000	$mmol C m^{-2}$	Maximum sponge biomass found with trawling surveys in Davis Strait.
m_{ASF}	0.000216	d^{-1}	Set to 15% (i.e. NGE) of the total respiration reported by (Kutti et al., 2013b; Leys et al., 2017)

Food supply The model equations were solved using an ODE solver from the R packages *deSolve* and *FME* (Soetaert et al., 2018; Soetaert and Petzoldt, 2010). Model simulations were run for four years and two different POM concentrations were used as a forcing function: a constant POM concentration of $0.10 mmol C m^{-3}$ for the entire simulation, and a variable POM concentration with every five days a food pulse of $0.10 mmol C m^{-3}$ (Figure 4242). For these two POM scenarios, we run the model simulations with five different flow velocities: 0.00, 0.25, 0.5, 0.75 and $1.00 m s^{-1}$.

Model results

At constant POM concentration, the PSFs grow to carrying capacity with flow velocity determining how quick their maximum benthic biomass is reached. However, when flow velocity is zero, the food ingestion for PSFs is zero and their biomass decreases to almost zero in the model. The here simulated maximum PSF benthic respiration ($500 \text{ mmol C m}^{-2} \text{ d}^{-1}$) is considerably higher than the reported maximum benthic respiration of a CWC reef ($250 \text{ mmol C m}^{-2} \text{ d}^{-1}$; Cathalot et al., 2015). The simulated benthic respiration when the PSF biomass is at its carrying capacity ($80 \text{ mmol C m}^{-2} \text{ d}^{-1}$) is similar to what observational studies reported ($20 - 140 \text{ mmol C m}^{-2} \text{ d}^{-1}$; D2.3., de Froe et al, in prep; Cathalot et al., 2015; Rovelli et al., 2015; White et al., 2012). However, when POM input is zero and growth respiration is not taken into account, the simulated total benthic respiration values are a factor 20 lower. The implied constant POM concentration of $0.1 \text{ mmol C m}^{-3}$ is not sufficient for ASF to increase its biomass. ASFs decrease from $1.0 \text{ mmol C m}^{-2}$ to $0.75 \text{ mmol C m}^{-2}$ over the course of the four-year simulation (Figure 4343).

At a variable POM concentration, the PSFs grow to carrying capacity when flow velocity is 0.50 m s^{-1} or higher. The PSF grow slower at a flow velocity of 0.25 m s^{-1} and reaches a biomass of $300 \text{ mmol C m}^{-2}$ after four years (Figure 4444). When flow velocity is 0.00 m s^{-1} the PSF biomass decreases to zero in the model. Benthic PSF's respiration varies with the enforced POM concentration and flow velocities. When POM is present, the flow velocity is higher than zero and the PSF biomass is at carrying capacity, the benthic PSF respiration ranges between $163 - 177 \text{ mmol C m}^{-2} \text{ d}^{-1}$. When POM is not present, the benthic PSF respiration of the populations at carrying capacity varies between $1.6 - 15 \text{ mmol C m}^{-2} \text{ d}^{-1}$. The POM pulse every five days is not sufficient to let the ASFs grow in the model. As in the constant POM concentration, the ASF biomass decreases from 1.0 to $0.75 \text{ mmol C m}^{-2}$ (Figure 445).

The lower POM *flux* in the variable POM scenario compared to the constant POM scenario causes a lower maximum PSF biomass in the models, and the PSF biomass follows different trajectories with the five different flow velocities. Also, the benthic PSF respiration differs between the two scenarios. The varying POM concentration causes, when POM is present in the model, the benthic PSF respiration to be twice as high than at a constant POM flux (80 vs $160 \text{ mmol C m}^{-2} \text{ d}^{-1}$). The varying POM concentration does not influence the trajectory of the ASF biomass, indicating the ASF need a much higher POM concentration than used in this model simulations. Looking closer at our model parameters, the decreasing ASF biomass also makes sense. The food supply for a PSF is determined by the water velocity times the food concentration, while for ASF food supply is determined by filtration velocity times the food concentration. The filtration capacity of PSFs can be determined by

multiplying its biomass specific surface area ($7.05e-05 \text{ m}^2 \text{ mmol C}^{-1}$) with the current velocity. Current velocities are typical between $0.1 - 0.2 \text{ m s}^{-1}$ and can reach up to 2.0 m s^{-1} , giving a filtration rate for PSFs between $7.05e-6$ and $1.41e-4 \text{ m}^3 \text{ mmol C}^{-1} \text{ s}^{-1}$. The filtration capacity of an active filter feeder is determined solely its filtration rate. For *Geodia* sp. the filtration rate is measured as from $4.166e-10 \text{ m}^3 \text{ mmol C}^{-1} \text{ s}^{-1}$ (Kutti et al., 2013b), which is 0.0005 % of the filtration capacity of a PSF in water flowing at 0.1 m s^{-1} . Therefore, in our current model, the ASFs need a high POM concentration to grow in biomass. Figure 45 presents the rate of change of ASF against the ASF's biomass for five POM concentrations. At a POM concentration of 50 mmol m^{-3} the ASF is able to grow in the model. This POM concentration is well above observed POM concentrations 10 meters above bottom (1.32 mmol m^{-3}) or even at the surface ($12.21 \text{ mmol m}^{-3}$) at sponge grounds in the Davis Strait. This finding provides evidence that for growth of ASF, we may need to consider adding the alternative food sources bacteria and dissolved organic matter (Leys et al., 2017) to the models in D2.5.

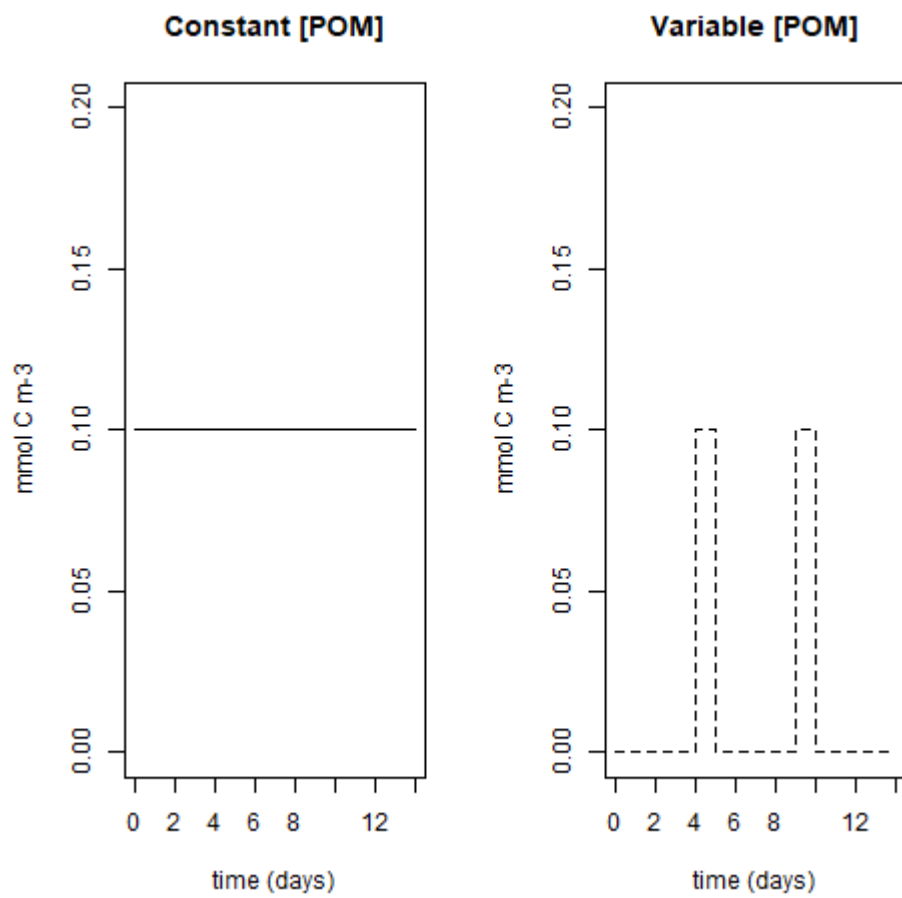


Figure 42: Two theoretical scenarios were simulated: one with a constant POM concentration (left panel) and one with a POM pulse every five days (right panel).

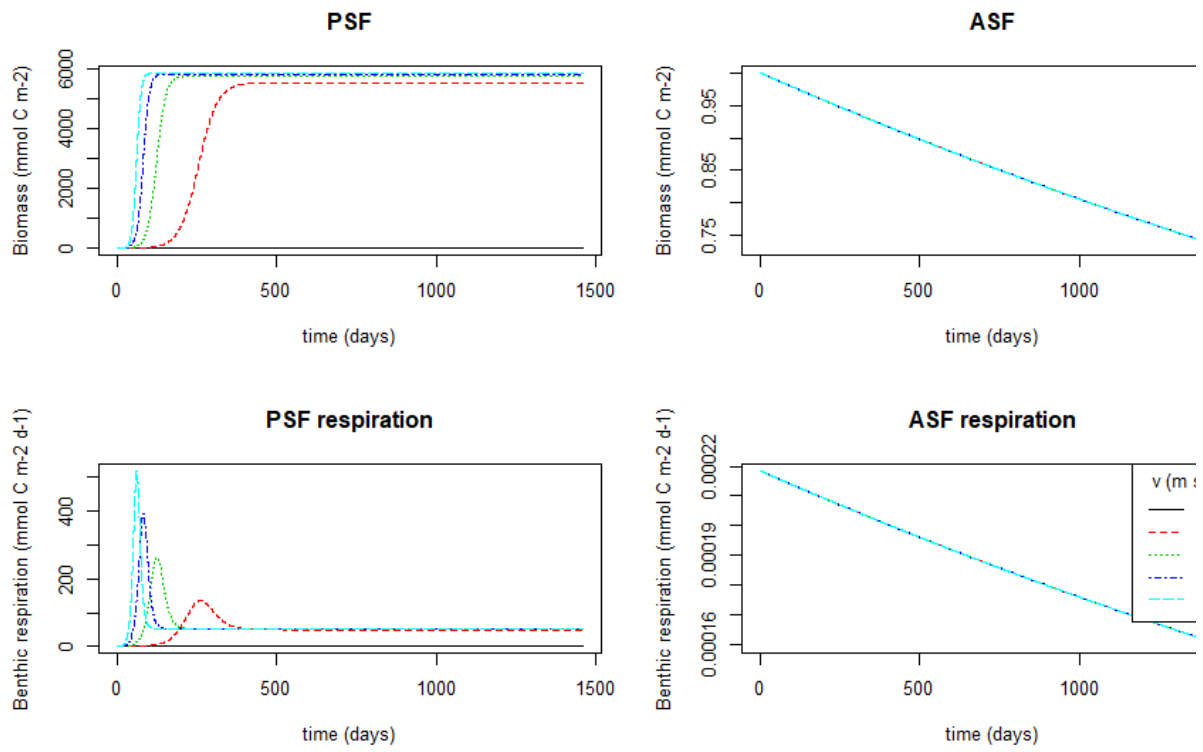


Figure 43: Model results at a constant POM concentration, for five flow velocities. PSF is the passive suspension feeders biomass, ASF is the active suspension feeders biomass, PSF and ASF respiration is the benthic respiration by PSF and ASF respectively.

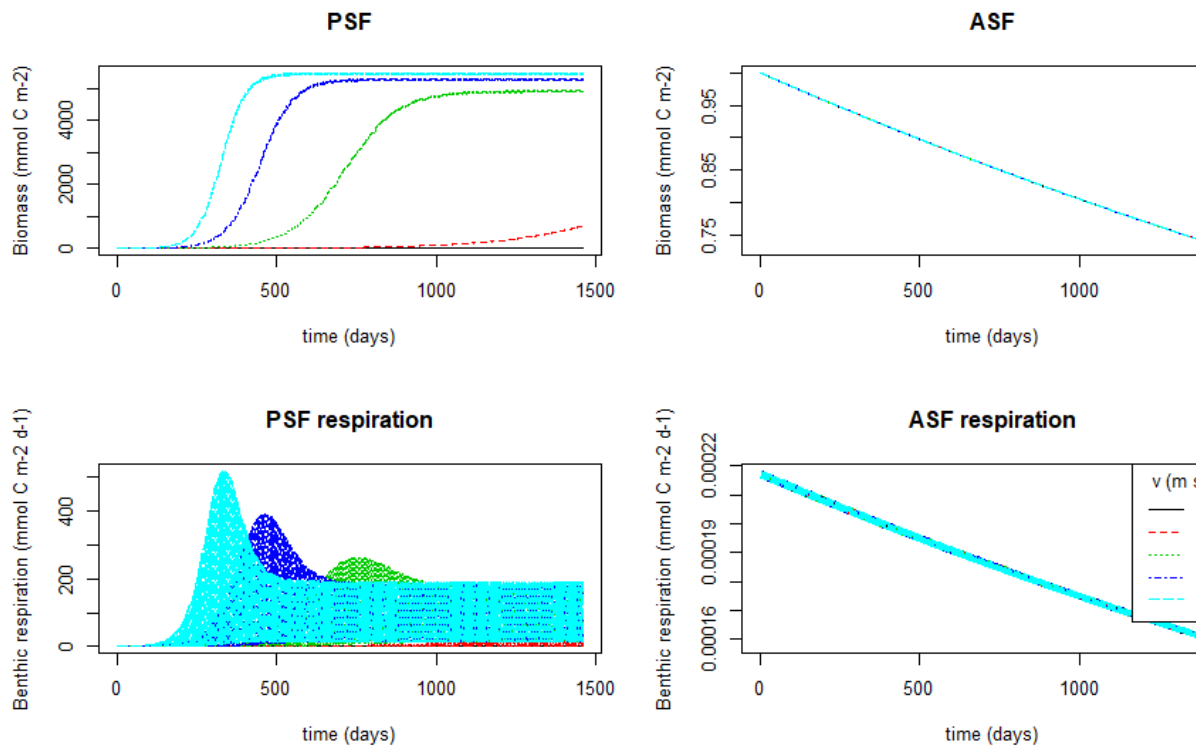


Figure 44: Model results at a variable POM concentration, for five flow velocities. PSF is the passive suspension feeders biomass, ASF is the active suspension feeders biomass, PSF and ASF respiration is the benthic respiration by PSF and ASF respectively.

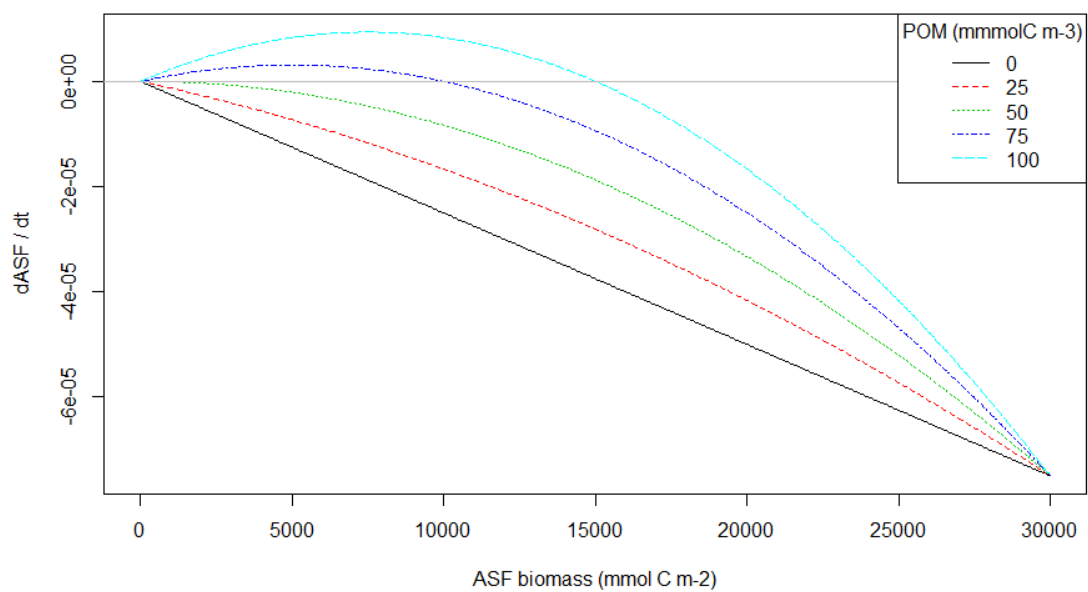


Figure 45: Rate of change for active suspension feeders (ASF) against the ASF biomass for five POM concentrations.

5 Conclusions and way forward

Experimental work conducted part of this deliverable has significantly contributed to improving our understanding of the feeding ecology and ecophysiology of important, but so far understudied, habitat forming species (e.g. black corals, octocorals, sponges). It has also shed some light on the potential consequences of altered food supply regimes and changes and OA on octocorals. However, there are other predicted climate-related changes, such as warming and deoxygenation, that may cause detrimental effects on these organisms and for which we did not have the opportunity to test here. Climate change is also occurring simultaneously to human pressures such as fisheries and deep-sea mining. It thus becomes urgent to determine the cumulative effects of climate change and local human stressors on these communities and on the functions and services they perform to meet ecological and societal needs.

Modelling results reported here improved our knowledge on how passive (i.e. CWC) and active (i.e. sponges) suspension feeders respond to different scenarios of environmental change (flow velocity and food supply). These physiological models will be linked to realistic food supply predictions from the coupled hydrodynamic (D2.4) and biogeochemical (D2.5) models, which will eventually be implemented in the computational heavy biogeochemical-hydrodynamic models in D2.5.

References

- Ackers, R. G., Moss, D., Picton, B. E., Stone, S. M. K., & Morrow, C. C. (2007). Sponges of the British Isles ("Sponge V"): A Colour Guide and Working Document. *Marine Conservation Society*.
- Alexander, B. E., Liebrand, K., Osinga, R., van der Geest, H. G., Admiraal, W., Cleutjens, J. P., ... & Goeij, J. M. (2014). Cell turnover and detritus production in marine sponges from tropical and temperate benthic ecosystems. *PLoS One*, 9(10), e109486.
- Althoff, K., Schütt, C., Steffen, R., Batel, R., & Müller, W. E. G. (1998). Evidence for a symbiosis between bacteria of the genus *Rhodobacter* and the marine sponge *Halichondria panicea*: Harbor also for putatively toxic bacteria?. *Marine Biology*, 130(3), 529–536. doi: 10.1007/s002270050273.
- Anthony, K. R. N. (1997). Prey capture by the sea anemone *Metridium senile* (L.): effects of body size, flow regime, and upstream neighbors. *The Biological Bulletin*, 192(1), 73-86.
- Anthony, K. R. N. (1999). Coral suspension feeding on fine particulate matter. *Journal of Experimental Marine Biology and Ecology*, 232, 85–106. doi:10.1016/S0022-0981(98)00099-9.
- Anthony, K. R. N., Connolly, S. R., & Willis, B. L. (2002). Comparative analysis of energy allocation to tissue and skeletal growth in corals. *Limnology and Oceanography*. 47, 1417–1429. doi:10.4319/lo.2002.47.5.1417.
- Aurand, D., & Coelho, G. (2005). Cooperative aquatic toxicity testing of dispersed oil and the chemical response to oil spills: Ecological Effects Research Forum (CROSERF). *Inc. Lusby, MD. Tech. Report*, 07-03.
- Baco, A. R., Morgan, N., Roark, E. B., Silva, M., Shamberger, K. E., & Miller, K. (2017). Defying dissolution: discovery of deep-sea scleractinian coral reefs in the North Pacific. *Scientific reports*, 7(1), 5436.
- Barthel, D. (1986). On the ecophysiology of the sponge *Halichondria panicea* in Kiel Bight . I . *Substrate specificity, growth and reproduction*, 32, 291–298.

- Barthel, D. (1988). On the ecophysiology of the sponge *Halichondria panicea* in Kile Bight. II. Biomass, production, energy budget and integration in environmental processes. *Marine Ecology Progress Series*, 43(April 1985), 87–93.
- Bates, D., Maechler, M., Bolker, B., & Walker S. (2015). Fitting Linear Mixed-Effects Models Using lme4. *Journal of Statistical Software*, 67(1), 1-48. doi:10.18637/jss.v067.i01.
- Batista, D., Tellini, K., Nudi, A. H., Massone, T. P., Scofield, A. D. L., & Wagener, A. D. L. R. (2013). Marine sponges as bioindicators of oil and combustion derived PAH in coastal waters. *Marine Environmental Research*, 92, 234–243. doi: 10.1016/j.marenvres.2013.09.022.
- Bell, J. J., Shaw, C., & Turner, J. R. (2006). Factors controlling the tentacle and polyp expansion behaviour of selected temperate Anthozoa. *Journal of the Marine Biological Association of the United Kingdom*, 86(5), 977-992.
- Berthet, B., Mouneyrac, C., Pérez, T., & Amiard-Triquet, C. (2005). Metallothionein concentration in sponges (*Spongia officinalis*) as a biomarker of metal contamination. *Comparative Biochemistry and Physiology - C Toxicology and Pharmacology*, 141(3), 306–313. doi: 10.1016/j.cca.2005.07.008.
- Birk, M.A. (2016). *presens: Interface for PreSens Fiber Optic Data. R package version 2.1.0.*
- BP Oil International Ltd (2017) *Schiehallion Crude oil from the UK's Quad 204 Development, Transportation and Trade*. Available at: <https://www.bp.com/content/dam/bp-trading/en/global/trading/crudes/brochures/SchiehallionBrochureMar17.pdf>. (last accessed: 01/09/18).
- Braga-Henriques, A., Porteiro, F. M., Ribeiro, P. A., Matos, V. D., Sampaio, Í., Ocaña, O., & Santos, R. S. (2013). Diversity, distribution and spatial structure of the cold-water coral fauna of the Azores (NE Atlantic). *Biogeosciences*, 10(6), 4009-4036.
- Bramanti, L., Movilla, J., Guron, M., Calvo, E., Gori, A., Dominguez-Carrió, C., ... & Ziveri, P. (2013). Detrimental effects of ocean acidification on the economically important Mediterranean red coral (*Corallium rubrum*). *Global Change Biology*, 19(6), 1897-1908.
- Brooke, S., Ross, S. W., Bane, J. M., Seim, H. E., & Young, C. M. (2013). Temperature tolerance of the deep-sea coral *Lophelia pertusa* from the southeastern United States. *Deep Sea Research Part II: Topical Studies in Oceanography*, 92, 240-248.
- Büscher, J. V., Form, A. U., & Riebesell, U. (2017). Interactive effects of ocean acidification and warming on growth, fitness and survival of the cold-water coral *Lophelia pertusa* under different food availabilities. *Frontiers in Marine Science*, 4, 101.
- Cahalan, J. A., Siddall, S. E., & Luckenbach, M. W. (1989). Effects of flow velocity, food concentration and particle flux on growth rates of juvenile bay scallops *Argopecten irradians*. *Journal of Experimental Marine Biology and Ecology*, 129(1), 45-60.
- Cathalot, C. C., Van Oevelen, D., Cox, T. J. S., Kutti, T., Lavaleye, M. S. S., Duineveld, G. C. A., et al. (2015). Cold-water coral reefs and adjacent sponge grounds: hotspots of benthic respiration and organic carbon cycling in the deep sea. *Frontiers in Marine Science* 2, 1–12. doi:10.3389/fmars.2015.00037.
- Carreiro-Silva, M., Cerqueira, T., Godinho, A., Caetano, M., Santos, R. S., & Bettencourt, R. (2014). Molecular mechanisms underlying the physiological responses of the cold-water coral *Desmophyllum dianthus* to ocean acidification. *Coral Reefs*, 33(2), 465-476.
- Cebrian, E., & Uriz, M. J. (2007). Contrasting effects of heavy metals and hydrocarbons on larval settlement and juvenile survival in sponges. *Aquatic Toxicology*, 81(2), 137–143. doi: 10.1016/j.aquatox.2006.11.010.
- Cerrano, C., Cardini, U., Bianchelli, S., Corinaldesi, C., Pusceddu, A., & Danovaro, R. (2013). Red coral extinction risk enhanced by ocean acidification. *Scientific reports*, 3, 1457.
- Chang-Feng, D., & Ming-Chao, L. (1993). The effects of flow on feeding of three gorgonians from southern Taiwan. *Journal of Experimental Marine Biology and Ecology*, 173(1), 57-69.

- Châtel, A., Talarmin, H., Hamer, B., Schröder, H. C., Müller, W. E. G., & Dorange, G. (2011). MAP kinase cell signaling pathway as biomarker of environmental pollution in the sponge *Suberites domuncula*. *Ecotoxicology*, *20*(8), 1727–1740. doi: 10.1007/s10646-011-0706-1.
- Cohen, A., & Holcomb, M. (2009). Why Corals Care About Ocean Acidification: Uncovering the Mechanism. *Oceanography*, *22*(4), 118-127. doi:10.5670/oceanog.2009.102.
- Crossland, C. J. (1987). In situ release of mucus and DOC-lipid from the corals *Acropora variabilis* and *Stylophora pistillata* in different light regimes. *Coral Reefs*, *6*(1), 35-42. doi:10.1007/BF00302210.
- Danovaro, R., Gambi, C., Dell'Anno, A., Corinaldesi, C., Fraschetti, S., Vanreusel, A., ... & Gooday, A. J. (2008). Exponential decline of deep-sea ecosystem functioning linked to benthic biodiversity loss. *Current Biology*, *18*(1), 1-8.
- Dasic International Limited, (2018) *Slickgone NS*. Available at: <http://oil.dasicinter.com/oil-dispersants/slickgone-ns-1> (last accessed: 14/08/18).
- Davies, P. S. (1984). The role of zooxanthellae in the nutritional energy requirements of *Pocillopora eydouxi*. *Coral Reefs*. doi:10.1007/BF00263571.
- Davies, A. J., & Guinotte, J. M. (2011). Global habitat suitability for framework-forming cold-water corals. *PLoS One* *6*. doi:10.1371/journal.pone.0018483.
- Davies, A. J., Duineveld, G. C. A., Lavaleye, M. S. S., Bergman, M. J. N., van Haren, H., & Roberts, J. M. (2009). Downwelling and deep-water bottom currents as food supply mechanisms to the cold-water coral *Lophelia pertusa* (Scleractinia) at the Mingulay Reef complex. *Limnology and Oceanography*, *54*, 620-629.
- Davies, A. J., & Guinotte, J. M. (2011). Global habitat suitability for framework-forming cold-water corals. *PloS one*, *6*(4), e18483.
- De Goeij, J. M., Moodley, L., Houtekamer, M., & Van Duyl, F. C. (2008). Tracing ¹³C-enriched dissolved and particulate organic carbon in the bacteria containing coral reef sponge *Halisarca caerulea* : Evidence for DOM feeding. *Limnology and Oceanography*, *53*(4), 1376–1386.
- De Goeij, J. M., De Kluijver, A., Van Duyl, F. C., Vacelet, J., Wijffels, R. H., De Goeij, A. F. P. M., ... & Schutte, B. (2009). Cell kinetics of the marine sponge *Halisarca caerulea* reveal rapid cell turnover and shedding. *Journal of Experimental Biology*, *212*(23), 3892-3900.
- de Matos, V., Gomes-Pereira, J. N., Tempera, F., Ribeiro, P. A., Braga-Henriques, A., & Porteiro, F. (2014). First record of *Antipathella subpinnata* (Anthozoa, Antipatharia) in the Azores (NE Atlantic), with description of the first monotypic garden for this species. *Deep Sea Research Part II: Topical Studies in Oceanography*, *99*, 113-121.
- Dickson, AG, Millero FJ. (1987). A comparison of the equilibrium constants for the dissociation of carbonic acid in seawater media. *Deep-Sea Research Part a-Oceanographic Research Papers*, *34*, 1733-1743.
- Dionísio, G., Faleiro, F., Bilan, M., Rosa, I. C., Pimentel, M., Serôdio, J., Calado R., & Rosa, R. (2017). Impact of climate change on the ontogenetic development of 'solar-powered' sea slugs. *Marine Ecology Progress, Series 578*: 87-97.
- Dodds, L. A., Roberts, J. M., Taylor, A. C., & Marubini, F. (2007). Metabolic tolerance of the cold-water coral *Lophelia pertusa* (Scleractinia) to temperature and dissolved oxygen change. *Journal of Experimental Marine Biology and Ecology*. *349*, 205–214. doi:10.1016/j.jembe.2007.05.013.
- Duineveld, G. C. A., Lavaleye, M. S. S., Bergman, M. J. N., De Stigter, H., & Mienis, F. (2007). Trophic structure of a cold-water coral mound community (Rockall Bank, NE Atlantic) in relation to the near-bottom particle supply and current regime. *Bulletin of Marine Science*. *81*, 449–467.
- Eerkes-Medrano, D., Feehan, C. J. & Leys, S. P. (2015). Sponge cell aggregation: Checkpoints in development indicate a high level of organismal complexity. *Invertebrate Biology*, *134*(1), 1–18. doi: 10.1111/ivb.12072.
- Form, A. U., & Riebesell, U. (2012). Acclimation to ocean acidification during long-term CO₂ exposure in the cold-water coral *Lophelia pertusa*. *Global change biology*, *18*(3), 843-853.

- Frøhlich, H. and Barthel, D. (1997). Silica uptake of the marine sponge *Halichondria panacea* in Kiel Bight. *Marine Biology*, 128, 115–125.
- Fry, B. (2006). *Stable isotope ecology* (Vol. 521). New York: Springer. doi:10.1007-0-387-33745-8.
- Gentric, C., Rehel, K., Dufour, A., & Sauleau, P. (2016). Bioaccumulation of metallic trace elements and organic pollutants in marine sponges from the South Brittany Coast, France. *Journal of Environmental Science and Health, Part A. Taylor & Francis*, 51(3), 213–219. doi: 10.1080/10934529.2015.1094327.
- Gehlen, M., Séférian, R., Jones, D. O., Roy, T., Roth, R., Barry, J. P., ... & Joos, F. (2014). Projected pH reductions by 2100 might put deep North Atlantic biodiversity at risk. *Biogeosciences*, 11, 6955–6967.
- Georgian, S. E., Dupont, S., Kurman, M., Butler, A., Strömberg, S. M., Larsson, A. I., & Cordes, E. E. (2016). Biogeographic variability in the physiological response of the coldwater coral *Lophelia pertusa* to ocean acidification. *Marine Ecology*, 37, 1345–1359.
- Giraudoux, P. (2018). *Package pgirmess: Spatial Analysis and Data Mining for Field Ecologists*. R package version 1.6.9. <https://CRAN.R-project.org/package=pgirmess>.
- Goldberg, W. M. (1991). Chemistry and structure of skeletal growth rings in the black coral *Antipathes fiordensis* (Cnidaria, Antipatharia). *Hydrobiologia*, 216, 403–409.
- Gori, A., Grover, R., Orejas, C., Sikorski, S. S., Ferrier-Pages, C., & Ferrier-Pagès, C. (2014). Uptake of dissolved free amino acids by four cold-water coral species from the Mediterranean. *Deep-Sea Research Part II: Topical Studies in Oceanography*, 99, 42–50. doi:10.1016/j.dsr2.2013.06.007.
- Gori, A., Reynaud, S., Orejas, C., & Ferrier-Pages, C. (2015). The influence of flow velocity and temperature on zooplankton capture rates by the cold-water coral *Dendrophyllia cornigera*. *Journal of Experimental Marine Biology and Ecology*, 466, 92–97.
- Gori, A., Ferrier-Pagès, C., Hennige, S. J., Murray, F., Rottier, C., Wicks, L. C. & Roberts, J. M. (2016). Physiological response of the cold-water coral *Desmophyllum dianthus* to thermal stress and ocean acidification. *PeerJ*, 4:e1606.
- Gómez, C. E., Wickes, L., Deegan, D., Etnoyer, P. J., & Cordes, E. E. (2018). Growth and feeding of deep-sea coral *Lophelia pertusa* from the California margin under simulated ocean acidification conditions. *PeerJ*, 6, e5671.
- Hatcher, A. (1989). RQ of benthic marine invertebrates. *Marine Biology*, 102(4), 445–452.
- Hebbeln, D., Portilho-Ramos, R. da C., Wienberg, C., & Titschack, J. (2019). The Fate of Cold-Water Corals in a Changing World: A Geological Perspective. *Frontiers in Marine Science*, 6, 1–8.
- Hennige, S. J., Wicks, L. C., Kamenos, N. A., Bakker, D. C. E., Findlay, H. S., Dumousseaud, C., & Roberts, J. M. (2014). Short-term metabolic and growth responses of the cold-water coral *Lophelia pertusa* to ocean acidification. *Deep-Sea Research Part II: Topical Studies in Oceanography*, 99, 2735.
- Hennige, S. J., Wicks, L. C., Kamenos, N. A., Perna, G., Findlay, H. S., & Roberts, J. M. (2015). Hidden impacts of ocean acidification to live and dead coral framework. *Proceedings of the Royal Society B: Biological Sciences*, 282(1813), 20150990.
- Hogg, M. M., Tendal, O. S., Conway, K. W., Pomponi, S. a, Van Soest, R. W. M., Gutt, J., et al. (2010). Deep-sea sponge grounds Regional Seas. Available at: http://epic.awi.de/epic/Main?entry_dn=Hog2010a&static=yes&page=abstract∓lang=en.
- Intergovernmental Panel on Climate Change (IPCC) (2014). *Climate Change 2014: Synthesis Report. Contribution of Working Groups I, II and III to the Fifth Assessment Report of the Intergovernmental Panel on Climate Change*, edited by Core Writing Team, R.K. Pachauri & L.A. Meyer. Geneva, Switzerland, IPCC. 151.
- Järnegren, J., & Altin, D. (2006). Filtration and respiration of the deep living bivalve *Acesta excavata* (JC Fabricius, 1779) (Bivalvia; Limidae). *Journal of Experimental Marine Biology and Ecology*, 334(1), 122–129.

- Kazanidis, G., Van Oevelen, D., Veuger, B., & Witte, U. F. M. (2018). Unravelling the versatile feeding and metabolic strategies of the cold-water ecosystem engineer *Spongosorites coralliophaga* (Stephens, 1915). *Deep-Sea Research Part I: Oceanographic Research Papers*, 141, 71–82. doi:10.1016/j.dsr.2018.07.009.
- Khalaman, V. V., & Komendantov, A. Y. (2016). Experimental study of the ability of the sponge *Halichondria panicea* (Porifera: Demospongiae) to compete for a substrate in shallow-water fouling communities of the White Sea. *Biology Bulletin*, 43(1), 69–74. doi: 10.1134/S1062359015060059.
- Khalaman, V. V., Sharov, A. N., Kholodkevich, S. V., Komendantov, A. Y., & Kuznetsova, T. V. (2017). Influence of the White Sea sponge *Halichondria panicea* (Pallas, 1766) on physiological state of the blue mussel *Mytilus edulis* (Linnaeus, 1758), as evaluated by heart rate characteristics. *Journal of Evolutionary Biochemistry and Physiology*, 53(3), 225–232.
- Kiriakoulakis, K., Fisher, E. L., Wolff, G. et al (2005). Lipids and nitrogen isotopes of two deep-water corals from the North-East Atlantic: initial results and implications for their nutrition. In *Cold-water Corals and Ecosystems*, 715–729. doi: 10.1007/3-540-27673-4_37.
- Knowlton, A. L., & Highsmith, R. C. (2005). Nudibranch-sponge feeding dynamics: Benefits of symbiont-containing sponge to *Archidoris montereyensis* (Cooper, 1862) and recovery of nudibranch feeding scars by *Halichondria panicea* (Pallas, 1766). *Journal of Experimental Marine Biology and Ecology*, 327(1), 36–46. doi: 10.1016/j.jembe.2005.06.001.
- Knudby, A., Kenchington, E., & Murillo, F. J. (2013). Modeling the distribution of *Geodia* sponges and sponge grounds in the Northwest Atlantic. *PLoS One*, 8, 1–20. doi:10.1371/journal.pone.0082306.
- Kooijman, S. A. L. M. (2000). *Dynamic energy and mass budgets in biological systems. Second*. Cambridge: Cambridge University Press.
- Koopmans, M., Martens, D., & Wijffels, R. H. (2010). Growth efficiency and carbon balance for the sponge *Haliclona oculata*. *Marine Biotechnology*, 12, 340–349. doi:10.1007/s10126-009-9228-8.
- Kroeker, K. J., Kordas, R. L., Crim, R. N., Singh, G. G. (2010). Meta-analysis reveals negative yet variable effects of ocean acidification on marine organisms. *Ecology Letters*, 13, 1419–1434.
- Kroeker, K. J., Kordas, R. L., Crim, R., Hendriks, I. E., Ramajo, L., Singh, G. S., ... & Gattuso, J. P. (2013). Impacts of ocean acidification on marine organisms: quantifying sensitivities and interaction with warming. *Global change biology*, 19(6), 1884–1896.
- Kumala, L., Riisgard, H. U., & Canfield, D. E. (2017). Osculum dynamics and filtration activity in small single-osculum explants of the demosponge *Halichondria panacea*. *Marine Ecology Progress Series*, 572(Wilkinson 1978), 117–128. doi: 10.3354/meps12155.
- Kurman, M. D., Gómez, C. E., Georgian, S. E., Lunden, J. J., & Cordes, E. E. (2017). Intra-specific variation reveals potential for adaptation to ocean acidification in a cold-water coral from the Gulf of Mexico. *Frontiers in Marine Science*, 4, 111.
- Kutti, T., Bannister, R. J., & Fosså, J. H. (2013). Community structure and ecological function of deep-water sponge grounds in the Traenadypet MPA-Northern Norwegian continental shelf. *Continental Shelf Research*, 69, 21–30. doi:10.1016/j.csr.2013.09.011.
- Lannig, G., Eilers, S., Pörtner, H. O., Sokolova, I. M., & Bock, C. (2010). Impact of ocean acidification on energy metabolism of oyster, *Crassostrea gigas* changes in metabolic pathways and thermal response. *Marine drugs*, 8(8), 2318–2339.
- Larsson, A. I., Lundälv, T., & Van Oevelen, D. (2013). Skeletal growth, respiration rate and fatty acid composition in the cold-water coral *Lophelia pertusa* under varying food conditions. *Marine Ecology Progress Series*. 483, 169–184. doi:10.3354/meps10284.
- Lenth, R. (2016). Least-Squares Means: The R Package lsmeans. *Journal of Statistical Software*, 69 (1), 1–33.

- Levin, L. A., Etter, R. J., Rex, M. A., Gooday, A. J., Smith, C. R., Pineda, J., ... & Pawson, D. (2001). Environmental influences on regional deep-sea species diversity. *Annual review of ecology and systematics*, 32(1), 51-93.
- Levin, L. A., & Le Bris, N. (2015). The deep ocean under climate change. *Science*, 350(6262), 766-768.
- Leys, S. P., & Eerkes-Medrano, D. I. (2006). Feeding in a calcareous sponge: particle uptake by pseudopodia. *The Biological Bulletin*, 211(2), 157-171.
- Leys, S. P., Kahn, A. S., Fang, J. K. H., Kutti, T., & Bannister, R. J. (2018). Phagocytosis of microbial symbionts balances the carbon and nitrogen budget for the deep-water boreal sponge *Geodia barretti*. *Limnology and Oceanography*, 63(1), 187-202.
- Leys, S. P., Yahel, G., Reidenbach, M. A., Tunnicliffe, V., Shavit, U., & Reiswig, H. M. (2011). The sponge pump: The role of current induced flow in the design of the sponge body plan. *PLoS One*, 6. doi:10.1371/journal.pone.0027787.
- Lubzens, E., Tandler, A., & Minkoff, G. (1989). Rotifers as food in aquaculture. *Hydrobiologia*, 186(1), 387-400.
- Lunden, J. J., McNicholl, C. G., Sears, C. R., Morrison, C. L., & Cordes, E. E. (2014). Acute survivorship of the deep-sea coral *Lophelia pertusa* from the Gulf of Mexico under acidification, warming, and deoxygenation. *Frontiers in Marine Science*, 1, 78.
- Mahaut, M. -L., Basuyaux, O., Baudinière, E., Chataignier, C., Pain, J., & Caplat, C. (2013). The porifera *Hymeniacidon perlevis* (Montagu, 1818) as a bioindicator for water quality monitoring. *Environmental Science and Pollution Research*, 20(5), 2984–2992. doi: 10.1007/s11356-012-1211-7.
- Maier, C., Watremez, P., Taviani, M., Weinbauer, M. G., & Gattuso, J. P. (2012). Calcification rates and the effect of ocean acidification on Mediterranean cold-water corals. *Proceedings of the Royal Society B: Biological Sciences*, 279(1734), 1716-1723.
- Maier, C., Schubert, A., Sánchez, M. M. B., Weinbauer, M. G., Watremez, P., & Gattuso, J. P. (2013). End of the century pCO₂ levels do not impact calcification in Mediterranean cold-water corals. *PLoS One*, 8(4), e62655.
- Maier, C., Popp, P., Sollfrank, N., Weinbauer, M. G., Wild, C., & Gattuso, J. P. (2016). Effects of elevated pCO₂ and feeding on net calcification and energy budget of the Mediterranean cold-water coral *Madrepora oculata*. *Journal of Experimental Biology*, 219: 3208-3217.
- Maier, C., Weinbauer, M.G. & Gattuso, J-P. (2019). Fate of Mediterranean cold-water corals as a result of global climate change. In C. Orejas & C. Jiménez, eds. *Mediterranean Cold-Water Corals: Past, Present and Future*. Springer (in press).
- Maier, S. R., Kutti, T., Bannister, R. J., van Breugel, P., van Rijswijk, P., & van Oevelen, D. (2019). Survival under conditions of variable food availability: Resource utilization and storage in the cold-water coral *Lophelia pertusa*. *Limnology and Oceanography*, 0, 1–21. doi:10.1002/lno.11142.
- Maldonado, M., Zhang, X., Cao, X., Xue, L., Cao, H., & Zhang, W. (2010). Selective feeding by sponges on pathogenic microbes: a reassessment of potential for abatement of microbial pollution. *Marine Ecology Progress Series*, 403, 75-89.
- Maldonado, M., Ribes, M., & van Duyl, F. C. (2012). Nutrient fluxes through sponges: biology, budgets, and ecological implications. In *Advances in marine biology*. Academic Press, Vol. 62, 113-182.
- Marine Management Organisation (2018). *Approved Oil Spill Treatment Products*. Available, at: <https://www.gov.uk/government/publications/approved-oil-spill-treatment-products/approved-oil-spill-treatment-products> (last accessed 02/09/2018).
- McClain, C. R., Allen, A. P., Tittensor, D. P., & Rex, M. A. (2012). Energetics of life on the deep seafloor. *Proceedings of the National Academy of Sciences of the United States of America*, 109, 15366–15371. doi:10.1073/pnas.1208976109.
- McCulloch, M., Trotter, J., Montagna, P., Falter, J., Dunbar, R., Freiwald, A., et al. (2012). Resilience of cold-water scleractinian corals to ocean acidification: Boron isotopic systematics of pH and saturation state up-regulation. *Geochimica et Cosmochimica Acta*, 87, 21–34. doi:10.1016/j.gca.2012.03.027.

- Mehrbach, C., Culbertson, C. H., Hawley, J. E., & Pytkowicz, R. M. (1973). Measurement of the apparent dissociation constants of carbonic acid in seawater at atmospheric pressure 1. *Limnology and Oceanography*, *18*(6), 897-907.
- Middelburg, J. J., Barranguet, C., Boschker, H. T. S., Herman, P. M. J., Moens, T., & Heip, C. H. R. (2000). The fate of intertidal microphytobenthos carbon: An in situ ¹³C-labeling study. *Limnology and Oceanography* *45*(6), 1224-1234.
- Middelburg, J. J., Mueller, C. E., Veuger, B., Larsson, A. I., Form, A., & Van Oevelen, D. (2015). Discovery of symbiotic nitrogen fixation and chemoautotrophy in cold-water corals. *Nature, Scientific Reports*, *5*, 17962. doi:10.1038/srep17962.
- Mienis, F., de Stigter, H. C., White, M., Duineveld, G., de Haas, H., & Van Weering, T. C. E. (2007). Hydrodynamic controls on cold-water coral growth and carbonate-mound development at the SW and SE Rockall Trough Margin, NE Atlantic. *Deep-Sea Research Part I: Oceanographic Research Papers*, *54*, 1655–1674.
- Moeller, R. E., Gilroy, S., Williamson, C. E., Grad, G., & Sommaruga, R. (2005). Dietary acquisition of photoprotective compounds (mycosporine-like amino acids, carotenoids) and acclimation to ultraviolet radiation in a freshwater copepod. *Limnology and Oceanography*, *50*(2), 427-439. doi:10.4319/lo.2005.50.2.0427.
- Moodley, L., Boschker, H. T. S., Middelburg, J. J., Pel, R., Herman, P. M. J., De Deckere, E., et al. (2000). Ecological significance of benthic foraminifera: ¹³ C Labelling experiments. *Marine Ecology Progress Series* *202*, 289-295. doi:10.3354/meps202289.
- Moodley, L., Middelburg, J. J., Soetaert, K., Boschker, H. T. S., Herman, P. M. J., & Heip, C. H. R. (2005). Similar rapid response to phytodetritus deposition in shallow and deep-sea sediments. *Journal of Marine Research*, *63*(2), 457-469.
- Movilla, J., Gori, A., Calvo, E., Orejas, C., López-Sanz, À., Domínguez-Carrió, C., ... & Pelejero, C. (2014). Resistance of two Mediterranean cold-water coral species to low-pH conditions. *Water*, *6*(1), 59-67.
- Mueller, C. E., Larsson, A. I., Veuger, B., Middelburg, J. J., & Van Oevelen, D. (2014). Opportunistic feeding on various organic food sources by the cold-water coral *Lophelia pertusa*. *Biogeosciences*, *11*, 123–133.
- Naumann, M. S., Orejas, C., Wild, C., & Ferrier-Pagès, C. (2011). First evidence for zooplankton feeding sustaining key physiological processes in a scleractinian cold-water coral. *Journal of Experimental Biology*, *214*(21), 3570-3576.
- Ocaña, O., Opresko, D. M., Brito, A. (2007). *Antipathella wollastoni* (Anthozoa: Antipatharia) outside of the Macaronesia waters. *Revista de la Academia Canaria de Ciencias*, *138*, 125–138.
- Olesen, T. M. E. & Weeks, J. M. (1994). Accumulation of Cd by the marine sponge *Halichondria panicea* pallas: effects upon filtration rate and its relevance for biomonitoring. *Bulletin of Environmental Contamination and Toxicology*, *52*(5), 722–728.
- Oliver, P. G. (1979). Adaptations of some deep-sea suspension-feeding bivalves (*Limopsis* and *Bathyarca*). *Sarsia*, *64*(1-2), 33-36.
- Orejas, C., Gili, J.M., & Arntz, W. (2003). Role of small-plankton communities in the diet of two Antarctic octocorals (*Primnoisis antarctica* and *Primnoella* sp.). *Marine Ecology Progress Series*, *250*, 105-116.
- Orejas, C., Gili, J. M., Lopez-Gonzalez, P. J., & Arntz, W. E. (2001). Feeding strategies and diet composition of four Antarctic cnidarian species. *Polar Biology*, *24*, 620-627.
- Orejas, C., Ferrier-Pagès, C., Reynaud, S., Gori, A., Beraud, E., Tsounis, G., et al. (2011). Long-term growth rates of four Mediterranean cold-water coral species maintained in aquaria. *Marine Ecology Progress Series*, *429*, 57–65. doi:10.3354/meps09104.
- Orejas, C., Gori, A., Rad-Menéndez, C., Last, K. S., Davies, A. J., Beveridge, C. M., Sadd, D., Kiriakoulakis, K., Witte, U., & Roberts, J. M. (2016). The effect of flow speed and food size on the capture efficiency and feeding behaviour of the cold-water coral *Lophelia pertusa*. *Journal of Experimental Marine Biology and Ecology*, *481*, 34-40.

- Orejas, C., Jimenez, C. (2019). *Mediterranean cold-water corals: Past, present and future*. Springer International Publishing, 581.
- Osinga, R., Tramper, J., & Wijffels, R. H. (1999). Cultivation of marine sponges. *Marine Biotechnology*, 1(6), 509–532.
- Palanques, A., Durrieu de Madron, X., Puig, P., Fabres, J., Guillén, J., Calafat, A., Canals, M., Heussner, S., & Bonnín, J. (2006). Suspended sediment fluxes and transport processes in the Gulf of Lions submarine canyons. The role of storms and dense water cascading. *Marine Geology*, 234, 43–61.
- Perea-Blázquez, A., Davy, S. K., & Bell, J. J. (2013). Low functional redundancy in sponges as a result of differential picoplankton use. *The Biological Bulletin*, 224(1), 29–34.
- Perez, F.F., Fontela, M., García-Ibáñez, M.I., Mercier, H., Velo, A., Lherminier, P., Zunino, P., la Paz, de, M., Alonso-Pérez, F., Gualart, E.F. & Padin, X.A. (2018). Meridional overturning circulation conveys fast acidification to the deep Atlantic Ocean. *Nature*, 554, 515–518.
- Pitt, K. A., Connolly, R. M., & Meziane, T. (2008). Stable isotope and fatty acid tracers in energy and nutrient studies of jellyfish: a review. In *Jellyfish Blooms: Causes, Consequences, and Recent Advances*, 119–132. Springer, Dordrecht.
- Previatti, M., Scinto, A., Cerrano, C. & Osinga, R. (2010). Oxygen consumption in Mediterranean octocorals under different temperatures. *Journal of Experimental Marine Biology and Ecology*, 390, 39–48.
- Pörtner, H. O. (2008). Ecosystem effects of ocean acidification in times of ocean warming: a physiologist's view. *Marine Ecology Progress Series*, 373, 203–217.
- Purser, A., Larsson, A. I., Thomsen, L., & Van Oevelen, D. (2010). The influence of flow velocity and food concentration on *Lophelia pertusa* (Scleractinia) zooplankton capture rates. *Journal of Experimental Marine Biology and Ecology*, 395, 55–62.
- R Core Team (2017). *R: A language and environment for statistical computing*, R Foundation for Statistical Computing, Vienna, Austria. Available at: <https://www.R-project.org/> (last accessed: 05/09/18).
- Regnier, P., Arndt, S., Goossens, N., Volta, C., Laruelle, G. G., Lauerwald, R., & Hartmann, J. (2013). Modelling estuarine biogeochemical dynamics: from the local to the global scale. *Aquatic geochemistry*, 19(5-6), 591–626.
- Rengstorf, A. M., Mohn, C., Brown, C., Wisz, M. S., & Grehan, A. J. (2014). Predicting the distribution of deep-sea vulnerable marine ecosystems using high-resolution data: Considerations and novel approaches. *Deep-Sea Research Part I: Oceanographic Research Papers*, 93, 72–82.
- Ribes, M., Coma, R., & Gili, J.M. (1999). Heterogeneous feeding in benthic suspension feeders: the natural diet and grazing rate of the temperate gorgonian *Paramuricea clavata* (Cnidaria: Octocorallia) over a year cycle. *Marine Ecology-Progress Series*, 183, 125–137.
- Riisgård, H. U., Thomassen, S., Jakobsen, H., Weeks, J. M., & Larsen, P. S. (1993). Suspension feeding in marine sponges *Halichondria panicea* and *Haliclona urceolus*: effects of temperature on filtration rate and energy cost of pumping. *Marine Ecology Progress Series*, 96(2), 177–188.
- Riisgård, H. U., Kumala, L., & Charitonidou, K. (2016). Using the F/R-ratio for an evaluation of the ability of the demosponge *Halichondria panicea* to nourish solely on phytoplankton versus free-living bacteria in the sea. *Marine Biology Research*. Taylor & Francis, 12(9), 907–916.
- Ritz, C., Baty, F., Streibig, J. C., & Gerhard, D. (2015). Dose-Response Analysis Using R'. *PLOS ONE*, 10(12), e0146021.
- Rix, L., de Goeij, J. M., Mueller, C. E., Struck, U., Middelburg, J. J., van Duyl, F. C., et al. (2016). Coral mucus fuels the sponge loop in warm- and cold-water coral reef ecosystems. *Nature, Scientific Reports*, 6, 18715.
- Rix, L., de Goeij, J. M., van Oevelen, D., Struck, U., Al-Horani, F. A., Wild, C., & Naumann, M. S. (2018). Reef sponges facilitate the transfer of coral-derived organic matter to their associated fauna via the sponge loop. *Marine Ecology Progress Series*, 589, 85–96.

- Roberts, J. M., Wheeler, A. J., & Freiwald, A. (2006). Reefs of the deep: The biology and geology of cold-water coral ecosystems. *Science* (80-.), 312, 543–547.
- Rossi, S., Ribes, M., Coma, R., & Gili, J. M. (2004). Temporal variability in Zooplankton prey capture rate of the passive suspension feeder *Leptogorgia sarmentosa* (Cnidaria: Octocorallia), a case study. *Marine Biology – Springer*, 144, 89–99.
- Rovelli, L., Attard, K. M., Bryant, L. D., Flögel, S., Stahl, H., Roberts, J. M., et al. (2015). Benthic O₂ uptake of two cold-water coral communities estimated with the non-invasive eddy correlation technique. *Marine Ecology Progress Series*, 525, 97–104.
- R-Studio Team (2016). RStudio: Integrated Development for R. RStudio, Inc., Boston, MA URL.
- Santos, M., Moita, M. T., Bashmachnikov, I., Menezes, G. M., Carmo, V., Loureiro, C. M., ... & Martins, A. (2013). Phytoplankton variability and oceanographic conditions at Condor seamount, Azores (NE Atlantic). *Deep Sea Research Part II: Topical Studies in Oceanography*, 98, 52-62.
- Sarazin, G., Michard, G., & Prevot, F. (1999). A rapid and accurate spectroscopic method for alkalinity measurements in sea water samples. *Water Research*, 33(1), 290-294.
- Schindelin, J., Arganda-Carreras, I., Frise, E., Kaynig, V., Longair, M., Pietzsh, T., Preibisch, S., Rueden, C., Saalfeld, S., Schmid, B., Tinevez, J. Y., White, D. J., Hartenstein, V., Eliceiri, K., Tomancak, P., & Cardona, A. (2012) Fiji: an Open-Source Platform for Biological-Image Analysis, *Nature Methods*, 9(7), 676-682.
- Schneemann, I., Nagel, K., Kajahn, I., Labes, A., Wiese, J., & Imhoff, J. F. (2010). Comprehensive investigation of marine actinobacteria associated with the sponge *Halichondria panicea*. *Applied and Environmental Microbiology*, 76(11), 3702–3714.
- Schönberg, C. H. L., & Barthel, D. (1997). Inorganic skeleton of the demosponge *Halichondria panicea*. Seasonality in spicule production in the Baltic Sea. *Marine Biology*, 130(2), 133–140.
- Schönberg, C. H., Fang, J. K., Carreiro-Silva, M., Tribollet, A., & Wisshak, M. (2017). Bioerosion: the other ocean acidification problem. *ICES Journal of Marine Science*, 74(4), 895-925.
- Sebens, K. P., & De Riemer, K. (1977). Diel cycles of expansion and contraction in coral reef anthozoans. *Marine Biology*, 43(3), 247-256.
- Sebens, K. P. (1984). Water flow and coral colony size: interhabitat comparisons of the octocoral *Alcyonium siderium*. *Proceedings of the National Academy of Sciences*, 81(17), 5473-5477.
- Sebens, K. P., Witting, J., & Helmuth, B. (1997). Effects of water flow and branch spacing on particle capture by the reef coral *Madracis mirabilis* (Duchassaing and Michelotti). *Journal of Experimental Marine Biology and Ecology*, 211(1), 1-28.
- Sebens, K. P., Grace, S. P., Helmuth, B., Maney Jr, E. J., & Miles, J. S. (1998). Water flow and prey capture by three scleractinian corals, *Madracis mirabilis*, *Montastrea cavernosa* and *Porites porites*, in a field enclosure. *Marine Biology*, 131(2), 347-360.
- Shimeta, J., & Jumars, P. A. (1991). Physical mechanisms and rates of particle capture by suspension feeders. *Oceanography and Marine Biology*, 29, 191–257.
- Soetaert, K., & Petzoldt, T. (2010). Inverse Modelling, Sensitivity and Monte Carlo Analysis in R Using Package FME. *Journal of Statistical Software*. 33, 1–28.
- Soetaert, K., Mohn, C., Rengstorf, A., Grehan, A., & Van Oevelen, D. (2016). Ecosystem engineering creates a direct nutritional link between 600-m deep cold-water coral mounds and surface productivity. *Nature - Scientific Reports*, 6, 35057.
- Soetaert, K., Petzoldt, T., Setzer, R. W., & Petzoldt, M. T. (2018). Package ‘deSolve’. *Writing Code in Compiled Languages*, 1-51.
- Stigebrandt, A. (2011). Carrying capacity: general principles of model construction. *Aquaculture Research*, 42, 41–50.
- Strohmeier, T., Strand, Ø., Alunno-Bruscia, M., Duinker, A., & Cranford, P. J. (2012). Variability in particle retention efficiency by the mussel *Mytilus edulis*. *Journal of Experimental Marine Biology and Ecology*, 412, 96-102.
- Swain, T. D., Schellinger, J. L., Strimaitis, A. M., & Reuter, K. E. (2015). Evolution of anthozoan polyp retraction mechanisms: convergent functional morphology and evolutionary allometry of the

- marginal musculature in order Zoanthidea (Cnidaria: Anthozoa: Hexacorallia). *BMC evolutionary biology*, 15(1), 123.
- Sweetman, A. K., Thurber, A. R., Smith, C. R., Levin, L. A., Mora, C., Wei, C. L., ... & Ingels, J. (2017). Major impacts of climate change on deep-sea benthic ecosystems. *Elementa: Science of the Anthropocene*, 5, Art-No.
- Tazioli S, Bo M, Boyer M, et al (2007) Ecological Observations of Some Common Antipatharian Corals in the. *Zoological Studies*, 46, 227–241.
- Tempera, F., Afonso, P., Gomes, T., & Santos, R. (2001). *Comunidades Biológicas do Sítio de Interesse Comunitário Ilhéus das Formigas e Recife Dollabarat*. Horta, Azores.
- Tempera, F., Atchoi, E., Amorim, P., Gomes-Pereira, J., & Gonçalves, J. (2013). Atlantic area marine habitats. Adding new Macaronesian habitat types from the Azores to the EUNIS Habitat Classification. In MeshAtlantic Technical Report, 4/2013. IMAR/DOP-UAç, Horta.
- Thomassen, S., & Riisgard, H. U. (1995). Growth and energetics of the sponge *Halichondria panicea*. *Marine Ecology Progress Series*, 128, 239-246.
- Thresher, R. E., Tilbrook, B., Fallon, S., Wilson, N. C., & Adkins, J. (2011). Effects of chronic low carbonate saturation levels on the distribution, growth and skeletal chemistry of deep-sea corals and other seamount megabenthos. *Marine Ecology Progress Series*, 442, 87-99.
- Tittensor, D. P., Baco, A. R., Hall-Spencer, J. M., Orr, J. C., & Rogers, A. D. (2010). Seamounts as refugia from ocean acidification for cold-water stony corals. *Marine Ecology*, 31, 212–225.
- Tsounis, G., Orejas, C., Reynaud, S., Gili, J.M., Allemand, D., & Ferrier-Pagès, C. (2010). Prey-capture rates in four Mediterranean cold-water corals. *Marine Ecology Progress Series*, 398, 149-155.
- Van Haren, H., Mienis, F., Duineveld, G. C. A., & Lavaleye, M. S. S. (2014). High-resolution temperature observations of a trapped nonlinear diurnal tide influencing cold-water corals on the Logachev mounds. *Progress in Oceanography*, 125, 16–25.
- Van Oevelen, D., Mueller, C. E., Lundälv, T., & Middelburg, J. J. (2016). Food selectivity and processing by the cold-water coral *Lophelia pertusa*. *Biogeosciences*, 13(20), 5789-5798.
- Van Oevelen, D., Mueller, C. E., Lundälv, T., Van Duyl, F. C., De Goeij, J. M., & Middelburg, J. J. (2018). Niche overlap between a cold-water coral and an associated sponge for isotopically enriched particulate food sources. *PLoS One*, 13, 1–16.
- Wagner, D., Luck, D. G., Toonen, R. J. (2012). The biology and ecology of black corals (Cnidaria: Anthozoa: Hexacorallia: Antipatharia). *Advances in Marine Biology*, 63, 67–132.
- Warner, G. F. (1981). Species descriptions and ecological observations black corals (Antipatharia) from Trinidad G. F. Warner. *Bulletin of Marine Science*, 31, 147–163.
- Warner, G. F, Pergamon, (1977). On the shapes of passive suspension feeders. *Biology of benthic organisms*, 567-576.
- Wei, C. L., Rowe, G. T., Hubbard, G. F., Scheltema, A. H., Wilson, G. D. F., Petrescu, I., et al. (2010). Bathymetric zonation of deep-sea macrofauna in relation to export of surface phytoplankton production. *Marine Ecology Progress Series*, 399, 1–14. doi:10.3354/meps08388.
- Weisz, J. B., Lindquist, N., & Martens, C. S. (2008). Do associated microbial abundances impact marine demosponge pumping rates and tissue densities?. *Springer-Oecologia*, 155(2), 367-376.
- White, M., Mohn, C., de Stigter, H., & Mottram, G. (2005). Deep-water coral development as a function of hydrodynamics and surface productivity around the submarine banks of the Rockall Trough, NE Atlantic. *SpringerLinks, Cold-Water Corals and Ecosystems*, 503–514.
- White, M., Wolff, G. A., Lundälv, T., Guihen, D., Kiriakoulakis, K., Lavaleye, M. S. S., et al. (2012). Cold-water coral ecosystem (Tisler Reef, Norwegian shelf) may be a hotspot for carbon cycling. *Marine Ecology Progress Series*, 465, 11–23.
- Wichels, A., Würtz, S., Döpke, H., Schütt, C., & Gerds, G. (2006). Bacterial diversity in the breadcrumb sponge *Halichondria panicea* (Pallas). *FEMS Microbiology Ecology*, 56(1), 102–118.
- Wild, C., Mayr, C., Wehrmann, L., Schöttner, S., Naumann, M., Hoffmann, F., et al. (2008). Organic matter release by cold water corals and its implication for fauna-microbe interaction. *Marine Ecology Progress Series*, 372, 67–75.

- Wildish, D., and Kristmanson, D. (2005) Benthic suspension feeders and flow. Cambridge University Press.
- Witte, U., Brattegard, T., Graf, G., & Springer, B. (1997). Particle capture and deposition by deep-sea sponges from the Norwegian-Greenland Sea. *Marine Ecology Progress Series*, 154, 241-252.
- Wohlers, J., Engel, A., Zollner, E., Breithaupt, P., Jurgens, K., Hoppe, H.-G., et al. (2009). Changes in biogenic carbon flow in response to sea surface warming. *Proceedings of the National Academy of Sciences of United States of America*, 106, 7067–7072.
- Xavier J., Carreiro-Silva M., Colaço A., Le Bris N., Levin L. (2019) Chapter 6. Vulnerabilities: Invertebrate taxa (VME indicators). In Levin, L., Baker, M., Thompson, A. (eds) *Deep-ocean climate change impacts on habitat, fish and fisheries*. FAO Fisheries and Aquaculture Technical Paper No. 638. Rome, FAO.
- Yahel, G., Whitney, F., Reiswig, H. M., Eerkes-Medrano, D. I., & Leys, S. P. (2007). In situ feeding and metabolism of glass sponges (Hexactinellida, Porifera) studied in a deep temperate fjord with a remotely operated submersible. *Limnology and Oceanography*, 52, 428–440.
- Yesson, C., Taylor, M. L., Tittensor, D. P., Davies, A. J., Guinotte, J., Baco, A., ... & Rogers, A. D. (2012). Global habitat suitability of cold-water octocorals. *Journal of Biogeography*, 39(7), 1278-1292.
- Zahn, R. K., Zahn, G. & Alii, E. (1981). Assessing consequence of marine pollution by hydrocarbons using sponges as model organisms. *The Science of the Total Environment*, 20, 147–169.
- Zahn, R. K., Zahn-Daimler, G., Müller, W. E. G., Michaelis, M. L., Kurelec, B., Rijavec, M., Batel, R., & Bihari, N. (1983). DNA damage by PAH and repair in a marine sponge. *The Science of the Total Environment*, 26, 137–156.
- Zetsche, E. M., Baussant, T., Meysman, F. J. R., & Van Oevelen, D. (2016). Direct visualization of mucus production by the cold-water coral *Lophelia pertusa* with digital holographic microscopy. *PLoS One*, 11, 1–17.
- Zhao, X., Shi, W., Han, Y., Liu, S., Guo, C., Fu, W., ... & Liu, G. (2017). Ocean acidification adversely influences metabolism, extracellular pH and calcification of an economically important marine bivalve, *Tegillarca granosa*. *Marine environmental research*, 125, 82-89.

